

Hydrocarbon Biomarkers for Biotic and Environmental Evolution through the
Neoproterozoic-Cambrian Transition

by

Amy Elizabeth Kelly

B.S. Chemistry and Geochemistry
Caltech, 2002

S.M. Chemistry
Massachusetts Institute of Technology, 2004

SUBMITTED TO THE DEPARTMENT OF EARTH, ATMOSPHERIC AND
PLANETARY SCIENCES IN PARTIAL FULFILLMENT OF THE REQUIREMENTS
FOR THE DEGREE OF

DOCTOR OF PHILOSOPHY IN GEOCHEMISTRY
AT THE
MASSACHUSETTS INSTITUTE OF TECHNOLOGY

JUNE 2009

© 2009 Massachusetts Institute of Technology
All rights reserved

Signature of Author.....

Department of Earth, Atmospheric and Planetary Sciences

April 10, 2009

Certified by.....

Roger E. Summons
Professor of Geobiology
Thesis Supervisor

Accepted by.....

Maria Zuber
E. A. Griswold Professor of Geophysics
Head of the Department

Hydrocarbon Biomarkers for Biotic and Environmental Evolution through the Neoproterozoic-Cambrian Transition

by

Amy E. Kelly

Submitted to the Department of Earth, Atmospheric and Planetary Sciences
on May 1, 2009 in Partial Fulfillment of the
Requirements for the Degree of Doctor of Philosophy in
Geochemistry

ABSTRACT

The sequence of events over the Neoproterozoic - Cambrian transition that led to the radiation of multicellular organisms has been an issue of debate for over a century. It is a critical interval in the history of life on Earth because it marks the first appearance of all extant animal phyla in the fossil record. We set out to improve understanding of environmental transitions during this key interval of Earth's history by studying chemical fossils (biomarkers) in Neoproterozoic to Cambrian aged sedimentary rocks and oils from Australia, Eastern Siberia and Oman. This thesis presents the distributions of steranes and other hydrocarbons through these various strata and the characterization of novel age and paleostratification biomarkers. Compound specific carbon isotopic data of *n*-alkanes and isoprenoids were also acquired and evaluated in the context of existing datasets with a focus on elucidating the processes responsible for anomalous trends. Consistent with current theory, our results indicate that there was a significant shift in the redox state the oceans and that this took place on a global scale. The biomarker and isotopic proxies we have measured help us further constrain the timing of this redox shift, and suggest a concomitant switch in the composition of marine photosynthetic communities, at termination of the Neoproterozoic Era.

Thesis Supervisor: Roger E. Summons
Title: Professor of Geobiology

Biographical Note

Amy Elizabeth Kelly was born in Washington D.C. on July 29, 1980 to Richard and Susan Kelly. She grew up in Paoli, PA and graduated from Conestoga High School where she was nominated to the National Honor Society and named an AP Scholar.

Then she attended Caltech in Pasadena, CA where she majored in both Chemistry and Geochemistry. During the summers, she had a variety of research opportunities. In the summer of 1999, she received an NSF-REU scholarship and worked with Professor Don Berry at the University of Pennsylvania. In the summer of 2000 she worked at the Australian National University under Professor Eric Wenger. In the summer of 2001, she worked at a Johns Hopkins CTY program, teaching 6th graders chemistry. Amy graduated from Caltech with a BS in June of 2002.

Amy came to MIT in the fall of 2002 to join the Chemistry Department. She quickly found a home in the Lippard lab where she worked on synthetically modeling the active site of methane monooxygenase. After receiving her Masters in Chemistry in the fall of 2004, she immediately joined the lab of Professor Roger E. Summons in the Department of Earth, Atmospheric and Planetary Science (EAPS) where she studied biomarkers from Neoproterozoic sedimentary rocks and oils for just under 5 years and advised three undergraduate students. In her time in EAPS she has received numerous awards including the Linden Fellowship from the Earth System Initiative at MIT in July of 2004, Eleanor and Anthony DeFrancis Scholarship from the National Italian American Foundation in January 2005, August 2005, June 2006, July 2007 and July 2008, Harrison Scholarship from the Tobacco Root Geological Society in April 2006, Outstanding Student Talk Award from the Ocean Sciences Meeting in March 2008 and ExxonMobil Geoscience Grant in March 2008. She was also privileged to be chosen to participate in the Agouron International Geobiology course on Catalina Island in June and July 2005.

During the summer of 2009 she plans to intern at Shell. She has also accepted an NAI Postdoctoral Scholarship split between Arizona State University, where she will work with Ariel Anbar, and the University of California at Riverside, where she will work with Timothy Lyons and Gordon Love.

Acknowledgement

I would like to begin by thanking my advisor, Roger Summons. Over the past five years he has helped me grow as a scientist not only in learning lab skills but also in the way I read and analyze articles. Thank you also to my thesis committee, led by Daniel Rothman and including Andrew Knoll and Christopher Reddy. Both Dan and Andy were also on my Generals committee and have seen me through most of my MIT career. Dan was especially helpful when interpreting isotope data and Andy, though immensely helpful scientifically, was most helpful as a mentor who supported me along my way. Ed Boyle was my second generals advisor and has been an excellent resource for oceanography knowledge and an amazing model for me to follow. He has always been here for me these past 5 years, and for that I am grateful.

I would also like to thank my collaborators Daniel Rothman, Gordon Love, Emmanuelle Grosjean, David Fike and John Zumberge. Gordon's guidance and support has been vital to my success. Thank you to John Zumberge, P.D.O., Andrew Hill and David Fike for helping me acquire samples. Thank you to John Hayes, Alexander Bradley and Sara Lincoln for valuable discussions about my research though they are not collaborators. I would also like to thank the entire Boyle and Summons labs, especially Rick Kayser, Seth John, Yanek Hebling, Alexander Bradley, Sara Lincoln and again Gordon Love. Thank you to the undergraduate researchers I have advised- Elisabetta Corradi, Sarah Hurley and Laurie Hakes. Elisabetta and Sarah are from Wellesley College and have opened my eyes to the vast potential of Liberal Arts colleges.

Thanks to those who have funded my research: the Linden Fellowship at MIT, Tobacco Root Geological Society, NSF and especially the National Italian American Foundation.

A final thank you goes, of course, to my family and friends. I would like to recognize Susan Kelly (mom), Richard Kelly (dad), Sara Lincoln and Brandon Sparks who saved my sanity and were even able to put a smile on my face no matter what I was facing. I would also like to dedicate this thesis to my late grandfather Joseph P. Kelly, an admirable microbiologist who initially sparked my passion for science at a young age.

Table of Contents

Chapter 1: Introduction	15
Cambrian explosion	15
Biomarker importance	18
Paleogeography	19
Thesis outline	20
Chapter 2: Biomarker Trends in Neoproterozoic to Lower Cambrian Oils from Eastern Siberia	25
Environmental interpretations	40
Comparison to Oman	42
Sterane patterns	43
Chapter 3: Novel Steranes in Neoproterozoic Sediments and Oils	59
Distribution of compound C through time	69
Distribution of C ₁₉ norsterane C with lithology and depositional environment	72
Identity of C ₁₉ norsterane C	72
Distribution of 21-norsteranes with lithology and depositional environment	79
Chapter 4: C-Isotopic Studies of Hydrocarbons in Neoproterozoic to Cambrian Samples	89
Chapter 5: Neoproterozoic Rocks with Confounding Biomarker Signatures: Novel Environmental Signals or Contamination?	117
Age-sensitive biomarkers	128
Maturity-sensitive parameters	129
Patterns of <i>n</i> -alkanes	130
General issues	135
Appendix 1: Biomarker Trends in Neoproterozoic to Lower Cambrian Rocks from the Centralian Superbasin in Australia	141
Interpretations for Australian samples	149
Appendix 2: Biomarker Trends in Ediacaran Rocks from the White Sea Region of Russia	153

List of Tables and Figures

Chapter 1	Introduction	
Figure 1.	Paleogeographic relationship of the world in the Late Proterozoic	19
Chapter 2	Biomarker Trends in Neoproterozoic to Lower Cambrian Oils from Eastern Siberia	
Figure 1.	Map of the sites from which the Eastern Siberian oil samples were taken	27
Table 1.	The provenance, age, lithology, and depositional environment of the Eastern Siberian oil samples	28
Figure 2.	A selection of GC-MS MRM chromatograms showing relative abundances of steranes in an Eastern Siberian oil from the Usol'ye Formation from the Nepa-Botuoba Basin, ES 083	30
Figure 3.	A selection of GC-MS MRM chromatograms showing relative abundances of hopanes in an Eastern Siberian oil from the Usol'ye Formation from the Nepa-Botuoba Basin, ES 083	31
Table 2.	Redox and possible stratification and hypersalinity indicators	32
Table 3.	Maturity indicators	34
Table 4.	Possible sponge indicators	36
Table 5.	A selection of source indicators	38
Figure 4.	Cross-plots of a selection of biomarkers	40
Figure 5.	Principal component analysis tree showing the main oil families in these Eastern Siberian oils	42
Figure 6.	C ₂₇ , C ₂₈ and C ₂₉ sterane distributions from representative samples of the Walcott Member, Q oil of Oman, the Amadeus Basin, Officer Basin, Eastern Siberia and the South Oman Salt Basin	44
Figure 7.	Sterane ternary diagram	45
Figure 8.	Schematics of the different redox conditions of Neoproterozoic water columns	52
Chapter 3	Novel Steranes in Neoproterozoic Sediments and Oils	
Figure 1.	GC-MS MRM chromatogram showing the pattern of C ₁₉ norsteranes in Q oil from Oman on a DB-1 column	61
Figure 2.	Hypothetical structures for C ₁₉ norsteranes identified in various rocks and oils	61
Figure 3.	Chemical structures of the 21-norsterane series	62
Figure 4.	GC-MS MRM chromatogram of 21-norcholestane in a Shuram Formation rock from Oman on a DB-1 column	62
Figure 5.	GC-MS MRM chromatogram of 21-norstigmastane in Q oil from Oman on a DB-1 column	62
Figure 6.	GC-MS MRM chromatograms of the full series of 21-norsteranes from the A2C rock sample OMR 235 of Oman on a DB-1 column	63
Table 1.	Identity, provenance, age, type and lithology of each carbonate sample	65

Table 2.	Identity, provenance, age, type and lithology of each siliciclastic sample	66
Figure 7.	GC-MS MRM chromatograms showing the distributions of C ₁₉ norsteranes in a selection of oils and rocks spanning the Neoproterozoic to Jurassic	69
Figure 8.	Cross-plot of C/ (A+B) vs. geologic time	70
Figure 9.	Cross-plot of C/ (A+B) with the gammacerane/ hopane (γ/ H) ratio	72
Figure 10.	Spectra of C ₁₉ norsteranes A, B, and C in Q oil sample OMO 001	73
Figure 11.	Fragmentation patterns used to identify the C ₁₉ norsteranes	74
Figure 12.	A GCxGC composite chromatogram of masses 203, 245, and 260 shown in two different views	75
Figure 13.	GC-MS chromatogram for a Q oil OMO 021 showing C ₁₉ A, C ₁₉ B, C ₁₉ C, and the isomers of androstane produced by sealed-tube isomerization	76
Figure 14.	Crossplot of γ/ H vs. 21-norstigmastane/ C ₂₈ $\alpha\beta\beta$ R	80
Figure 15.	Crossplot of γ/ H vs. 21-norstigmastane/ C ₂₈ $\alpha\beta\beta$ R without post-mature samples	80
Figure 16.	GC-MS data showing the C ₂₆ and C ₂₈ 21-norsterane abundances in bitumen and kerogen hydropyrolysate of rock sample OMR 235 of the A2C from Oman	81
Figure 17.	Crossplot of C ₂₇ steranes/ C ₂₉ steranes vs. 21-norcholestane/ 21-norstigmastane	82
Chapter 4	C-Isotopic Studies of Hydrocarbons in Neoproterozoic to Cambrian Samples	
Figure 1.	Food chain with appropriate δ labels	91
Figure 2.	Isotopic ordering of isoprenoids vs. <i>n</i> -alkanes in Proterozoic and Phanerozoic marine systems	92
Figure 3.	The South Oman Salt Basin (SOSB) and detail of the region	95
Figure 4.	Compound specific isotopic data from the carbonate platform of the SOSB	96
Figure 5.	Compound specific isotopic data from the Athel Sub-basin of the SOSB	96
Figure 6.	Compound specific isotope data for the entire SOSB	97
Table 1.	Δ data for the SOSB with sample IDs, formations, and approximate ages	98
Figure 7.	Compound specific isotopic data from Eastern Siberia	99
Table 2.	Δ data for Eastern Siberia with sample IDs, formations, and approximate ages	100
Figure 8.	Compound specific isotopic data from the Amadeus Basin of the Centralian Superbasin in Australia	101
Table 3.	Δ data for the Amadeus Basin of the Centralian Superbasin in Australia with sample IDs, formations, and approximate ages	101
Figure 9.	Compound specific isotopic data from Oman with bulk δ_a and δ_o data from Fike et al., 2006	102

Figure 10.	Inorganic and organic carbon isotope signatures of the carbonate platform of the SOSB	104
Figure 11.	Depiction of the Phanerozoic ocean vs. the hypothesized Neoproterozoic ocean	107
Chapter 5	Neoproterozoic Rocks with Confounding Biomarker Signatures: Novel Environmental Signals or Contamination?	
Table 1.	Information on areas and strata studied including their collection type, age, lithology, depositional setting, total organic carbon (TOC), and fossils	122
Table 2.	Key age and maturity parameters	127
Figure 1.	C ₃₁ hopane distributions in saturate fractions of samples from St. Petersburg collected by GC-MS MRM	130
Figure 2.	GC-MS full scans of the saturate fractions of samples from China	131
Figure 3.	GC-MS full scan data for the saturate fractions of outcrop samples from Arkhangelsk	132
Figure 4.	GC-MS full scan data for the saturate fractions of outcrop samples from St. Petersburg	133
Figure 5.	GC-MS full scan data for the saturate fractions of samples from the Wonoka Formation	134
Figure 6.	GC-MS full scan data for the saturate fractions of samples from the Coppercap Formation	135
Appendix 1	Biomarker Trends in Neoproterozoic to Lower Cambrian Rocks from the Centralian Superbasin in Australia	
Figure 1.	Location of the Centralian Superbasin	142
Figure 2.	Stratigraphic columns of the eastern Officer Basin and the Amadeus Basin	143
Table 1.	Australian samples and their identities	145
Table 2.	Australian full scan data	147
Table 3.	Salinity indicators from GC-MS MRM analyses of Australian samples	148
Table 4.	Maturity indicators from GC-MS MRM analyses of Australian samples	149
Table 5.	Sponge and other source markers from GC-MS MRM analyses of Australian samples	149
Appendix 2	Biomarker Trends in Ediacaran Rocks from the White Sea Region of Russia	

1. Introduction

Abstract

The Neoproterozoic Era was a time of great change in Earth's surface environment and its biota. It is necessary to study this era, as it set the stage for the rapid diversification of multicellular life in the Cambrian. In order to understand these developments, we studied biomarkers of sedimentary rocks and oils from three areas of the world. This chapter provides a review of existing knowledge for the Neoproterozoic - Cambrian transition, how biomarker geochemistry can provide new insights and how we chose localities for sampling.

Introduction

Cambrian explosion.

The Cambrian explosion marks the initial appearance of taxonomically diverse multicellular life, beginning around 542 Ma. It is important to understand this episode because, from many lines of evidence, it represents a globally significant biogeochemical event (e.g., Cloud Jr., 1968; Derry et al., 1992; Canfield & Teske, 1996; Knoll & Carroll, 1999; Anbar & Knoll, 2002; Rothman et al., 2003; Porter, 2004; Fike et al., 2006; McFadden et al., 2008). In many sections around the world, the Neoproterozoic - Cambrian boundary is marked by a rapid increase in trace fossil diversity above Ediacaran-type fossils and below trilobites (Kaufman et al., 1991). Simple trace fossils occur below the boundary and the more complex ichnofossil *Treptichnus pedum* was used to guide the placement of the beginning of the Cambrian (Narbonne et al., 1987). At several localities the first appearance of small shelly fossils and/ or a strong, short-lived negative carbon isotopic excursion in carbonates also closely approximate the boundary (e.g., Magaritz et al., 1986; Lambert et al., 1987; Narbonne et al., 1994).

The environmental and biological triggers for this radiation are still unclear. Some argue that the concept of a rapid increase in diversity at this time is a preservational artifact (Darwin, 1859; Bromham et al, 1998). However, sequence stratigraphy, the Precambrian fossil record and molecular clock studies with which the fossil record is congruent

support the concept of a rapid radiation in the diversity of life (Knoll, 2003; Peterson et al., 2004).

Many contend that an increase in dioxygen levels was a driving force (e.g., Cloud Jr., 1968; Knoll & Carroll, 1999; Porter, 2004). This is supported by carbon and sulfur isotopic data (Derry et al., 1992; Canfield & Teske, 1996; Fike et al., 2006; McFadden et al., 2008) and by basic animal and algal physiology (Runnegar, 1991; Anbar & Knoll, 2002). Both animals and algae also have absolute requirements for molecular oxygen in order to biosynthesize sterols for their cell membranes (Bloch, 1983; Runnegar, 1991; Summons et al., 2006), though this requirement is low compared to that required by macroscopic bilaterian physiology. Sterols are synthesized almost exclusively by eukaryotes and are used to modify membrane rigidity and curvature and as signaling compounds (Bacia et al., 2005; Summons et al., 2006). These sterols, through the processes of diagenesis, become transformed into sterane hydrocarbons that are stable on geological time scales. Such steranes can be extracted from rocks and analyzed by conventional analytical techniques in order to trace aspects of animal evolution.

Other theories for the sudden diversification of life invoke environmental perturbation. These include tectonic factors, changes in ocean chemistry and changes in biogeochemical cycling (Rothman et al., 2003; Porter, 2004). The Neoproterozoic - Cambrian boundary coincided with enhanced tectonic activity, which led to changes in ocean circulation and nutrient levels, transgressions, and the formation of shallow seas. Though these conditions were not unique to the late Neoproterozoic, they likely contributed to the diversification of life at that time (Tucker, 1992).

Strong, short-lived negative carbon isotopic excursions in carbonates, analogous to the one near the Neoproterozoic - Cambrian boundary, can be caused by rapid decreases in biological productivity, and/ or increased oxidation of organic carbon (Lambert et al., 1987). Similar isotopic events in Earth's history are known to accompany widespread extinctions (Knoll & Carroll, 1999). The last appearance of the early calcareous fossils *Cloudina* and *Namacalathus* correlate with the isotopic excursion, so this faunal

transition has been hypothesized to be a mass extinction (e.g., Amthor et al., 2003). In rare cases, others have found an overlap in Ediacaran and small shelly fossils, conventionally considered to be of Cambrian age, and consider the evolutionary events to be continuous (Grotzinger et al., 1995). This leads to the hypothesis that the usually large gap seen in the fossil record may be more of a preservational feature than evidence of a mass extinction (Grotzinger et al., 1995). If there was an extinction event prior to the Cambrian - pre-Cambrian boundary, permissive ecology could also be used to explain the sudden diversification at this time. Permissive ecology is a concept Knoll (2003) employs to propose that “these intervals of rapid environmental change caused temporary breakdowns of the established ecosystems with their harsh competition for resources and thereby permitted the new experiments in life that ultimately led to our modern world,” (Narbonne, 2003).

Evolutionary innovations such as sexual reproduction, multicellularity and the acquisition of plastids have also been proposed as explanations for the ‘explosion’. However, all of these biological innovations have a complex genetic basis and must have their roots in evolutionary events that took place long before the rapid, visible radiation and thus were probably not a primary influence in the diversification (Porter, 2004). Predation is another innovation that has been proposed. The first mineralized skeletons have borings, suggestive of predation (Bengtson & Zhao, 1992). It is possible that skeletons arose as a response to predation, which also induced a variety of other changes, leading to the radiation (Bengtson & Zhao, 1992). Another development that possibly appeared near the boundary was the production of fecal pellets which package and ballast organic matter into fast-sinking particles. These would likely have increased the flux of organic matter to the ocean floor, thereby circumventing its remineralization and assisting burial. The oxidation of organic matter is one sink for oxygen. When this material is buried without being oxidized, the level of oxygen in the water column and thus in the atmosphere increases. This could have been one mechanism by which more oxygen became available in surface waters, thereby propagating the radiation of metazoan life (Logan et al., 1995), however macrozooplankton with fecal pellets big enough to sink likely did not evolve until around 520 Ma (Chen & Zhou, 1997; Vannier & Chen, 2000; Peterson et al., 2005).

Coincident with the animal radiation was increased diversity of acritarchs. Acritarchs are eukaryotic microfossils that have traditionally been considered to be the cysts of planktonic algae (Porter, 2004). More recently, some have also been proposed to be animal egg hulls (Van Waveren & Marcus, 1993; Yin et al., 2004; Knoll et al., 2006). If many are derived from algae, this would suggest that the impact of biogeochemical changes at this time affected disparate forms of life and therefore that ecology must have played some role (Knoll, 1994). It is probable that no single factor led to the diversification of life at the Neoproterozoic - Cambrian boundary, but a complex combination of intrinsic and extrinsic factors (Knoll & Carroll, 1999).

Biomarker importance.

Though the term biomarkers can refer to both those found in living organisms and those found in sediments, in this thesis biomarkers refers to molecular fossils, derived from biochemicals, mainly lipids. Lipid biomarkers can be preserved when morphological remains cannot, even when the precursor organisms have no hard parts. The structural and isotopic information lipid biomarkers provide can be diagnostic of specific taxa, biosynthetic pathways, physiology, depositional environments, thermal maturity and used to place broad constraints on geological age (Peters et al., 2005). A biomarker may be diagnostic of a particular biosynthetic pathway because it is the product of a specific physiology or requires certain chemicals or other factors such as light, dioxygen, reduced sulfur, anoxia, or others. For example, in a sedimentary rock extract the presence of isorenieratane, derived from the carotenoid isorenieratene, suggests that green sulfur bacteria, which require sulfide and light, were active when the sediment was deposited and thus that the ancient photic zone included a euxinic layer (Brocks & Summons, 2003).

Although the Cambrian explosion is mainly associated with the rapid diversification of metazoans, biomarkers that are proxies for bacteria or protists can provide information about the prevailing environment. Triterpenoids derived from bacteria can provide information complementary to that derived from molecules specific for animals. As described above, molecules useful for directly studying eukaryotes include steranes. As

many researchers have put forward the increase in dioxygen levels as an important factor in multicellular diversity, we decided to use biomarkers to explore the issues of the redox state and ventilation of the ocean.

Paleogeography.

A broad paleogeographic range must be studied in order to complete a global environmental reconstruction of this time period. There are, however, mandatory conditions that must be met when choosing where to sample. Not all areas of the world have well preserved Neoproterozoic sections, if they occur at all. Additionally, certain conditions are mandatory for the preservation of indigenous biomarkers, including low thermal alteration, a low degree of oxidation and careful collection and handling. Further, it is advantageous if the rock has high organic content since indigenous hydrocarbon abundances will then be vastly in excess of contaminants, improving ‘signal to noise’ measured on a mass spectrometer. Thus the areas of the Earth that are explored in this thesis are from Australia, Eastern Siberia and Oman. These regions were likely disparate enough at the time of the latest Proterozoic to give a sense of the global environment at that time (Figure 1).

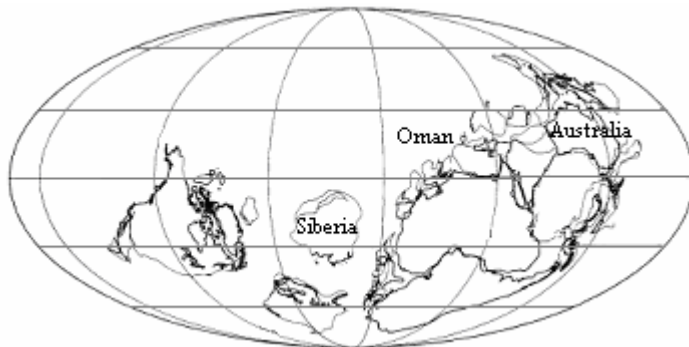


Figure 1. Paleogeographic relationship of the world in the Late Proterozoic modified from McKerrow et al., 1992.

Australian samples.

Samples from Australia have been collected from the Officer and Amadeus Basins, which, although now separate entities, were contiguous over the critical interval as the Centralian Superbasin (Walter et al., 1995; Logan et al., 1997). This area is of interest

because of the range of depositional environments represented and the unique fauna and acritarch assemblages observed in these sediments. For example, the Amadeus Basin of the Centralian Superbasin is home to the Pertatataka acritarch assemblage and body fossils of Ediacara fauna (Zang & Walter, 1989; Grey, 2005). In the Centralian Superbasin, both major Neoproterozoic snowball events are observed and detailed carbon, sulfur and strontium data have been collected and correlated worldwide (Walter et al., 1995; Walter et al., 2000).

Eastern Siberian samples.

The formations in Eastern Siberia range in age from the Riphean (650-1650 Ma), through the Vendian (570-650 Ma) and into the Early Cambrian. The biomarker work presented in this thesis suggests that all of the samples are from the late Cryogenian to Early Cambrian. The samples are all oils, primarily sourced by dolomites from a shallow water depositional setting. The biomarkers found follow very similar patterns to those extracted from Neoproterozoic rocks and oils of the South Oman Salt Basin.

South Oman Salt Basin samples.

Oman was chosen as an area of interest because the sediments are rich in organic matter, both major Neoproterozoic glaciations can be identified and because of the dating and carbon and sulfur isotope work being performed on these same samples in our lab or otherwise at MIT (Fike et al., 2006; Bowring et al., 2007).

Thesis outline

Chapter 2 presents the biomarkers extracted from Neoproterozoic oils from Eastern Siberia and the environmental interpretations that can be derived from that data. A brief overview of areas with C₂₉ steranes vs. C₂₇ steranes dominance and the environmental significance of this difference follow. Most likely the type of sterane dominance is due to the abundances of red vs. green algae, which may be ultimately determined by the redox of the deepwaters. **Chapter 3** presents the use and origins of novel biomarkers. A C₁₉ norsterane and 21-norsteranes have been found to be useful indicators of water column stratification. The C₁₉ norsterane is suggested to be an A-norsterane and is also viable as

an age marker for Neoproterozoic to Early Cambrian sedimentary rocks and oils. **Chapter 4** presents compound specific carbon isotopic data for *n*-alkanes and isoprenoids from Neoproterozoic samples of the South Oman Salt Basin, Eastern Siberia and Australia. The changes in their relative isotopic values are interpreted with regards to the ventilation of the global ocean. **Chapter 5** gives a thorough assessment of the possible contaminants faced when studying ancient rocks.

References

- Amthor, J. E.; Grotzinger, J. P.; Schröder, S.; Bowring, S. A.; Ramezani, J.; Martin, M. W.; Matter, A. **2003**. Extinction of *Cloudina* and *Namacalathus* at the Precambrian-Cambrian boundary in Oman. *Geology* **31**, 431-434.
- Anbar, A. D.; Knoll, A. H. **2002**. Proterozoic ocean chemistry and evolution: A bioinorganic bridge? *Science* **297**, 1137-1142.
- Bacia, K.; Schwille, P.; Kurzchalia, T. **2005**. Sterol structure determines the separation of phases and the curvature of the liquid-ordered phase in model membranes. *Proc. Natl. Acad. Sci. USA* **102**, 3272-3277.
- Bengtson, S.; Zhao, Y. **1992**. Predatorial borings in late Precambrian mineralized exoskeletons. *Science* **257**, 367-369.
- Bloch, K. **1983**. Sterol structure and membrane function. *CRC Crit. Rev. Biochem.* **14**, 47-92.
- Bowring, S. A.; Grotzinger, J. P.; Condon, D. J.; Ramezani, J.; Newall, M. J.; Allen, P. A. **2007**. Geochronologic constraints on the chronostratigraphic framework of the Neoproterozoic Huqf Supergroup, Sultanate of Oman. *Am. J. Sci.* **307**, 1097-1145.
- Brocks, J. J.; Summons, R. E. **2003** Sedimentary hydrocarbons, biomarkers for early life. In: *Treatise on Geochemistry* **8** (H. D. Holland and K. Turekian, eds.) Elsevier, 63-115.
- Bromham, L.; Rambaut, A.; Fortey, R.; Cooper, A.; Penny, D. **1998**. Testing the Cambrian explosion hypothesis by using a molecular dating technique. *Proc. Natl. Acad. Sci. USA* **95**, 12386-12389.
- Canfield, D. E.; Teske, A. **1996**. Late Proterozoic rise in atmospheric oxygen concentration inferred from phylogenetic and sulphur-isotope studies. *Nature* **382**, 127-132.
- Chen, J.; Zhou, G.-Q. **1997**. Biology of the Chenjiang fauna. In: The Cambrian Explosion and the fossil record. (J. Chen, Y. N. Cheng & H. V. Iten, eds.), Bulletin of the National Museum of Natural Science, Vol. 10, Taichung, pp. 11-105.
- Cloud, P. E. Jr. **1968**. Atmospheric and hydrospheric evolution on the primitive Earth. *Science* **160**, 729-736.
- Darwin, C. **1859**. On the Origin of Species by Means of Natural Selection: London, J. Murray.
- Derry, L. A.; Kaufman, A. J.; Jacobsen, S. B. **1992**. Sedimentary cycling and environmental change in the Late Proterozoic: Evidence from stable and

- radiogenic isotopes. *Geochim. et Cosmochim. Acta* **56**, 1317-1329.
- Fike, D. A.; Grotzinger, J. P.; Pratt, L. M.; Summons, R. E. **2006**. Oxidation of the Ediacaran Ocean. *Nature* **444**, 744-747.
- Grey, K. **2005**. In: Ediacaran Palynology of Australia. Mem. 31 (Laurie, J. R., ed.) Association of the Australasian Palaeontologists, Canberra.
- Grotzinger, J. P.; Bowring, S. A.; Saylor, B. Z.; Kaufman, A. J. **1995**. Biostratigraphic and geochronologic constraints on early animal evolution. *Science* **270**, 598-604.
- Kaufman, A. J.; Hayes, J. M.; Knoll, A. H.; Germs, G. J. B. **1991**. Isotopic compositions of carbonates and organic carbon from upper Proterozoic successions in Namibia: stratigraphic variation and the effects of diagenesis and metamorphism. *Precambrian Res.* **49**, 301-327.
- Knoll, A. H. **1994**. Proterozoic and Early Cambrian protists: Evidence for accelerating evolutionary tempo. *Proc. Natl. Acad. USA* **91**, 6743-6750.
- Knoll, A. H. **2003**. Life on a Young Planet: The First Three Billion Years of Evolution on Earth. Princeton University Press, Princeton, NJ.
- Knoll, A. H.; Carroll, S. B. **1999**. Early animal evolution: Emerging views from comparative biology and geology. *Science* **284**, 2129-2137.
- Knoll, A. H.; Javaux, E. J.; Hewitt, D.; Cohen, P. **2006**. Eukaryotic organisms in Proterozoic oceans. *Phil. Trans. R. Soc. B* **361**, 1023-1038.
- Lambert, I. B.; Walter, M. R.; Wenlong, Z.; Songnian, L.; Guogan, M. **1987**. Palaeoenvironment and carbon isotope stratigraphy of Upper Proterozoic carbonates of the Yangtze Platform. *Nature* **325**, 140-142.
- Logan, G. A.; Hayes, J. M.; Hieshima, G. B.; Summons, R. E. **1995**. Terminal Proterozoic reorganization of biogeochemical cycles. *Nature* **376**, 53-56.
- Logan, G. A.; Summons, R. E.; Hayes, J. M. **1997**. An isotopic biogeochemical study of Neoproterozoic and Early Cambrian sediments from the Centralian Superbasin, Australia. *Geochim. Cosmochim. Acta* **61**, 5391-5409.
- Magaritz, M.; Holser, W. T.; Kirschvink, J. L. **1986**. Carbon-isotope events across the Precambrian/Cambrian boundary on the Siberian Platform. *Nature* **320**, 258-259.
- McFadden, K. A.; Huang, J.; Chu, X.; Jiang, G.; Kaufman, A. J.; Zhou, C.; Yuan, X.; Xiao, S. **2008**. Pulsed oxidation and biological evolution in the Ediacaran Doushantuo Formation. *Proc. Natl. Acad. USA* **105**, 3197-3202.
- McKerrow, W. S.; Scotese, C. R.; Brasier, M. D. **1992**. Early Cambrian continental reconstructions. *J. Geol. Soc.* **149**, 599-606.
- Narbonne, G. M. **2003**. The crucial 80 % of life's epic. *Science* **301**, 919.
- Narbonne, G. M.; Myrow, P. M.; Landing, E.; Anderson, M. M. **1987**. A candidate stratotype for the Precambrian-Cambrian boundary, Fortune Head, Burin Peninsula, southeastern Newfoundland. *Can. J. Earth Sci.* **24**, 1277-1293.
- Narbonne, G. M.; Kaufman, A. J.; Knoll, A. H. **1994**. Integrated chemostratigraphy and biostratigraphy of the Windermere Supergroup, northwestern Canada: Implications for Neoproterozoic correlations and the early evolution of animals. *Geol. Soc. Amer. Bull.* **106**, 1281-1292.
- Peters, K. E.; Walters, C. C.; Moldowan, J. M., eds. **2005**. The Biomarker Guide, second edition. Cambridge University Press.
- Peterson, K. J.; Lyons, J. B.; Nowak, K. S.; Takacs, C. M.; Wargo, M. J.; McPeck, M. A. **2004**. Estimating metazoan divergence times with a molecular clock. *Proc. Natl.*

- Acad. USA* **101**, 6536-6541.
- Peterson, K. J.; McPeck, M. A.; Evans, D. A. D. **2005**. Tempo and mode of early animal evolution: inferences from rocks, Hox, and molecular clocks. *Paleobiology* **31**, 36-55.
- Porter, S. H. **2004**. The fossil record of early eukaryotic diversification. *Paleontological Society Papers* **10**, 35-50.
- Rothman, D. H.; Hayes, J. M.; Summons, R. E. **2003**. Dynamics of the Neoproterozoic carbon cycle. *Proc. Natl. Acad. USA* **100**, 8124-8129.
- Runnegar, B. **1991**. Precambrian oxygen levels estimated from the biochemistry and physiology of early eukaryotes. *Palaeogeogr. palaeoclimatol. palaeoecol.* **97**, 97-111.
- Summons, R. E.; Bradley, A. S.; Jahnke, L. J.; Waldbauer, J. R. **2006**. Steroids, triterpenoids and molecular oxygen. *Phil. Trans. R. Soc. B* **361**, 951-968.
- Tucker, M. E. **1992**. The Precambrian-Cambrian boundary: seawater chemistry, ocean circulation and nutrient supply in metazoan evolution, extinction and biomineralization. *J. Geol. Soc., London* **149**, 655-668.
- Van Waveren, I.; Marcus, N. **1993**. Morphology of recent copepod egg-envelopes from Turkey Point (Gulf of Mexico) and their implications for acritarch affinity. *Spec. Pap. Palaeontol.* **48**, 111-124.
- Vannier, J.; Chen, J.-Y. **2000**. The Early Cambrian colonization of pelagic niches exemplified by *Isoxys* (Arthropoda). *Lethaia* **33**, 295-311.
- Walter, M. R.; Veevers, J. J.; Calver, C. R.; Grey, K. **1995**. Neoproterozoic stratigraphy of the Centralian Superbasin, Australia. *Precambrian Res.* **73**, 173-195.
- Walter, M. R.; Veevers, J. J.; Calver, C. R.; Gorjan, P.; Hill, A. C. **2000**. Dating the 840-544 Ma Neoproterozoic interval by isotopes of strontium, carbon, and sulfur in seawater, and some interpretative models. *Precambrian Res.* **100**, 371-433.
- Yin, C. Y.; Bengtson, S.; Yue, Z. **2004**. Silicified and phosphatized *Tianzhushania*, spheroidal microfossils of possible animal origin from the Neoproterozoic of South China. *Acta Palaeontol. Polonica* **49**, 1-12.
- Zang, W. L.; Walter, M. R. **1989**. Latest Proterozoic plankton from the Amadeus Basin in central Australia. *Nature* **337**, 642-645.

2. Biomarker Trends in Neoproterozoic to Lower Cambrian Oils from Eastern Siberia

Abstract

The Neoproterozoic Era is of widespread geobiological interest because it marks the first appearance of animals in the fossil record. Much Neoproterozoic research has been focused on the ventilation of the global ocean, as this is considered a primary factor in the diversification of complex, multicellular life. Neoproterozoic to Cambrian aged oils from Eastern Siberia were analyzed for their hydrocarbon biomarker contents in order to further our understanding of the prevailing environment and its microbial and metazoan communities. Sterane patterns from these oils are compared to those of Neoproterozoic sections in Oman to help reconstruct ecological relationships. Eastern Siberian oils and Oman Huqf oils are, overall, very similar. Although age constraints on the Siberian section are poor, the Huqf and Siberian petroleum source rocks appear to be broadly coeval. The abundance of sponge biomarkers in these samples allow us to better constrain the ages of the Siberian section. The predominance in these and other Neoproterozoic sediments of C₂₉ or C₂₇ steranes seems to be influenced by redox of deep waters that likely determined whether green or red algae dominated the local ecosystem, respectively. This yields another potential proxy with which to understand ancient deep water redox.

Introduction

The Neoproterozoic Era was a time of great change in Earth's surface environment and its biota. It is proposed that there were two episodes when the Earth was entirely covered with ice, known as snowball Earth episodes: the Sturtian episode around 710 Ma and the Marinoan episode around 635 Ma (Hoffmann et al., 2004). There was also a more regional, short-term event referred to as the Gaskiers glaciation that occurred around 580 Ma (Bowring et al., 2003). The ocean was in transition from having a deep anoxic water column with oxygenated surface waters to one with a fully ventilated water column (e.g., Lambert et al., 1987; Des Marais et al., 1992; Knoll & Carroll, 1999; Porter, 2004; Cloud Jr., 1968; Derry et al., 1992; Canfield & Teske, 1996; Anbar & Knoll, 2002; Fike et al., 2006; McFadden et al., 2008). Toward the end of the Neoproterozoic Era we observe the

first metazoan body-fossils; this is followed by the rapid diversification of modern animal phyla during the Cambrian Period. Many forms of geological and geochemical evidence illuminate unprecedented and globally significant biogeochemical changes taking place during this entire interval (e.g., Knoll & Carroll, 1999; Porter, 2004; Cloud Jr., 1968; Derry et al., 1992; Canfield & Teske, 1996; Anbar & Knoll, 2002; Rothman et al., 2003; Fike et al., 2006; McFadden et al., 2008). The spatial and temporal patterns as well as the trigger for these profound environmental changes, however, remain unclear and subject to intense debate. The goal of this research is to use lipid biomarker proxies for microbial and metazoan communities in order to gain further insight into biological and redox processes taking place in the marine water column during these times of transition.

We chose to study Eastern Siberian oils because Eastern Siberia is one of the few places in the world where Neoproterozoic sediments that have not been through extensive maturation and where high abundances of organic carbon and bitumen can be found in sediments (Hayes et al., 1992). Eastern Siberia is also host to numerous Neoproterozoic oils fields. Six petroleum samples were taken from the Baykit Basin of the Baykit High region, four from the Katanga Basin within the Cis-Sayan Basin, and fifteen from the Nepa-Botuoba Basin of the Nepa-Botuoba High region (Figure 1).

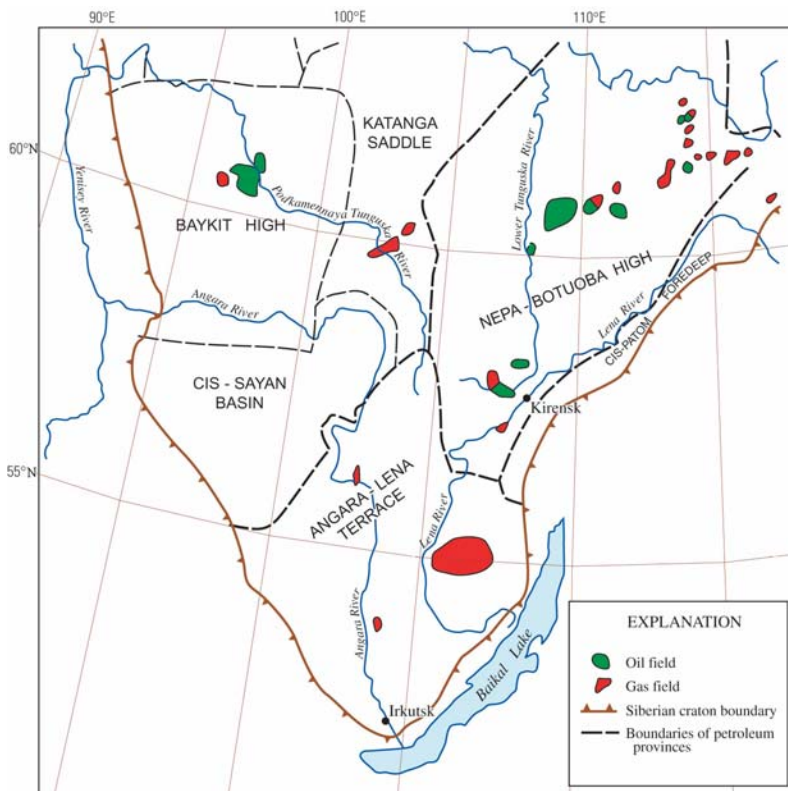


Figure 1. Map of the sites from which the Eastern Siberian oil samples were taken, adapted from Ulmishek, 2001a. Samples from the Baykit Basin are from the Baykit High region, from the Katanga Basin are from within the Cis-Sayan Basin, and from the Nepa-Botuoba Basin are from the Nepa-Botuoba High region.

Experimental Prodecures

Sampling.

Samples were selected from an oil collection provided by John Zumberge of Geomark Research, Houston, Texas. Being oils, the samples from Eastern Siberia are of uncertain stratigraphic placement within each formation. Sample information is given in Table 1.

Sample	Basin	Group	Age	Lithology	Dep. Env.	Key References
ES 001	Baykit	Kamov	Riphean	dolomite with minor sandstone, shale, mudstone and marl	marine to shallow marine	IHS charts
ES 005						
ES 010						
ES 015						
ES 018						
ES 020						
ES 022	Katanga	Vanavara	Vendian	shale, dolomite and sandstone	shallow marine	Ulmishek, 2001b; IHS charts
ES 024						
ES 026						
ES 030	Nepa-Botuoba	Kursoy	Vendian	siltstone and sandstone		Sokolov & Fedonkin, 1990
ES 035	Katanga	Vanavara	Vendian			
ES 036	Nepa-Botuoba	Nepa	Vendian	siltstone and sandstone	continental depositional setting	IHS charts
ES 040						
ES 043		Parshino	Vendian			
ES 048		Byuk	Vendian	dolomite, dolomitic marl and anhydrite		Sokolov & Fedonkin, 1990
ES 053						
ES 057		Katanga	Vendian	dolomite, clayey dolomite and dolomitic marl	shallow marine to restricted	Ulmishek, 2001b; IHS charts
ES 064		Tetere	Vendian-Cambrian	dolomite	shallow marine to restricted	Ulmishek, 2001b; IHS charts
ES 066						
ES 068		Usol'ye	Lower Cambrian	salt and dolomite	shallow marine to restricted	Ulmishek, 2001b; IHS charts
ES 080						
ES 083						
ES 087						
ES 089						
ES 091	Bilir	Lower Cambrian				

Table 1. The provenance, age, lithology, and depositional environment of the Eastern Siberian oil samples.

General Procedure.

Organic free solvents from OmniSolv were used. Prior to use, all glassware and aluminum foil were fired at 550°C for 8h and glass wool; pipettes and silica gel were fired at 450°C for 8h.

Each sample was separated by liquid chromatography on a silica gel 60 (Merck, 230-400 mesh) column using hexane to elute the saturate fraction, 4:1 hexane/dichloromethane to

elute the aromatic fraction, and 7:3 dichloromethane/ methanol to elute the polar fraction. Activated Cu was added to the saturate fraction to remove elemental sulfur. One milligram aliquots of the saturate and aromatic fractions were then reduced to 0.1 mL and added to insert vials with an internal standard. The saturate fraction was run on the Autospec with the following standards: 50 ng D4 (D₄- $\alpha\alpha\alpha$ -ethylcholestane, Chiron) or 50 ng D4 (D₄- $\alpha\alpha\alpha$ -ethylcholestane, Chiron) + 1 μ g *aiC*₂₂ (3-methylheneicosane, ULTRA Scientific). The aromatic fraction was run with 100 ng of D14 standard (d₁₄ p-terphenyl, Cambridge Isotope Laboratories).

Gas Chromatography-Mass Spectrometry (GC-MS) was performed using a Micromass Autospec-Ultima instrument equipped with an Agilent 6890N Series gas chromatograph. For analysis of the saturated hydrocarbons, a 60 m J&W Scientific DB-1 fused silica capillary column (0.25 mm i.d., 0.25 μ m film thickness) was used with helium as carrier gas. Injection was performed at 60°C in splitless mode and, after a delay of 2 min the oven was programmed from 60°C to 150°C at 10°C/min, then to 315°C at 3°C/min where it was held isothermal for 24 min. The source was operated in EI-mode at 70 eV ionization energy. For full scan analyses the scan rate was 0.80 s/decade over a mass range of 50 to 600 m/z with a total cycle time of 1.06 s. Data were acquired and processed using MassLynx v4.0 software. Biomarkers in the saturated hydrocarbon fraction were analyzed by GC-MS with the Autospec operated in the metastable reaction monitoring (MRM) mode under the same GC conditions as described for the full scan experiments. Peak identification was based on retention time comparisons with the hydrocarbons present in a synthetic standard oil (AGSO Standard Oil) and abundances measured by comparing peak areas to the internal D₄ sterane standard without any adjustment for possible differential responses.

Aromatics were analysed using a DB-5MS column in selected ion monitoring (SIM) mode. The source was operated in EI+ mode at 250°C with 70 eV ionization energy and 8000 V acceleration voltage. The injection method was the same as for the saturates.

Principal components analysis and hierarchical cluster analysis were conducted using the Pirouette software (Infometrix Corporation).

Results and Discussion

The biomarker data are subdivided into four categories: redox and possible stratification and hypersalinity indicators (Table 2), maturity indicators (Table 3), possible sponge biomarkers (Table 4), and other source biomarkers (Table 5). The sterane and hopane distributions for a typical Eastern Siberian oil sample are shown in Figures 2 and 3.

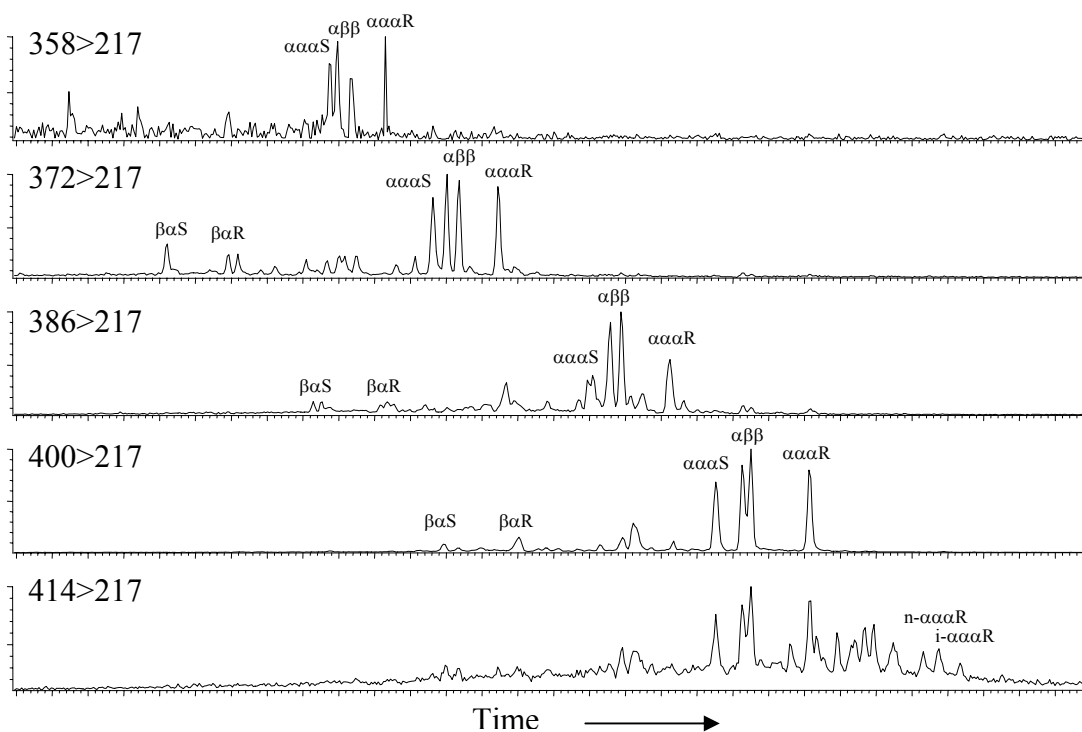


Figure 2. A selection of GC-MS MRM chromatograms showing relative abundances of steranes in an Eastern Siberian oil from the Usol'ye Formation from the Nepa-Botuoba Basin, ES 083.

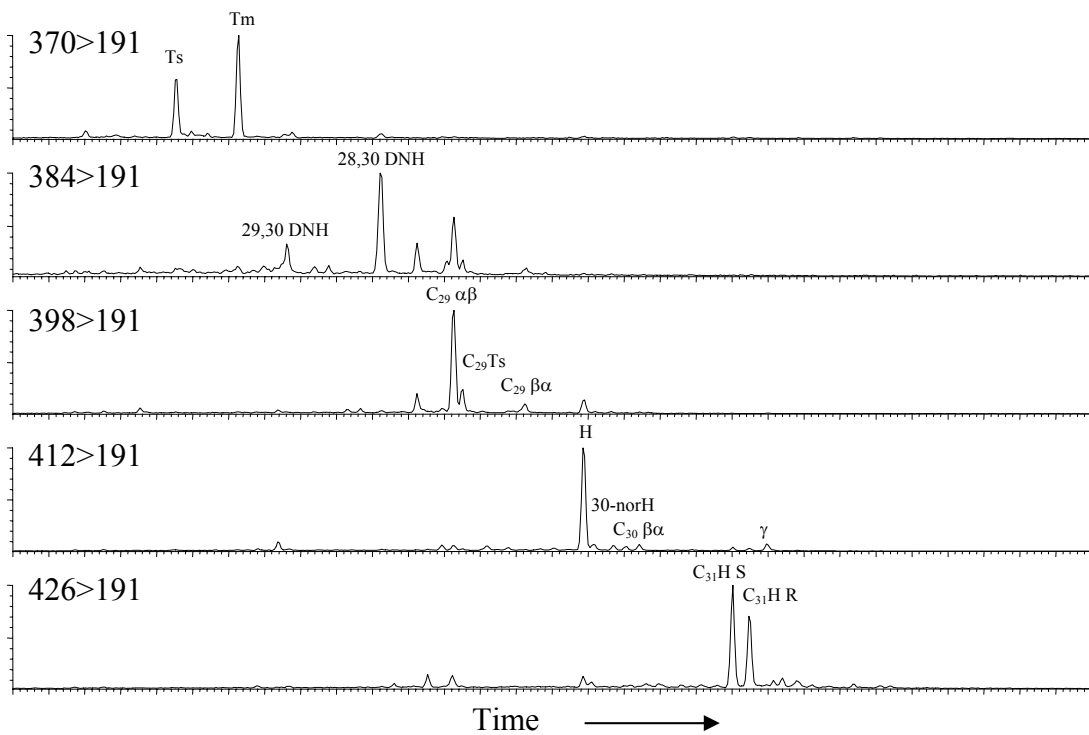


Figure 3. A selection of GC-MS MRM chromatograms showing relative abundances of hopanes in an Eastern Siberian oil from the Usol'ye Formation from the Nepa-Botuoba Basin, ES 083.

Redox and Possible Stratification and Hypersalinity Indicators									
	Pr/ Ph	HomoH Index %	γ / C ₃₀ H	R ₂₂ index	21-norchol/ 27-norchol	21-norC ₂₈ St/ C ₂₈ $\alpha\beta\beta$ R	21-norC ₂₈ St/ C ₂₈ Sts	C/ A+B	C/ A
ES 001	0.94	0.08	0.09	0.80	0.05	0.39	0.08	0.11	0.71
ES 005	1.06	0.10	0.09	1.02	0.06	0.38	0.08	0.09	0.60
ES 010	0.89	0.09	0.10	0.82	0.08	0.23	0.05	0.12	0.77
ES 015	1.26	0.10	0.10	0.98	0.08	0.43	0.10	0.10	0.59
ES 018	1.01	0.09	0.11	0.99	0.09	0.33	0.08	0.13	0.80
ES 020	1.14	0.08	0.07	0.91	0.09	0.25	0.05	0.12	0.85
ES 022	0.75	0.10	0.11	0.99	0.10	0.45	0.11	0.14	0.74
ES 024	0.79	0.10	0.10	0.99	0.07	0.29	0.07	0.15	0.77
ES 026	0.77	0.07	0.08	0.97	0.04	0.23	0.06	0.13	0.75
ES 030	0.83	0.11	0.13	1.00	0.05	0.30	0.07	0.15	0.75
ES 035	0.76	0.09	0.08	0.98	0.08	0.24	0.06	0.12	0.91
ES 036	0.72	0.09	0.09	0.93	0.06	0.50	0.10	0.10	0.58
ES 040	0.68	0.10	0.07	0.98	0.04	0.31	0.08	0.19	1.06
ES 043	0.77	0.09	0.09	0.96	0.04	0.33	0.09	0.11	0.67
ES 048	0.66	0.12	0.07	1.05	0.05	0.21	0.05	0.09	0.55
ES 053	0.85	0.12	0.08	0.95	0.04	0.32	0.07	0.08	0.48
ES 057	0.74	0.08	0.07	0.97	0.04	0.23	0.06	0.20	1.45
ES 064	0.69	0.10	0.07	1.05	0.05	0.21	0.06	0.18	0.98
ES 066	0.67	0.09	0.09	1.03	0.06	0.37	0.10	0.11	0.72
ES 068	0.72	0.11	0.07	0.98	0.04	0.23	0.06	0.13	0.98
ES 080	0.74	0.06	0.11	0.94	0.06	0.35	0.09	0.07	0.45
ES 083	0.75	0.10	0.07	0.98	0.04	0.22	0.05	0.12	0.82
ES 087	0.63	0.10	0.07	0.98	0.05	0.24	0.06	0.21	1.38
ES 089	0.64	0.10	0.08	1.00	0.06	0.31	0.08	0.12	0.77
ES 091	0.76	0.10	0.07	1.03	0.03	0.34	0.08	0.12	0.78

Table 2. Redox and possible stratification and hypersalinity indicators showing differences in the depositional environment of the Kamov Group samples (ES 001 - ES 020) compared to the younger samples (ES 022 – ES 091). None of the samples appear to have been deposited in a stratified environment and the Kamov samples were likely deposited in a more oxidized environment than the younger samples. H denotes hopane, γ gammacerane, and St for sterane. The homohopane index is calculated as C₃₅H (R+S) *100/ C₃₁-C₃₅H (R+S) %. The R₂₂ index is $2 * n\text{-C}_{22} / (n\text{-C}_{21} + n\text{-C}_{23})$.

The pristane (Pr)/ phytane (Ph) ratio provides information on the redox conditions under which sediments were deposited (Powell & McKirdy, 1973; Didyk et al., 1978; ten Haven et al., 1987; Peters et al., 2005). However, as with all geochemical proxies, there needs to be caution in using one parameter in isolation. Pristane and phytane are both formed during the diagenesis of chlorophyll. When oxygen is present, pristane can be formed from phytol through a sequence of oxidation and decarboxylation reactions. When the depositional environment is anoxic, reductive processes prevail and phytane is the predominant product. Empirical evidence suggests that a Pr/ Ph value <0.8 is diagnostic for an anoxic environment as commonly encountered in strongly stratified

water columns. On the other hand, Pr/ Ph >1 suggests more oxygenated environments, while Pr/ Ph >3 is generally observed in terrestrial settings where organic matter is transported and sedimented in oxygenated water bodies (Peters et al., 2005). Further, Pr/ Ph ratios that are <1 are most commonly observed in marine carbonates while values in the range of 2-4 for are common in deltaic shales. Intermediate values are common in clastic marine settings. As shown in Table 2 and Figure 4a, the Pr/ Ph values are around 1 for the Kamov Group oils and significantly lower, between 0.6 and 0.85, for the younger samples. This indicates that the samples are all marine, and that the depositional environment of the Kamov Group samples was more oxidizing than that of the other samples, which may have been deposited in more restricted environments.

The two most widely used ‘salinity’ indicators are the C₃₅ homohopane index, measured as C₃₅H (R+S) *100/ C₃₁-C₃₅H (R+S) %, and gammacerane to hopane ratio. Both are more accurately indicators of stratification that can occur due to redox, temperature or salinity stratification (Peters et al., 2005). Gammacerane is formed through the dehydration and reduction of tetrahymanol (ten Haven et al., 1989; Harvey & McManus, 1991), which is synthesized by bacterivorous ciliates that prefer stratified zones of the water column (Harvey & McManus, 1991; Sinninghe Damsté et al., 1995). The values for the homohopane index are all around 0.1% and the gammacerane to hopane values are all around 0.1. The R₂₂ index is $2 * n\text{-C}_{22} / (n\text{-C}_{21} + n\text{-C}_{23})$ and is considered by some to be a salinity marker; a value greater than 1.5 is typical for hypersaline environments (ten Haven et al., 1988). This index is similar throughout all of the oils with values around 1. Use of 21-norsteranes and compound C as indicators of water column stratification is discussed in Chapter 3. As with the other stratification indicators, there is not much change in any of these indicators. There is a significant difference in the range of abundances of compound B, however, with the younger samples having a wider range (Figure 4b). As a whole these indicators suggest that none of the oils were deposited in stratified or hypersaline environments.

Maturity Indicators							
	Ts/ (Ts+Tm)	C ₃₁ H 22S/ S+R	C ₂₉ ααα St S/ (S+R)	C ₃₀ H/ M	Ts/ H	Ph/ n-C ₁₈	OEP
ES 001	0.52	0.66	0.54	20.88	0.38	0.24	0.98
ES 005	0.58	0.59	0.51	20.31	0.38	0.20	0.99
ES 010	0.51	0.59	0.54	20.62	0.41	0.22	0.96
ES 015	0.63	0.59	0.54	20.45	0.51	0.14	0.96
ES 018	0.63	0.65	0.58	21.11	0.49	0.18	0.99
ES 020	0.52	0.51	0.51	11.41	0.36	0.19	0.97
ES 022	0.58	0.52	0.55	11.97	0.48	0.51	0.99
ES 024	0.43	0.52	0.54	12.40	0.32	0.86	0.99
ES 026	0.43	0.52	0.54	12.36	0.35	1.11	0.97
ES 030	0.38	0.58	0.52	12.40	0.32	1.08	0.98
ES 035	0.42	0.51	0.53	16.48	0.23	0.95	0.93
ES 036	0.67	0.57	0.54	15.58	0.64	0.95	1.05
ES 040	0.41	0.52	0.52	14.80	0.31	1.38	0.95
ES 043	0.37	0.58	0.53	14.77	0.34	1.22	0.96
ES 048	0.38	0.60	0.54	20.65	0.25	1.38	1.00
ES 053	0.45	0.60	0.55	23.24	0.23	1.05	0.98
ES 057	0.40	0.59	0.52	18.94	0.29	1.43	1.00
ES 064	0.57	0.56	0.51	19.30	0.50	1.56	1.02
ES 066	0.56	0.59	0.56	20.41	0.67	1.24	1.02
ES 068	0.40	0.59	0.54	20.17	0.29	1.35	0.40
ES 080	0.72	0.53	0.57	22.72	1.11	1.23	0.37
ES 083	0.37	0.57	0.53	17.21	0.26	1.39	0.39
ES 087	0.43	0.59	0.52	17.74	0.31	1.64	0.41
ES 089	0.48	0.54	0.57	19.46	0.34	1.38	0.40
ES 091	0.39	0.58	0.52	18.63	0.28	1.31	0.36

Table 3. Maturity indicators suggesting that all of the oils are of moderate thermal maturity, with the older samples being slightly more mature, and that ES 080 has an anomalous abundance of Ts. H denotes hopane, M moretane and St for sterane. The OEP is measured as $(n-C_{25} + 6 * n-C_{27} + n-C_{29}) / (4 * n-C_{26} + 4 * n-C_{28})$.

Ts/ (Ts+Tm) values are commonly used to evaluate thermal maturity, with higher values indicating higher maturities (Seifert & Moldowan, 1978). However, there is a strong facies control on this ratio, so it is most reliable when compared among samples of similar lithology. As shown in Table 3 the values vary from around 0.4 to 0.7. The αβ-homohopane 22S/ 22S + 22R and C₂₉ ααα sterane 20S/ 20S + 20R ratios are also used to assess thermal maturity. Values at or near 0.55 indicate oil-mature samples (Seifert & Moldowan, 1986), as do high C₃₀ hopane/ moretane ratios (Seifert & Moldowan, 1980). The homohopane S/ S+R values are all above 0.55 and the sterane S/ S+R values are all between 0.5 and 0.6, suggesting moderate thermal maturity. The hopane to moretane ratios are all around 20 with the exception of samples 020 to 043, which are between 10

and 16. All of these values suggest moderate maturity, with the samples with lower values having slightly lower thermal maturity. For post-mature samples, Ts/ H can be used as a maturity marker (Volkman et al., 1983). The samples all have values between 0.2 and 0.7, except for sample 080 which also has the highest Ts/ (Ts+Tm) value. The phytane/ *n*-C₁₈ ratio can be used as a maturity marker (ten Haven et al., 1987). Values >>1 suggest a sample is immature. It is also often used as an indicator for biodegradation. Within a family of oils, slightly to moderately biodegraded oils have higher phytane/ *n*-C₁₈ ratios (Peters et al., 2005). The Kamov Group oils have values around 0.2, whereas most of the other samples have values greater than 1. Samples ES 022 and ES 024 fall in between. This may suggest that the older samples are slightly more mature. OEP is the odd over even carbon number preference and is measured by $(n\text{-}C_{25} + 6 * n\text{-}C_{27} + n\text{-}C_{29}) / (4 * n\text{-}C_{26} + 4 * n\text{-}C_{28})$. Values around 1 suggest that the bitumen is thermally mature (Scalan & Smith, 1970). Most of the oils have OEPs around 1, however samples ES 068 - ES 091 have much lower values, around 0.4, suggesting they are slightly less mature. Together these indicators suggest that the samples are all of moderate thermal maturity, with the older samples being slightly more mature than the younger samples, and that ES 080 has an anomalous abundance of Ts.

Possible Sponge Biomarkers			
	i-C ₃₀ / n-C ₃₀	i-C ₃₀ αααR/ n-C ₃₀ αααR	27-norSts/ C ₂₇ Sts
ES 001	3.03	1.81	0.30
ES 005	2.52	2.20	0.28
ES 010	4.02	1.70	0.29
ES 015	1.73	0.96	0.23
ES 018	2.37	1.15	0.26
ES 020	0.74	0.32	0.14
ES 022	1.75	1.91	0.27
ES 024	2.78	1.20	0.24
ES 026	2.28	1.21	0.37
ES 030	2.95	1.76	0.26
ES 035	2.76	1.27	0.25
ES 036	1.12	0.52	0.31
ES 040	2.43	1.38	0.30
ES 043	2.09	1.75	0.35
ES 048	2.32	1.77	0.26
ES 053	2.26	1.63	0.27
ES 057	2.81	1.24	0.30
ES 064	1.95	0.99	0.30
ES 066	1.91	1.36	0.35
ES 068	2.10	1.24	0.26
ES 080	1.43	0.51	0.32
ES 083	2.22	1.03	0.24
ES 087	1.97	1.09	0.26
ES 089	2.20	1.32	0.29
ES 091	2.01	1.41	0.31

Table 4. Possible sponge indicators suggesting that demosponges were prevalent in the ancient depositional environment for all of the oils, but with samples 020, 036 and 080 as outliers. St denotes sterane. The *i*-C₃₀ and *n*-C₃₀ refer to iso- and *n*-propylcholestanes, respectively.

The ratio of 24-isopropylcholestanes to 24-*n*-propylcholestanes is useful as an indicator of demosponges and as an age marker since it is only high in the Neoproterozoic to Ordovician (McCaffrey et al., 1994; Love et al., 2009). The *n*-propyl isomers likely originated from a marine algal source while the isopropyl isomers are hypothesized to be derived from demosponge input. Sponges, being the most basal metazoan clade, likely evolved in the Neoproterozoic and had comparatively lower abundances through the Phanerozoic (McCaffrey et al., 1994; Sperling et al., 2007; Love et al., 2009). Almost all of the Eastern Siberian oil samples have values well above 1 for both isopropylcholestanes/ *n*-propylcholestanes ratios, suggesting the presence of demosponges in the ancient depositional environment for all of the oils. Abnormally low

values are found in samples 020, 036 and 080. Another possible indicator of demosponges biomass contributions to sediments is a high abundance of 27-norcholestanes relative to cholestanes (Kelly et al., 2007). The values here are all between 0.2 and 0.4 suggesting that if certain demosponges do give rise to a high abundance of 27-norcholestanes, they were not prevalent in the environment here. Altogether, these ratios suggest that demosponges were prevalent in the ancient depositional environment for all of the oils.

Other Source Biomarkers								
	Sts/ Hs	2 α MeHI%	3 β MeHI%	28,30 BNH/ C30 H	C ₂₇ Sts/ C ₂₉ Sts	<i>n</i> -C ₂₂ / x-C ₂₂	<i>n</i> -C ₂₄ / x-C ₂₄	x-C ₂₀ / Ph
ES 001	0.61	6.55	3.59	0.18	0.20	2.66	2.68	0.90
ES 005	0.67	8.30	4.64	0.17	0.16	3.33	2.79	1.10
ES 010	0.63	8.78	5.50	0.18	0.17	3.08	3.10	0.96
ES 015	0.72	8.47	5.58	0.17	0.21	3.71	2.66	1.31
ES 018	0.73	6.10	4.33	0.18	0.19	3.89	3.35	0.95
ES 020	0.85	8.44	5.22	0.17	0.33	2.99	3.17	0.96
ES 022	0.47	12.69	8.60	0.14	0.15	2.44	2.40	0.44
ES 024	0.64	11.01	5.39	0.24	0.17	1.47	1.25	0.42
ES 026	0.86	11.09	5.57	0.42	0.16	1.26	1.14	0.40
ES 030	0.86	10.47	6.34	0.32	0.17	1.96	2.59	0.32
ES 035	0.61	9.13	4.30	0.13	0.15	1.51	1.32	0.49
ES 036	2.23	8.42	5.46	0.42	0.18	1.20	1.18	0.53
ES 040	1.26	10.73	4.77	0.39	0.18	1.31	1.25	0.25
ES 043	1.20	11.31	4.95	0.37	0.16	1.28	1.19	0.37
ES 048	0.82	6.67	4.22	0.15	0.20	1.34	0.79	0.35
ES 053	0.79	8.25	4.27	0.12	0.19	1.71	1.63	0.30
ES 057	1.10	8.33	3.83	0.30	0.18	1.23	1.22	0.30
ES 064	1.77	8.77	3.48	0.55	0.20	1.35	1.21	0.28
ES 066	2.59	10.39	4.61	0.52	0.24	1.45	1.54	0.29
ES 068	1.01	8.61	3.94	0.30	0.19	1.30	1.25	0.31
ES 080	4.63	8.74	5.43	0.41	0.30	1.36	1.92	0.26
ES 083	1.00	8.54	3.78	0.25	0.22	1.36	1.53	0.23
ES 087	1.10	8.36	3.89	0.30	0.19	1.16	1.15	0.29
ES 089	1.34	10.15	4.89	0.28	0.18	1.38	1.28	0.35
ES 091	1.03	9.39	4.04	0.34	0.17	1.25	1.05	0.41

Table 5. A selection of source indicators showing differences in the depositional environment of the Kamov Group samples (ES 001 - ES 020) compared to the younger samples (ES 022 – ES 091). The steranes/ hopanes ratios suggest that eukaryotic input increased through time in this area. The 2- and 3-methylhopane indices suggest a small but steady input from both cyanobacteria and methanotrophic proteobacteria, respectively. The 28,30-bisnorhopane to hopane ratios suggest that the Kamov Group oils were deposited in a more oxic depositional environment than the younger oils. The C₂₇/ C₂₉ steranes ratios suggest a predominance of green algae in all of these samples. The ratios of *n*-alkanes to X-peaks suggest that there was an abundance of sponges or colorless sulfide oxidizing bacteria, especially in the samples younger than the Kamov Group. The x-C₂₀/ phytane signals appear to be dominated by the lack of abundance of phytane in the Kamov Group with respect to the younger oils. H denotes hopane and St for sterane.

The ratio of steranes/ hopanes is primarily used as an indicator of input from eukaryotes relative to bacteria (Moldowan et al., 1985). The values for samples ES 001 through ES 035 are all below 1 whereas those between ES 057 and ES 091 are all greater than 1. The samples between ES 035 and ES 057 vary in this respect. This suggests that the eukaryotic input increased through time in this area. The 2-methylhopane index (2MeHI) has been proposed as a molecular proxy for cyanobacteria (Summons et al., 1999) while

the 3-methylhopane index (3MeHI) is potentially useful as a proxy for methanotrophic proteobacteria (Collister et al., 1992; Farrimond et al., 2004). The 2MeHI values are all between 6 and 12 %, and the 3MeHI values are all between 3 and 9 % suggesting a small but steady input from both cyanobacteria and methanotrophic proteobacteria (Figure 4c). The 28,30-bisnorhopane to C₃₀ hopane ratio, when high, suggests a clay-poor, anoxic depositional environment. 28,30-Bisnorhopane may be biosynthesized by chemoautotrophic bacteria that grow at the oxic-anoxic interface of a water body, but since it is only found in bitumen it is more likely that it is the diagenetic product of hopanols formed under conditions where bacteria like sulfide oxidizers thrive (Peters et al., 2005). The Kamov Group values are all around 0.18, whereas the younger oils have higher values, generally ranging between 0.3 and 0.5 (Figure 4a). This again suggests that the Kamov Group oils were deposited in a more oxic depositional environment. However, there is also a significant increase in the diasteranes to steranes ratio in the Kamov Group oils relative to the younger oils, so the change in 28,30-bisnorhopane abundance could also be related to a clay rich depositional environment for the Kamov Group. The C₂₇/ C₂₉ steranes ratios are all around 0.2, suggesting a predominance of green algae in all of these samples; this will be discussed further below. There are two ratios provided in Table 5 with *n*-C_#/ *x*-C_# and one *x*-C₂₀/ Ph. The X-peaks are mid-chain monomethylalkanes which may suggest the presence of cyanobacteria, sponges or colorless sulfide oxidizing bacteria (Shiea et al., 1990; Thiel et al., 1999; Love et al., 2008). The *n*-C₂₂/ *x*-C₂₂ and *n*-C₂₄/ *x*-C₂₄ are both greater than 2 for the Kamov Group and on average less than 2 for the younger samples. This abundance of X-peaks likely suggests the abundance of sponges or colorless sulfide oxidizing bacteria, especially in the samples younger than the Kamov Group. The *x*-C₂₀/ Ph values are around 1 for the Kamov Group samples and significantly lower, between 0.2 and 0.6, for the younger samples. Given the *n*-alkane to X-peak ratios, this signal appears to be dominated by the lack of abundance of Ph in the Kamov Group sample rather than an abundance of X-peaks in the Kamov Group oils (Figure 4d). In summary, eukaryotic input increased through time in this area, there was a small but steady input from both cyanobacteria and methanotrophic proteobacteria, the Kamov Group oils were deposited in a more oxic depositional environment than the younger oils, there was a predominance of green algae

in all of these samples and an abundance of sponges or colorless sulfide oxidizing bacteria, especially in the samples younger than the Kamov Group.

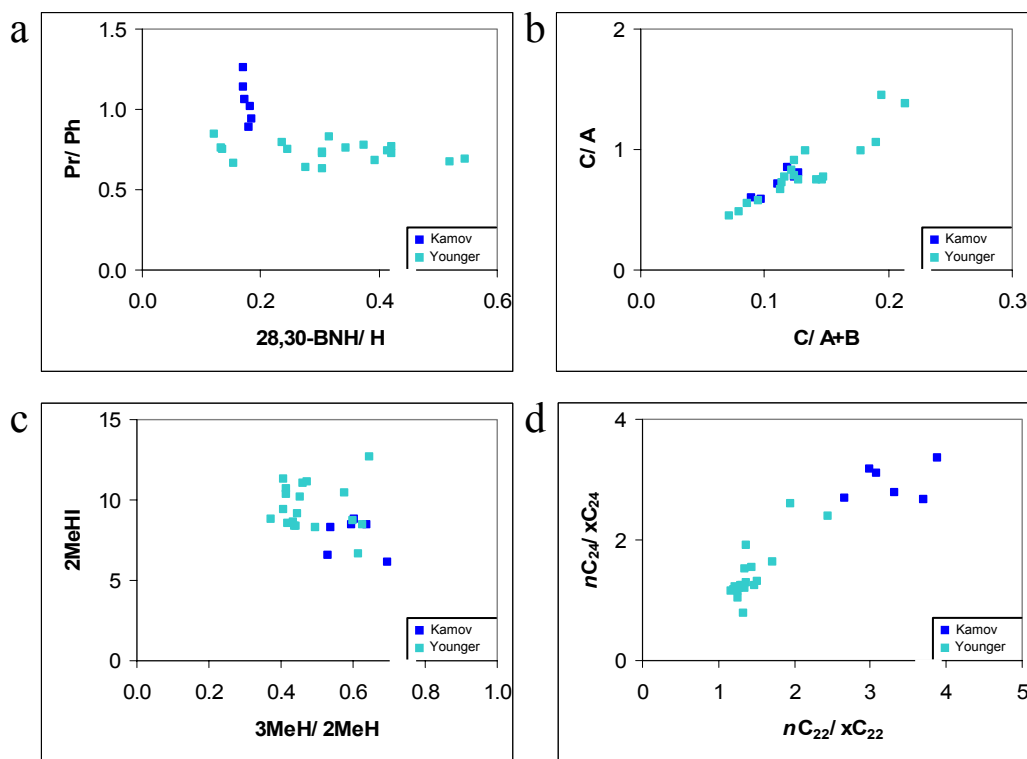


Figure 4. Cross-plots of a selection of biomarkers. Samples from the Kamov Group are in dark blue, whereas the younger oils are in light blue. a) Pristane/ phytane vs. 28,30-bisnorhopane/ hopane, showing that the Kamov Group oils plot in a different region than the rest of the Eastern Siberian oils that are younger. b) C/ A vs. C/ A+B showing a greater variance of the abundance of B in the younger samples in comparison to the Kamov Group oils. c) 2-methylhopane/ (2-methylhopane + hopane) vs. 3-methylhopane/ 2-methylhopane showing that the Kamov Group oils generally plot in a different region than the rest of the Eastern Siberian oils that are younger. d) $n\text{-C}_{24}/x\text{-C}_{24}$ vs. $n\text{-C}_{22}/x\text{-C}_{22}$ showing a clear separation between the Kamov Group oils and the younger Eastern Siberian oils.

Environmental interpretations.

In previous studies of Eastern Siberian oils the main features were recorded as low Pr/ Ph values, $\text{C}_{35}\text{H}/\text{C}_{34}\text{H} > 1$, trace gammacerane, $\text{T}_s/\text{T}_m < 1$, a high relative abundance of mid-chain monomethyl alkanes, 30-norhopanes, C_{29} steranes and acyclic isoprenoids, a greater abundance of hopanes relative to steranes, the presence of 2-methylhopanes, 2,3,6-trimethyl aryl isoprenoids and C_{30} methylsteranes, and a lack of diasteranes (Fowler & Douglas, 1987; Summons & Powell, 1992). The low Pr/ Ph values, presence of C_{30}

norhopanes, $C_{35}H/C_{34}H > 1$, $Ts/Tm < 1$, and lack of diasteranes led the authors to suggest a carbonate source.

Generally, our data agree with these past studies. The Pr/Ph values show that the samples are all marine, and that the depositional environment of several of the Kamov Group oils was more oxidizing or less restricted than that of the younger samples. The low homohopane index, gammacerane to hopane ratio and concentrations of 21-norsteranes suggest that none of these samples were from hypersaline or stratified depositional environments. Combined, the $Ts/(Ts+Tm)$, C_{31} hopane S/ S+R, C_{29} sterane S/ S+R and hopane to moretane ratios suggest that all of the samples are of moderate thermal maturity. The isopropylcholestane sponge biomarkers are relatively high in all of the samples, providing evidence that even the oldest samples are likely Ediacaran or at least latest Cryogenian in age (Love et al., 2009). On average, the steranes to hopanes ratio was less than 1 in the early Ediacaran and greater than 1 in the later Ediacaran in these samples, suggesting more eukaryotic input closer to the Cambrian. The 2-MeHI shows an appreciable contribution from cyanobacteria throughout the sections. The 3-MeHI shows a small contribution from methanotrophic bacteria throughout as well. The 28,30-bisnorhopane to hopane ratio is higher in the younger samples than the Kamov Group samples, supporting the hypothesis that the Kamov Group samples were deposited in a more oxic setting. C_{29} steranes predominate in all of the samples, suggesting a predominance of green algae. The abundance of X-peaks likely suggests the presence of sponges or colorless sulfide oxidizing bacteria. Though there were peaks that appeared at similar retention times to 2,3,6-trimethyl aryl isoprenoids, further spectroscopic analysis showed that 2,3,6-trimethyl aryl isoprenoids could not be detected in these samples.

A principal components analysis of the MRM-derived biomarker parameters showed three main clusters, with ES 020 and ES 080 as outliers (Figure 5). The most relevant factors that made up the principal components were the steranes/ hopanes ratio, % C_{27} steranes, % C_{28} steranes, $n-C_{22}/x-C_{22}$, $n-C_{24}/x-C_{24}$, $\alpha\alpha\alpha R$ isopropylcholestane/ $\alpha\alpha\alpha R$ n -propylcholestane, 2-methylhopane index, and isotopic compositions of the saturate and aromatic fractions (proprietary to Geomark).

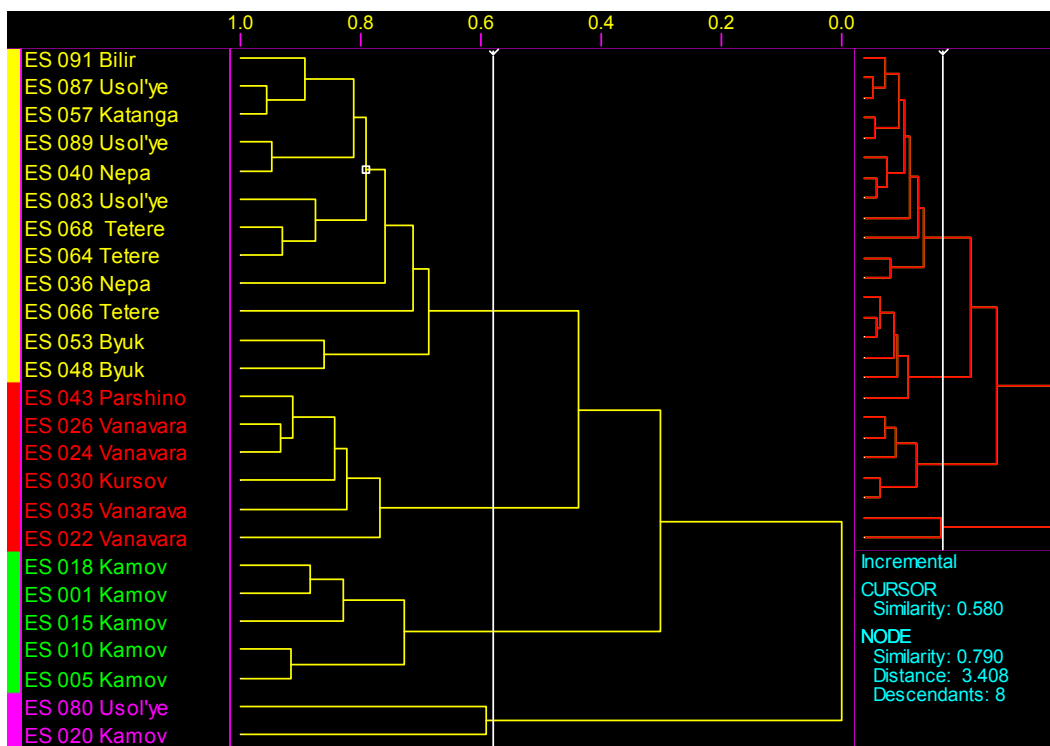


Figure 5. Principal component analysis tree showing the main oil families in these Eastern Siberian oils, with ES 020 and ES 080 as outliers. Notice that the rest of the Kamov Group samples separate quite strongly from the younger samples.

Comparison to Oman.

Previous studies have compared Eastern Siberian oils to Huqf oils of Oman due to their high abundance of monomethyl alkanes and C_{29} steranes (Fowler & Douglas, 1987; Summons & Powell, 1992). The Huqf oils of Oman, recently discussed in Grosjean et al. (2009) have abundant C_{29} steranes, associated with an abundance of green algae, and mid-chain monomethyl alkanes. More interestingly, we have found that the Eastern Siberian Kamov Group samples are very similar to those of the Nafun group of Oman and the younger Eastern Siberian samples are very similar to those of the Ara group of Oman. Grosjean et al. (2009) showed that the main differences between the Nafun and Ara hydrocarbon assemblages are that the Nafun has a lower ratio of 28,30-bisnorhopane to hopane, 2-methylhopanes to 3-methylhopanes and $C_{35}H/C_{34}H$, lower concentrations of 21-norsteranes, X-peaks and gammacerane, higher Pr/Ph, and higher relative abundance of diasteranes. Interestingly, these exact same parameters distinguish the Kamov Group vs. the younger Eastern Siberian oils with a few notable exceptions. In the Siberian samples, there is no significant difference in gammacerane to hopane or $C_{35}H/C_{34}H$

ratios and 21-norsteranes are actually more abundant in the Kamov Group samples. All of the other parameters behave similarly, suggesting that the Nafun Group and Kamov Group samples may be coeval. The Nafun Group is dated to an age range of 635 to 547 Ma (Bowring et al., 2007). Geochemical parameters suggest the source rocks of the younger oils of Eastern Siberia are coeval with the Ara Group, which is dated to be 547 to < 541 Ma (Bowring et al., 2007).

Sterane patterns.

It appears that in Neoproterozoic rocks and oils C₂₉ steranes are usually dominant with a few exceptions where C₂₇ steranes are dominant (Knoll et al. 2007). In this section we explore what areas of the world at this time have which sterane dominance and try to relate that to known sterol patterns in modern algae in order to address the possible redox conditions of their depositional environments.

The dominant steranes in the Awatubi and Walcott Members of the Chuar Group in Arizona, the Q oil of Oman, and the Ediacaran Formations of the Amadeus Basin in Australia are C₂₇ steranes (Ventura et al., 2009; Grantham 1986; Summons & Walter 1990; Appendix 1). In the lower Walcott Member, this dominance is strong and the average C₂₇/ C₂₉ steranes ratios are 17.1 (Ventura et al., 2009). The values for the Awatubi Member, which lies beneath the Walcott Member and for the upper Walcott Member are 2.7 and 6.8, respectively (Ventura et al., 2009). The dominance is also relatively strong in Q oil, which has average ratios of 2.6 (Grosjean et al., 2009). In the Amadeus Basin samples the average C₂₇/ C₂₉ steranes ratio is closer to unity at 1.4 (Appendix 1). However, in rocks and oils (aside from Q oil) of the South Oman Salt Basin, Cryogenian to Early Cambrian oils of Eastern Siberia, and Ediacaran samples from the Officer Basin in Australia C₂₉ steranes are dominant (Grantham 1986; Fowler & Douglas, 1987; Summons & Walter, 1990; Grosjean et al., 2009; this Chapter; Appendix 1). The dominance of C₂₉ steranes is clear in the South Oman Salt Basin (- Q oil) samples and Eastern Siberian oils where the average C₂₇/ C₂₉ steranes ratios are 0.3 and 0.2, respectively (Grosjean et al., 2009; this Chapter). In the Officer Basin samples the

average C_{27}/C_{29} steranes ratio is closer to unity at 0.8 (Appendix 1). This is clearly visible in the chromatograms in Figure 6 and ternary diagram in Figure 7.

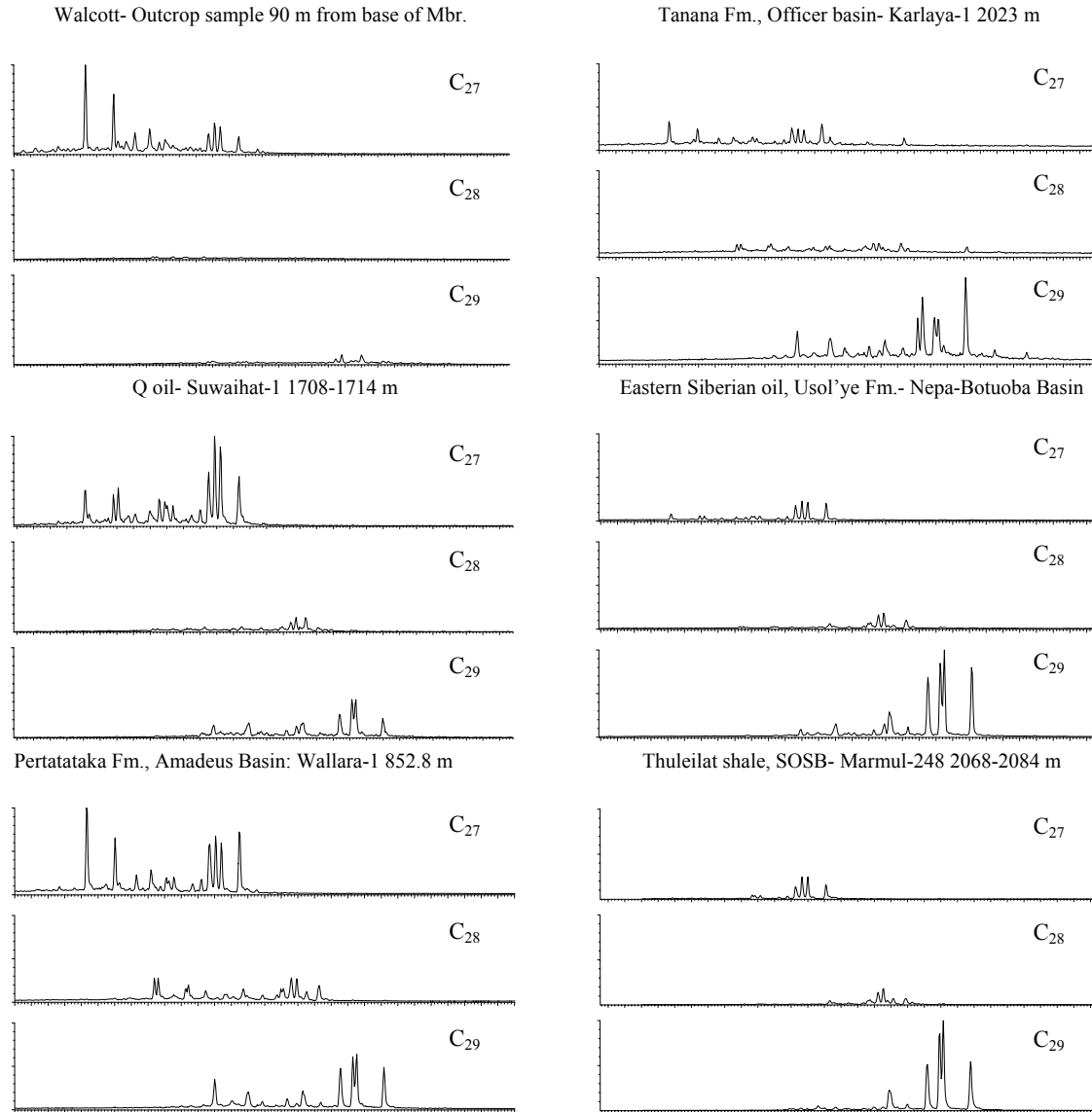


Figure 6. C_{27} , C_{28} and C_{29} sterane distributions from representative samples of the Walcott Member, Q oil of Oman, the Amadeus Basin, Officer Basin, Eastern Siberia and the South Oman Salt Basin (SOSB). For each sample the axes are linked to show relative distributions. In the Walcott Member of the Chuar Group in Arizona, Q oil of Oman and Amadeus Basin samples of Australia a predominance of C_{27} steranes is visible, whereas in the Officer Basin samples of Australia, the oils from Eastern Siberia, and rocks and oils (aside from Q oil) of the South Oman Salt Basin C_{29} steranes are predominant.

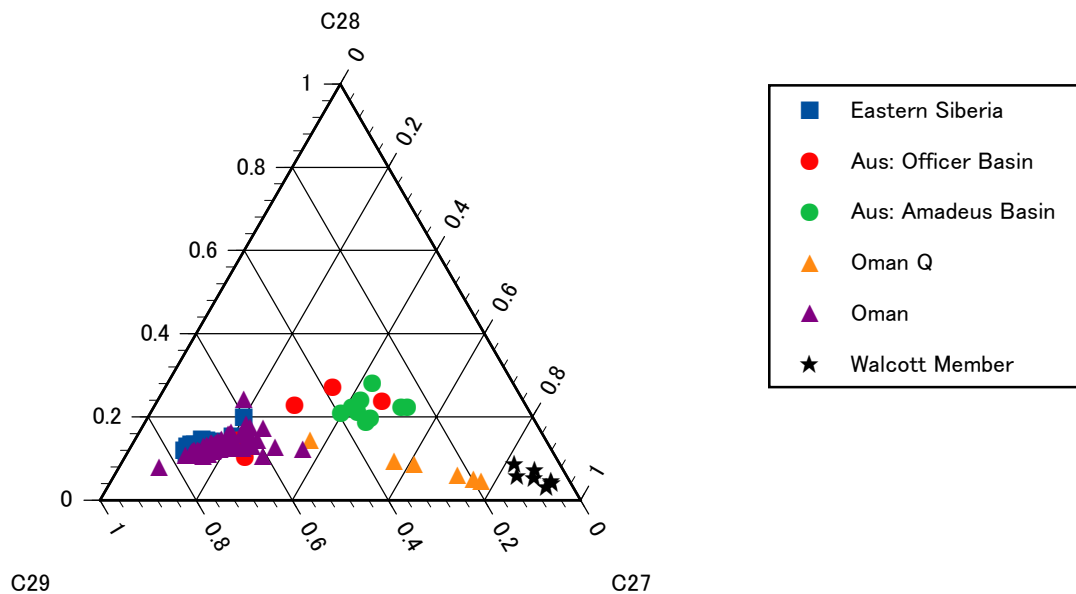


Figure 7. Sterane ternary diagram showing that rocks from the Walcott Member of the Chuar Group and Oman Q oils have a predominance of C_{27} steranes, the other Oman samples (mainly Huqf oils and Nafun or Ara Group rocks) and Eastern Siberian oils have a predominance of C_{29} steranes, and the Australian rock samples from the Amadeus and Officer Basins lie roughly in the middle with slightly more abundant C_{27} steranes in the Amadeus Basin samples and C_{29} steranes in the Officer Basin samples. None of these samples have an abundance of C_{28} steranes, which is expected for samples of Neoproterozoic to Cambrian age.

The abundance of C_{28} steranes is generally quite low in Neoproterozoic to Cambrian sediments. The increase in $C_{28}/(C_{28}+C_{29})$ steranes through the geological record may be associated with the diversification of phytoplankton assemblages through the Mesozoic (Grantham & Wakefield, 1988; Schwark & Empt, 2006). In rocks, as opposed to oils, the abundance of C_{28} steranes spikes at some extinctions events (Schwark & Empt, 2006). So, another interpretation for high $C_{28}/(C_{28}+C_{29})$ sterane ratios may be an increase in contribution from resilient prasinophytes (Schwark & Empt, 2006), some of which are known to make C_{28} sterols (Volkman, 1986; Kodner et al., 2008).

The green algal classes Ulvophyceae and Prasinophyceae may be responsible for C_{29} dominance in late Neoproterozoic rocks (Kodner et al., 2008). Green algae became ecologically important 600-800 Ma (Knoll et al., 2007) likely due to an increase in the essential nutrient of dissolved iron in the ocean (Canfield et al., 2008; Love, 2008). The 700-750 Ma Svanbergfjellet Formation of Spitsbergen contains fossils of at least two classes of green algae, including a morphological analogue to Ulvophyceae (Butterfield

et al., 1988; Butterfield et al., 1994). Microfossil data also support the idea that C₂₉ sterane dominance in the Officer Basin samples of Australia was due to the prevalence of green algae. Acritarchs consistent with chlorophycean affinity are found in the Ediacaran lower Ungoolya Group, including the Tanana Formation (Arouri et al., 1999).

There are several potential explanations for the dominance of C₂₇ steranes in some Neoproterozoic sediments, but C₂₉ sterane dominance in most. It is likely that the areas with C₂₉ sterane dominance were those with a prevalence of green algae. Environments with C₂₇ sterane dominance may have been areas where there was a prevalence of red algal clades, since green algae produce sterols with C₂₉ dominance.

Red algae produce cholesterol as their main sterol (Patterson 1971; Volkman, 1986). As early as ~1200 Ma, Bangiacean red algae were extant (Butterfield, 2000; Butterfield et al., 1990). Nearly all living marine red algae are multicellular benthos that would be expected to live close to the shoreline. Any samples with C₂₇ sterane dominance due to red algal influence would have to be from areas shallow enough to have a major input from the photosynthetic benthos. Importantly, red algae have an advantage over green algae in euxinic waters. Sulfide strips the water column of Fe²⁺ and red algae have a lower Fe²⁺ requirement than green algae (Falkowski et al., 2004).

Most green algae produce dominantly C₂₉ sterols (Kodner et al., 2008; Volkman 1986). However, there are a few green algae that dominantly produce C₂₇ sterols. In stationary phase, *Dunaliella minuta* may produce C₂₇ sterols dominantly (Ballantine et al., 1979). *Dictyosphaerium pulchellum* produces C₂₇ sterols dominantly, however it is a freshwater species, so it is not likely to be the source of the signal we are seeing in the geological record in marine rocks (Cranwell et al., 1990). Though *Dunaliella salina* (UTEX 1644) grown at 0.85, 1.7 and 3.4 M NaCl was found to dominantly produce C₂₉ sterols (Peeler et al., 1989), I found that at ~4 M NaCl *Dunaliella salina* dominantly produces C₂₇ sterols. This may be due to use of different strains. The prasinophytes *Tetraselmis sueica* and two *Tetraselmis sp.* strains may also dominantly produce C₂₇ sterols (Patterson et al., 1993). Lastly, *Ulva pertusa* dominantly produces C₂₇ sterols (Ikekawa et al., 1968). It

may not be that any of these taxa were responsible for the dominant C₂₇ sterane signal in some of the Neoproterozoic sediments, but it is important to note that not all green algae produce C₂₉ sterols as the predominant pseudohomologue.

C₂₇ sterols were the dominant sterols for half of the dinoflagellates studied by Volkman (1986). The glaucophyte *Cyanophora paradoxa* produces a predominance of C₂₇ sterols, but is a freshwater organism (Kodner et al., 2008). Though it is unclear whether they evolved by the Neoproterozoic, a few Prymnesiophyceae dominantly produce C₂₇ sterols. These include *Chrysochromulina polylepis*, *Prymnesium patellifera* and *Ochrosphaera neapolitana* (Volkman, 1986). The most likely of the above organisms to have been prolific in Neoproterozoic oceans are the dinoflagellates, which also make the unique compound dinosterol (Withers, 1983). Through diagenesis, dinosterol becomes a set of dinosteranes, which have been identified in sediments as old as the Early Cambrian (Moldowan & Talyzina, 1998).

In order to identify the organisms that are most likely responsible for C₂₇ sterane dominance in some Neoproterozoic sediments, it is important to first present the depositional environments of the areas studied. According to Canfield et al. (2008), during much of the late Neoproterozoic sub-surface oceans were anoxic with deep water being sometimes sulfidic, but usually ferruginous. Ferruginous deep waters were identified in two regions of South Australia, the Caribou and Mackenzie Mountains of Canada, Avalon Peninsula of Newfoundland, East Greenland, Spitzbergen of Svalbard and Siberia.

Fe speciation data for the Walcott Member of the Chuar Group by Canfield et al. (2008), however, was suggestive of sulfidic deep waters. Though aryl isoprenoids are not present (Love, 2008), molecular fossil evidence is not inconsistent with the proposal for sulfidic deep waters in the Walcott Member. The apparent absence of aryl isoprenoids suggests that the sulfidic waters never entered the photic zone, but the Canfield et al. (2008) work focuses on bottom water environments. Also, work by Ventura et al. (2009) shows gammacerane to hopane ratios greater than 0.5 in the upper Awatubi Member and lower

Walcott Member, suggestive of stratification. Work by Nagy et al. (2009) shows the lower Chuar Group had diverse acritarchs, which are commonly interpreted as being green algae. The ratios of highly reactive iron vs. total iron are variable, suggestive of both an oxic and an anoxic water column; however, the ratio of pyrite to highly reactive iron is low, suggesting a lack of euxinia (Johnston et al., 2008). The Fe speciation in the upper Chuar Group, which includes the Walcott Member, shows an abundance of highly reactive iron, suggestive of an anoxic water column, and high pyrite to highly reactive iron, suggestive of euxinic conditions (Johnston et al., 2008). This trend towards values indicative of euxinia begins in the upper Awatubi Member where the TOC starts to increase as well. The sample density is low at the top of the Walcott Member, so though it stays anoxic it is difficult to say whether or not it is still euxinic (Johnston et al., 2008). From the middle of the Awatubi Member up through the Walcott Member, diverse acritarchs are absent, but vase shaped microfossils and possibly bacterial blooms are present (Porter & Knoll, 2000; Porter et al., 2003; Nagy et al., 2009). The TOC, Fe and microfossil data suggest eutrophication during late Chuar time. There is no direct fossil evidence for red algae in the Walcott Member, but non-calcareous reds do not have a good fossil record and Xiao et al. (2004) suggest the even the coralline clade may have had an uncalcified evolutionary history in the Ediacaran.

Grantham (1986) studied the composition of two Oman crude oils and found one to have C₂₇ steranes dominant. Subsequent publications defined the oils with high C₂₇ steranes as Q oils, meaning they have an unknown source (Grantham et al., 1988). These Q oils have a high abundance of gammacerane and 21-norsteranes, suggestive of a stratified water column (Grosjean et al., 2009). The presence of sponge biomarkers shows input from more oxygenated environments. Without knowing the source rocks for Q oils or having iron speciation data from those rocks, it is difficult to say for sure what the redox of the bottom waters was like in this area, but the high gammacerane abundances is consistent with sulfidic deep waters (Sinninghe Damsté et al., 1995).

In the Ediacaran, the Amadeus basin likely had at least an upper oxic layer as the Pertatataka Fm. contains acritarchs of possible green algal affinity (Walter et al., 1995;

Zhang & Walter, 1989). The pristane to phytane values are variable, ranging from 0.5 to 2.5 (Logan et al., 1997; McKirdy et al., 2006; Appendix 1). The gammacerane to hopane values are very low, all less than 0.1 (Appendix 1). The redox state of the deep water is unknown.

The other oil Grantham (1986) studied had dominantly C_{29} steranes and was later identified as Huqf oil (Grantham et al., 1988). These oils are geochemically very similar to the Huqf rocks, in which C_{29} steranes dominate as well (Grosjean et al., 2009). They have very low Pr/ Ph values suggestive of an anoxic water column. Supporting this is a high C_{35} homohopane abundance. Gammacerane concentrations are low and aryl isoprenoids could not be identified. X-peaks are present in all samples as are 24-isopropylcholestanes (Grosjean et al., 2009). Together this suggests deposition in a water column with a shallow oxic layer where sponges lived and an anoxic lower layer.

The Eastern Siberian oils younger than the Kamov Group generally have values of Pr/ Ph less than 0.8 suggestive of an anoxic depositional environment. The abundance of demosponge markers suggests there was also an upper oxic layer. Though the gammacerane to hopane ratios are all less than 0.13, the presence of both anoxia and sponges is suggestive of a stratified water column with a shallow oxic layer above an anoxic water column.

The Ediacaran Officer Basin samples have demosponge markers, suggestive of an upper oxic layer. Pristane to phytane values are highly variable, ranging from 0.5 to 2.2 (Logan et al., 1997; McKirdy et al., 2006; Appendix 1). The gammacerane to hopane values are all very low, less than 0.12 (Appendix 1). The redox state of the deep water is unknown.

The most important factor in determining sterane abundances may be the redox environment of the deep water. From the Fe speciation evidence, we predict that in Neoproterozoic samples high C_{27}/ C_{29} steranes ratios compared to nearby strata, especially in conjunction with high gammacerane abundances (gammacerane to hopane > 0.5), are indicative of euxinic deep waters. Conversely, high C_{29}/ C_{27} steranes ratios are

indicative of ferruginous deep waters. This hypothesis will be tested as we collect more Fe speciation data with which to compare our biomarker results. Though a gammacerane to hopane ratio of 0.3 is not insignificant, in the Phanerozoic, where stratification exists either due to salinity gradients or sulfidic deep waters, gammacerane to hopane ratios are generally quite high, reaching values around 1 (Wang & Fu, 1997; Bao & Li, 2001). Perhaps the organisms that make tetrahymanol, the precursor to gammacerane, would not live in water columns stratified due to ferruginous bottom waters. Though both the Awatubi and Walcott Members of the Chuar Group have a predominance of C_{27}/C_{29} steranes, there is only strong evidence for euxinic deep waters in the upper Awatubi Member and lower Walcott Member. This is also where gammacerane abundances are highest. The lower Walcott Member is also where the C_{27}/C_{29} steranes ratios increase dramatically compared to the strata above and below. It is interesting that the gammacerane values indicate the switch in deep water before the C_{27}/C_{29} steranes ratios.

The presence of sulfidic deep waters in the lower Walcott Member may have caused an increase in C_{27} steranes because Fe and Mo are removed from sulfidic water, leading to a limitation in fixed nitrogen and dissolved ferrous iron (Anbar & Knoll, 2002; Falkowski et al., 2004). Due to their lesser requirement for iron than that of green algae, red algae would then become abundant, leading to C_{27} steranes dominance. A schematic of this water column is shown in Figure 8a. A similar situation occurred at the P/T boundary, where extensive anaerobic waters led to a radiation in red lineage groups (Falkowski et al., 2004). Do note that algae grow in the oxic, shallow layer.

Less certain is the deep water redox environment of the source rocks for the Oman Q oil. Due to the high abundance of gammacerane, we hypothesize that the C_{27} sterane dominance may be due to an origin from sediments deposited in a sulfidic deep water environment leading to a predominance of red algae, but it may be from a significant input of sterols from dinoflagellates or a significant input of sterols from ancient relatives of the modern hypersaline tolerant green alga *Dunaliella salina*.

In the rest of the South Oman Salt Basin and the Eastern Siberian basins there may have been enough mixing with a ferruginous deep zone to allow the green algae to out-compete the red algae, leading to a dominance of C₂₉ steranes. A schematic of this type of water column is shown in Figure 8b.

The evidence for the redox state of the deep waters in the Amadeus and Officer Basins are the weakest. Interestingly, they are also the basins with samples where C₂₇/ C₂₉ sterane ratios are close to unity. Additionally, these basins were likely were likely connected as regions of the Centralian Superbasin in the Ediacaran (Logan et al., 1997; Walter et al., 1995). Perhaps they each had stronger characteristics of sulfidic versus ferruginous bottom waters, but since they were connected they mixed enough for the signal to be sufficiently convoluted and muted. As neither have strong gammacerane abundances, we tentatively consider both to have ferruginous deep waters. Another possibility for the Amadeus Basin is that the bottom waters were euxinic as the sterane signature suggests but there were limited shallow waters where the benthic, phototrophic red algae could live.

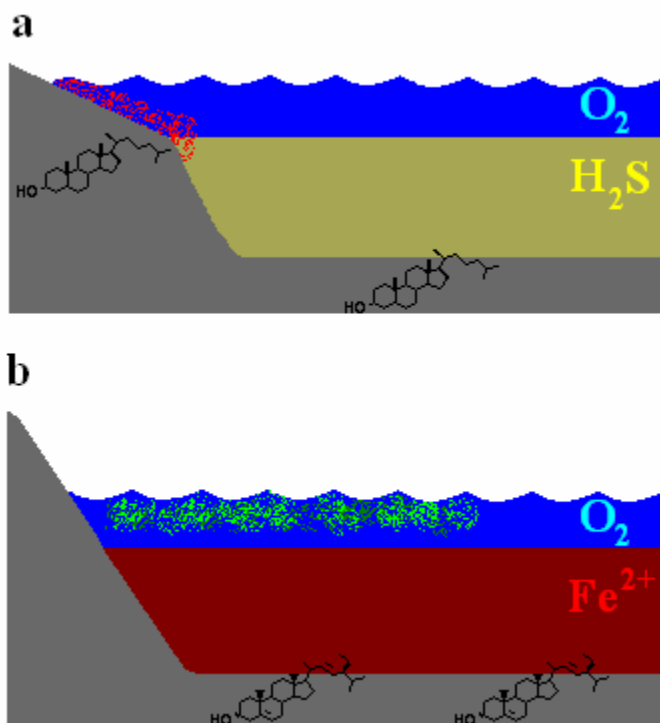


Figure 8. Schematics of the different redox conditions of Neoproterozoic water columns. The Amadeus and Officer basins are enigmatic and not identified in either of these scenarios. In both cases, the algae are growing in the oxic, shallow ocean layer. a) Example of a water column with sulfidic deepwater, allowing red algae, which are benthic, to outcompete green algae and causing cholesterol to form in the sediments. This may have been the scenario for the Walcott Member and Q oil of the South Oman Salt Basin. b) Example of a water column with ferruginous deepwater, allowing green algae to dominate and leave C₂₉ sterols in the sediment. This was likely the case for the South Oman Salt Basin (minus the source of the Q oils) and Eastern Siberian basins.

Conclusions

From this new biomarker data we have an improved understanding of the sedimentary environment during source rock deposition during the late Neoproterozoic in Eastern Siberia. Though there was more eukaryotic input closer to the Cambrian, the older samples were deposited in a more oxic setting. Sponges, cyanobacteria, green algae and possibly sulfide oxidizing bacteria were relatively abundant throughout.

The hydrocarbon compositions of the Eastern Siberian oils studied here have a strong resemblance to the Huqf oils of the South Oman Salt Basin. This and the substantial abundance of demosponge markers throughout the Siberian oils suggests that the samples assigned as Riphean age by Russian geologists are likely to be of Cryogenian to

Ediacaran age and those thought to be Vendian to Early Cambrian are likely Ediacaran to Early Cambrian.

The C₂₇/ C₂₉ steranes ratio is important in understanding the Neoproterozoic ecology worldwide. Especially in conjunction with gammacerane to hopane values, it may be useful as an indicator of the redox conditions of deep water environments and thus of the dominant organisms of regions during this era.

Acknowledgements

The author wishes to thank Roger Summons for the principle component analysis and John Zumberge for the isotopic compositions of the saturate and aromatic fractions of the Eastern Siberian oils and access to the IHS charts.

References

- Anbar, A. D.; Knoll, A. H. **2002**. Proterozoic ocean chemistry and evolution: A bioinorganic bridge? *Science* **297**, 1137-1142.
- Arouri, K.; Greenwood, P. F.; Walter, M. R. **1999**. A possible chlorophycean affinity of some Neoproterozoic acritarchs. *Org. Geochem.* **30**, 1323-1337.
- Ballantine, J. A.; Lavis, A.; Morris, R. J. **1979**. Sterols of the phytoplankton- effects of illumination and growth stage. *Phytochemistry* **18**, 1459-1466.
- Bao, J.; Li, M. **2001**. Unprecedented occurrence of novel C₂₆-C₂₈ 21-norcholestanes and related triaromatic series in evaporitic lacustrine sediments. *Org. Geochem.* **32**, 1031-1036.
- Bowring, S.; Myrow, P.; Landing, E.; Ramezani, J.; Grotzinger, J. **2003**. Geochronological constraints on terminal Neoproterozoic events and the rise of metazoans. *Geophysical Research Abstracts* **13**, 219.
- Bowring, S. A.; Grotzinger, J. P.; Condon, D. J.; Ramezani, J.; Newall, M. J.; Allen, P. A. **2007**. Geochronologic constraints on the chronostratigraphic framework of the Neoproterozoic Huqf Supergroup, Sultanate of Oman. *Am. J. Sci.* **307**, 1097-1145.
- Butterfield, N. J. **2000**. *Bangiomorpha pubescens* n. gen., sp.: implications for the evolution of sex, multicellularity, and the Mesoproterozoic/ Neoproterozoic radiation of eukaryotes. *Paleobiology* **26**, 386-404.
- Butterfield, N. J.; Knoll, A. H.; Swett, K. **1988**. Exceptional preservation of fossils in an Upper Proterozoic shale. *Nature* **334**, 424-427.
- Butterfield, N. J.; Knoll, A. H.; Swett, K. **1990**. A Bangiophyte red alga from the Proterozoic of arctic Canada. *Science* **250**, 104-107.
- Butterfield, N. J.; Knoll, A. H.; Swett, K. **1994**. Paleobiology of the Neoproterozoic Svanbergfjellet Formation, Spitsbergen. *Lethaia* **27**, 76.

- Canfield, D. E.; Teske, A. **1996**. Late Proterozoic rise in atmospheric oxygen concentration inferred from phylogenetic and sulphur-isotope studies. *Nature* **382**, 127-132.
- Canfield, D. E.; Poulton, S. W.; Knoll, A. H.; Narbonne, G. M.; Ross, G.; Goldberg, T.; Strauss, H. **2008**. Ferruginous conditions dominated later Neoproterozoic deep-water chemistry. *Science* **321**, 949-952.
- Cloud, P. E. Jr. **1968**. Atmospheric and hydrospheric evolution on the primitive Earth. *Science* **160**, 729-736.
- Collister, J. W.; Summons, R. E.; Lichtfouse, E.; Hayes, J. M. **1992**. An isotopic biogeochemical study of the Green River oil shale. *Org. Geochem.* **19**, 265-276.
- Cranwell, P. A.; Jaworshi, G. H. M.; Bickley, H. M. **1990**. Hydrocarbons, sterols, esters and fatty acids in six freshwater Chlorophytes. *Phytochemistry* **29**, 145-151.
- Derry, L. A.; Kaufman, A. J.; Jacobsen, S. B. **1992**. Sedimentary cycling and environmental change in the Late Proterozoic: Evidence from stable and radiogenic isotopes. *Geochim. et Cosmochim. Acta* **56**, 1317-1329.
- Des Marais, D. J.; Strauss, H.; Summons, R. E.; Hayes, J. M. **1992**. Carbon isotope evidence for the stepwise oxidation of the Proterozoic environment. *Nature* **359**, 605-609.
- Didyk, B. M.; Simoneit, B. R. T.; Brassell, S. C.; Eglinton, G. **1978**. Organic geochemical indicators of palaeoenvironmental conditions of sedimentation. *Nature* **272**, 216-222.
- Falkowski, P. G.; Katz, M. E.; Knoll, A. H.; Quigg, A.; Raven, J. A.; Schofield, O.; Taylor, F. J. R. **2004**. The evolution of modern eukaryotic phytoplankton. *Science* **305**, 354-360.
- Farrimond, P.; Talbot, H. M.; Watson, D. F.; Schulz, L. K.; Wilhelms, A. **2004**. Methylhopanoids: Molecular indicators of ancient bacteria and a petroleum correlation tool. *Geochim. et Cosmochim. Acta* **68**, 3873-3882.
- Fike, D. A.; Grotzinger, J. P.; Pratt, L. M.; Summons, R. E. **2006**. Oxidation of the Ediacaran Ocean. *Nature* **444**, 744-747.
- Fowler, M. G.; Douglas, A. G. **1987**. Saturated hydrocarbon biomarkers in oils of Late Precambrian age from Eastern Siberia. *Org. Geochem.* **11**, 201-213.
- Grantham, P. J. **1986**. The occurrence of unusual C₂₇ and C₂₉ sterane predominances in two types of Oman crude oil. *Org. Geochem.* **9**, 1-10.
- Grantham, P. J.; Wakefield, L. L. **1988**. Variations in the sterane carbon number distributions of marine source rock derived crude oils through geological time. *Org. Geochem.* **12**, 61-73.
- Grantham, P. J.; Lijmbach, G. W. M.; Posthuma, J.; Hughes Clarke, M. W.; Willink, R. J. **1988**. Origin of crude oils in Oman. *J. Pet. Geol.* **11**, 61-80.
- Grosjean, E.; Love, G. D.; Stalvies, C.; Fike, D. A.; Summons, R. E. **2009**. Origin of petroleum in the Neoproterozoic-Cambrian South Oman Salt Basin. *Org. Geochem.* **40**, 87-110.
- Harvey, H. R.; McManus, G. B. **1991**. Marine ciliates as a widespread source of tetrahymanol and hopan-3 β -ol in sediments. *Geochim. Cosmochim. Acta* **55**, 3387-3390.
- Hayes, J. M.; Summons, R. E.; Strauss, H.; Des Marais, D. J.; Lambert, I. B. **1992**. Proterozoic biogeochemistry. In: The Proterozoic Biosphere: A Multidisciplinary

- Study. (J. W. Schopf & C. Klein, eds.), Cambridge University Press, pp. 81-133.
- Hoffman, K.-H.; Condon, D. J.; Bowring, S. A.; Crowley, J. L. **2004**. U-Pb zircon data from the Neoproterozoic Ghaub Formation, Namibia: Constraints on Marinoan glaciation. *Geology* **32**, 817-820.
- IHS Charts from John Zumberge.
- Ikekawa, N. **1968**. Sterol compositions in some green algae and brown algae. *Steroids* **12**, 41-8.
- Johnston, D. T.; Poulton, S. W.; Dehler, C. M.; Canfield, D. E.; Knoll, A. H. **2008**. Early Neoproterozoic ocean chemistry: Fe-S systematics from the Chuar Group. *Eos Trans. AGU*, **89** Fall Meet. Suppl., Abstract PP33D-01.
- Kelly, A. E.; Love, G. D.; Grosjean, E.; Zumberge, J. E.; Summons, R. E. **2007**. Temporal and facies controls on the distributions of uncommon steranes from Neoproterozoic sediments and oils. Abstr. 23rd IMOG. Torquay, P203.
- Knoll, A. H.; Carroll, S. B. **1999**. Early animal evolution: Emerging views from comparative biology and geology. *Science* **284**, 2129-2137.
- Knoll, A.H.; Summons, R. E.; Waldbauer, J; Zumberge, J. **2007**. The geological succession of primary producers in the oceans. In: The Evolution of Primary Producers in the Sea. (P. Falkowski & A.H. Knoll, eds.), Elsevier, Burlington, pp. 133-163.
- Kodner, R. B.; Pearson, A.; Summons, R. E.; Knoll, A. H. **2008**. Sterols in red and green algae: quantification, phylogeny, and relevance for the interpretation of geologic steranes. *Geobiology* **6**, 411-420.
- Lambert, I. B.; Walter, M. R.; Wenlong, Z.; Songnian, L.; Guogan, M. **1987**. Palaeoenvironment and carbon isotope stratigraphy of Upper Proterozoic carbonates of the Yangtze Platform. *Nature* **325**, 140-142.
- Logan, G. A.; Summons, R. E.; Hayes, J. M. **1997**. An isotopic biogeochemical study of Neoproterozoic and Early Cambrian sediments from the Centralian Superbasin, Australia. *Geochim. Cosmochim. Acta* **61**, 5391-5409.
- Love, G. D. **2008**. pers. comm.
- Love, G. D.; Stalvies, C.; Grosjean, E.; Meredith, W.; Snape, C. E. **2008**. Analysis of molecular biomarkers covalently bound within Neoproterozoic sedimentary kerogen. In: Paleontological Society Papers, Volume 14. (P. H. Kelley & R. K. Bambach, eds.), The Paleontological Society, 67-83.
- Love, G. D.; Grosjean, E.; Stalvies, C.; Fike, D. A.; Grotzinger, J. P.; Bradley, A. S.; Kelly, A. E.; Bhatia, M.; Meredith, W.; Snape, C. E.; Bowring, S. A.; Condon, D. J.; Summons, R. E. **2009**. Fossil steroids record the appearance of Demospongiae during the Cryogenian Period. *Nature* **457**, 718-721.
- McCaffrey, M. A.; Moldowan, J. M.; Lipton, P. A.; Summons, R. E.; Peters, K. E.; Jeganathan, A.; Watt, D. S. **1994**. Paleoenvironmental implications of novel C₃₀ steranes in Precambrian to Cenozoic age petroleum and bitumen. *Geochim. Cosmochim. Acta* **58**, 529-532.
- McFadden, K. A.; Huang, J.; Chu, X.; Jiang, G.; Kaufman, A. J.; Zhou, C.; Yuan, X.; Xiao, S. **2008**. Pulsed oxidation and biological evolution in the Ediacaran Doushantuo Formation. *Proc. Natl. Acad. USA* **105**, 3197-3202.
- McKirby, D. M.; Webster, L. J.; Arouri, K. R.; Grey, K.; Gostin, V. A. **2006**. Contrasting sterane signatures in Neoproterozoic marine rocks of Australia before and after

- the Acraman asteroid impact. *Org. Geochem.* **37**, 189-207.
- Moldowan, J. M.; Talyzina, N. M. **1998**. Biogeochemical evidence for dinoflagellate ancestors in the Early Cambrian. *Science* **281**, 1168-1170
- Moldowan, J. M.; Seifert, W. K.; Gallegos, E. J.; **1985**. Relationship between petroleum composition and depositional environment of petroleum source rocks. *Am. Assoc. Pet. Geol. Bull.* **69**, 1255-68.
- Nagy, R. M.; Porter, S. M.; Dehler, C. M.; Shen, Y. **2009**. Biotic turnover driven by eutrophication prior to Sturtian low latitude glaciation. *Nature Geoscience* in press.
- Patterson, G. W. **1971**. The distributions of sterols in algae. *Lipids* **6**, 120-127.
- Patterson, G. W.; Tsitsa-Tzardis, E.; Wikfors, G. H.; Gladu, P. K.; Chitwood, D. J.; Harrison, D. **1993**. Sterols of Tetraselmis (Prasinophyceae). *Comp. biochem. physiol., B. Comp. biochem.* **105**, 253-256.
- Peeler, T. C.; Stephenson, M. B.; Einspahr, K. J.; Thompson Jr., G. A. **1989**. Lipid characterization of an enriched plasma membrane fraction of *Dunaliella salina* grown in media of varying salinity. *Plant Physiol.* **89**, 970-976.
- Peters, K. E.; Walters, C. C.; Moldowan, J. M., eds. **2005**. The Biomarker Guide, second edition. Cambridge University Press, 41-44.
- Porter, S. H. **2004**. The fossil record of early eukaryotic diversification. *Paleontological Society Papers* **10**, 35-50.
- Porter, S. M.; Knoll, A. H. **2000**. Testate amoebae in the Neoproterozoic Era: evidence from vase-shaped microfossils in the Chuar Group, Grand Canyon. *Paleobiology* **26**, 360-385.
- Porter, S. M.; Meisterfeld, R.; Knoll, A. H. **2003**. Vase-shaped microfossils from the Neoproterozoic Chuar Group, Grand Canyon: A classification guided by modern testate amoebae. *J. Paleont.* **77**, 409-429.
- Powell, T. G.; McKirdy, D. M. **1973**. Relationship between ratio of pristane and phytane, crude oil composition and geological environment in Australia. *Nature Phys. Sci.* **243**, 37-39.
- Rothman, D. H.; Hayes, J. M.; Summons, R. E. **2003**. Dynamics of the Neoproterozoic carbon cycle. *Proc. Natl. Acad. USA* **100**, 8124-8129.
- Scalan, R. S.; Smith, J. E. **1970**. An improved measure of the odd-even predominance in the normal alkanes of sediment extracts and petroleum. *Geochim. et Cosmochim. Acta* **34**, 611-620.
- Schwark, L.; Empt, P. **2006**. Sterane biomarkers as indicators of palaeozoic algal evolution and extinction events. *Palaeogeogr. palaeoclimatol. palaeoecol.* **240**, 225-236.
- alkanes in hot spring cyanobacterial mats: a direct biogenic source for branched alkanes in ancient sediments? *Org. Geochem.* **15**, 223-231.
- Seifert, W. K.; Moldowan, J. M. **1978**. Applications of steranes, terpanes and monoaromatics to the maturation, migration and source of crude oils. *Geochim. Cosmochim. Acta* **42**, 77-95.
- Seifert, W. K.; Moldowan, J. M. **1980**. The effect of thermal stress on source-rock quality as measured by hopane stereochemistry. *Physics and Chemistry of the Earth* **12**, 229-237.
- Seifert, W. K.; Moldowan, J. M. **1986**. Use of biological markers in petroleum

- exploration. In: Methods in Geochemistry and Geophysics Vol. 24 (R. B. Johns, ed.), Elsevier, Amsterdam, pp. 261-290.
- Shiea, J.; Brassell, S. C.; Ward, D. M. **1990**. Mid-chain branched mono- and dimethyl
Sinninghe Damsté, J. S.; Kenig, F.; Koopmans, M. P., Köster, J.; Schouten, S.; Hayes, J. M.; de Leeuw, J. W. **1995**. Evidence for gammacerane as an indicator of water-column stratification. *Geochim. Cosmochim. Acta* **59**, 1895-1900.
- Sokolov, B. S.; Fedonkin, M. A. (eds.) **1990**. The Vendian System. Vol. 2. Regional Geology. Springer-Verlag, Berlin, Heidelberg, New York.
- Sperling, E. A.; Pisani, D.; Peterson, K. J. **2007**. Poriferan paraphyly and its implications for Precambrian palaeobiology. In: The Rise and Fall of the Ediacaran Biota. (P. Vickers-Rich & P. Komarower, eds.), The Geological Society of London, Special Publications 286, London, pp. 355-368.
- Summons, R. E.; Powell, T. G. **1992**. Hydrocarbon composition of the Late Proterozoic oils of the Siberian Platform: Implications for the depositional environment of source rocks. In: Early Organic Evolution: Implications for Mineral and Energy Resources. (M. Schidowski et al., eds.) Springer-Verlag, Berlin, Heidelberg, pp. 296-307.
- Summons, R. E.; Walter, M. R. **1990**. Molecular fossils and microfossils of prokaryotes and protists from Proterozoic sediments. *Am. J. Sci.* **290A**, 212-244.
- Summons, R. E.; Jahnke, L. L.; Hope, J. M.; Logan, G. A. **1999**. 2-Methylhopanoids as biomarkers for cyanobacterial oxygenic photosynthesis. *Nature* **400**, 554-557.
- ten Haven, H. L.; de Leeuw, J. W.; Rullkötter, J.; Sinninghe Damsté, J. S. **1987**. Restricted utility of the pristane/ phytane ratio as a palaeoenvironmental indicator. *Nature* **330**, 641-643.
- ten Haven, H. L.; de Leeuw, J. W.; Sinninghe Damsté, J. S.; Schenck, P. A.; Palmer, S. E.; Zumberge, J. E. **1988**. Application of biological markers in the recognition of palaeohypersaline environments. Geological Society Special Publication No. 40, 123-130.
- ten Haven, H. L.; Rohmer, M.; Rullkötter, J.; Bisseret, P. **1989**. Tetrahymanol, the most likely precursor of gammacerane, occurs ubiquitously in marine sediments. *Geochim. Cosmochim. Acta* **56**, 1993-2000.
- Thiel, V.; Jenisch, A.; Wörheide, G.; Löwenberg, A.; Reitner, J.; Michaelis, W. **1999**. Mid-chain branched alkanolic acids from “living fossil” demosponges: a link to ancient sedimentary lipids? *Org. Geochem.* **30**, 1-14.
- Ulmishek, G. F. **2001a**. Petroleum Geology and Resources of the Nepa-Botuoba High, Angara-Lena Terrace, and Cis-Patom Foredeep, Southeastern Siberian Craton, Russia. U.S. Geological Survey Bulletin 2201-C.
- Ulmishek, G. F. **2001b**. Petroleum Geology and Resources of the Baykit High Province, East Siberia, Russia. U.S. Geological Survey Bulletin 2201-F.
- Ventura, G. T.; Kenig, F.; Kelly, A. E.; Summons, R. E. **2009**. Biomarker patterns of the late Neoproterozoic Kwagunt Formation, Chuar Group (~800-742 Ma), Grand Canyon USA – A record of biogeochemical instability prior to the Cryogenian Period. In revision.
- Volkman, J. K. **1986**. A review of sterol markers for marine and terrigenous organic matter. *Org. Geochem.* **9**, 83-99.
- Volkman, J. K.; Alexander, R.; Kagi, R. I.; Woodhouse, G. W. **1983**. Demethylated

- hopanes in crude oils and their applications in petroleum geochemistry. *Geochim. Cosmochim. Acta* **47**, 785-794.
- Walter, M. R.; Veevers, J. J.; Calver, C. R.; Grey, K. **1995**. Neoproterozoic stratigraphy of the Centralian Superbasin, Australia. *Precambrian Res.* **73**, 173-195.
- Wang, R.; Fu, J. **1997**. Variability in biomarkers of different saline basins in China. *Int. J. Salt Lake Res.* **6**, 25-53.
- Withers, N. **1983**. Dinoflagellate sterols. In: Marine Natural Products 5 (P. J. Scheuer, ed.), Academic Press, New York, pp. 87-130.
- Xiao, S.; Knoll, A. H.; Yuan, X.; Poeschel, C. M. **2004**. Phosphatized multicellular algae in the Neoproterozoic Doushantuo Formation, China, and the early evolution of Florideophyte red algae. *Amer. J. Bot.* **91**, 214-227.
- Zang, W. L.; Walter, M. R. **1989**. Latest Proterozoic plankton from the Amadeus Basin in central Australia. *Nature* **337**, 642-645.

3. Novel Steranes in Neoproterozoic Sediments and Oils

Abstract

The Neoproterozoic Era, which immediately precedes the sudden explosion of diverse animal life in the Cambrian, is of widespread scientific interest because it is here that we observe the first tangible evidence that complex organisms were present and interacting with their environment. However, Neoproterozoic rocks, other than a few Lagerstätten of the Ediacaran Period, do not contain an abundance of well-preserved macrofossils like those found in Phanerozoic rocks. Moreover, Ediacaran fossils are so unlike later organisms that it is difficult to discern taxonomic relationships or the specific conditions that characterized the paleoenvironments that were their habitats. Since few body fossils can be found, and these are difficult to interpret, chemical fossils provide a particularly important window into this chapter of Earth's history. Though many types of biomarker hydrocarbons can be found in the sedimentary rock record, only a few of these are well enough understood to provide any information about the environment at the time of deposition. This study concerns the patterns of two types of norsteranes in Neoproterozoic sediments, C₁₉ norsteranes and 21-norsteranes. Although the precise structures and biological origins of the C₁₉ norsteranes remain to be determined, the relative abundance of one of the isomers appears to correlate with indicators of water column stratification. Because of its restricted temporal distribution, this C₁₉ norsterane (designated C₁₉C) may also serve as an age marker for Neoproterozoic to Early Cambrian rocks and oils. The second series, comprising C₂₆-C₂₈ pseudohomologues, are tentatively identified as 21-norsteranes based on their retention times relative to 21-norcholestane. These two series of compounds can be used to help characterize depositional environments, especially where there are no body fossils to allow interpretation.

Introduction

The Neoproterozoic Era was a period of transformation in Earth's history. During this time, the ocean was in transition from an anoxic water column with oxygenated surface waters to a fully ventilated water column (e.g., Cloud Jr., 1968; Lambert et al., 1987; Derry et al., 1992; Des Marais et al., 1992; Canfield & Teske, 1996; Knoll & Carroll,

1999; Anbar & Knoll, 2002; Porter, 2004; Fike et al., 2006; McFadden et al., 2008). This era preceded the initial radiation of multicellular life, including representatives of all of the modern animal phyla in the Early Cambrian. Yet, only in the latest Neoproterozoic are body fossils of even simple animals found. Thus, chemical, or molecular, fossils offer an alternative for investigating the composition of contemporaneous microbial communities and, potentially, early metazoans (e.g. Love et al., 2009).

Molecular fossils are useful tools to evaluate paleoenvironmental conditions, age of the host rock, and other factors. Though there are many hydrocarbon species found in rocks, the origins of only a few are understood well enough to provide tangible information. Of these, steranes are abundant in the geological record. Most have structures based on the cholestane skeleton, with the side-chain supplemented with up to 3 additional carbon atoms. The most ubiquitous steranes comprise cholestanes, ergostanes and stigmastanes. Eukaryotes biosynthesize a wide range of precursor sterols that are transformed upon burial and diagenesis into these sterane subclasses. Less common are steranes with reduced side-chains or modifications to the A-ring. These likely have fewer organismic sources and, as a consequence, could be source-specific.

Current interest in the origins and implications of C₁₉ norsteranes stems from observations of their high relative abundances in oils from the Neoproterozoic South Oman Salt Basin (SOSB) (Grosjean et al., 2009). The C₁₉ norsteranes have a specific mass spectrometric fragmentation pattern. Because the A, B, C ring unit has one less methyl group than conventional steranes, the main fragment is 203 m/z, instead of the usual sterane 217 m/z fragment. The chromatogram in Figure 1 shows that the transition of 260>203 on a GC-MS with metastable reaction monitoring (MRM) allows these steranes to be visualized with excellent selectivity and a high signal to noise ratio. Though the structures are not known for certain, the diagnostic 260>203 parent to daughter transition used to identify these compounds suggests three primary skeletal possibilities. These are A-norsterane (1), 18-norsterane (2) and 19-norsterane (3) (Figure 2). Of course, there would be numerous possibilities for distinct stereochemistries.

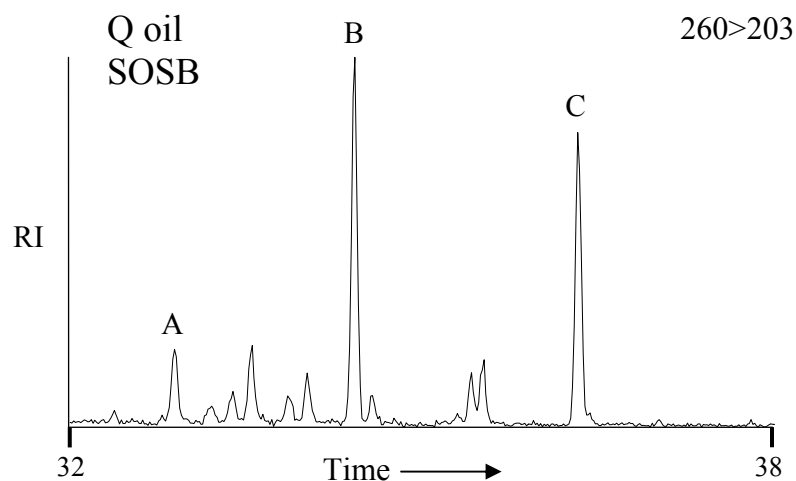


Figure 1. GC-MS MRM chromatogram showing the pattern of C₁₉ norsteranes in Q oil from Oman on a DB-1 column.

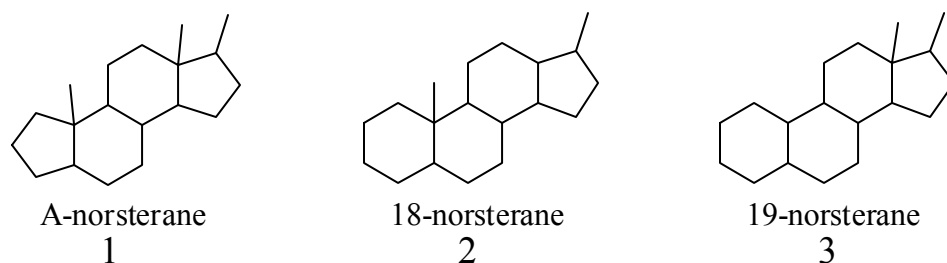


Figure 2. Hypothetical structures for C₁₉ norsteranes identified in various rocks and oils.

21-Norsteranes are already known to exist in the form of 21-norcholestane, which was first identified by Moldowan et al. (1991) based on chemical synthesis. More recently their 24-methyl and 24-ethyl homologues were tentatively identified (Bao & Li, 2001; Grosjean et al., 2009). The structures of these compounds are given in Figure 3. GC-MS MRM chromatograms of 21-norcholestane and 21-norstigmastane are given in Figure 4 and 5, respectively. In contrast to the four regular sterane isomers ($\alpha\alpha\alpha + \alpha\beta\beta$ each with 20S + 20R) seen with cholestane, the 21-norsteranes only appear as a single peak in each trace. This is due to the absence of chiral a center at C₂₀ and co-elution of the $\alpha\alpha\alpha + \alpha\beta\beta$ isomers. It is more difficult to observe 21-norergostane since it coelutes on a DB-1 column with the $\alpha\alpha\alpha$ 20R isomer of cholestane, as seen in Figure 6.

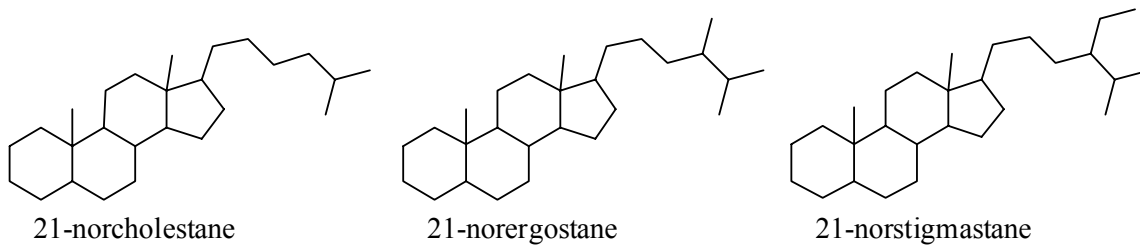


Figure 3. Chemical structures of the 21-norsterane series.

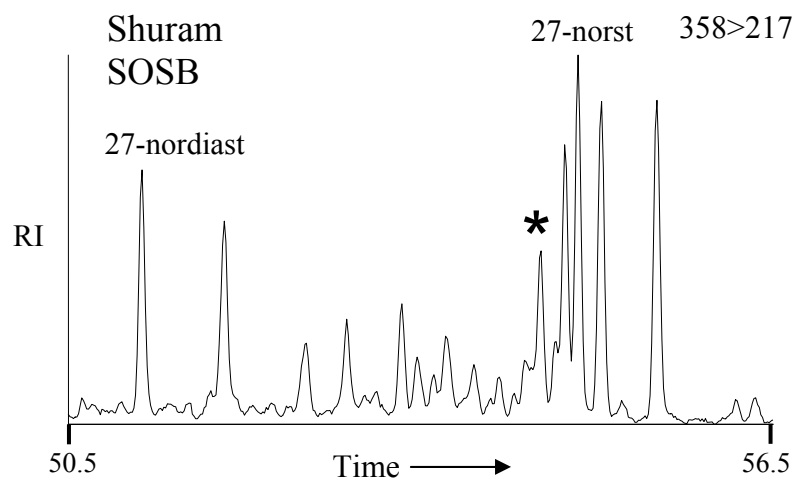


Figure 4. GC-MS MRM chromatogram of 21-norcholestane (marked with an asterisk) in a Shuram Formation rock from Oman on a DB-1 column.

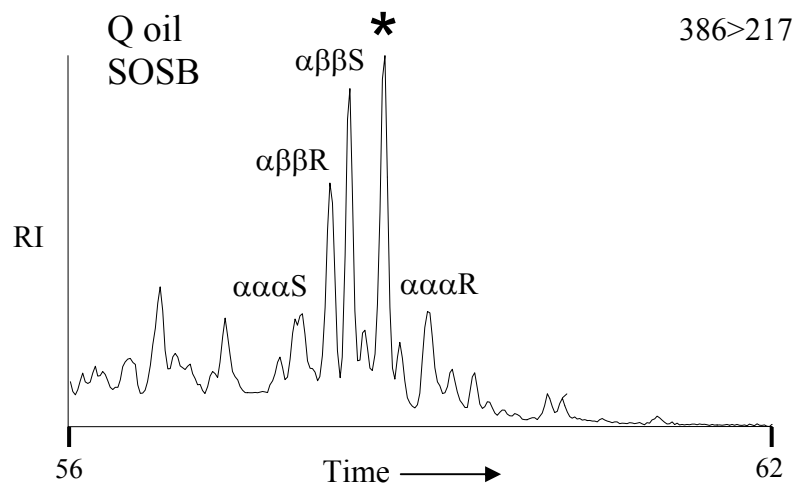


Figure 5. GC-MS MRM chromatogram of 21-norstigmastane (marked with an asterisk) in Q oil from Oman on a DB-1 column.

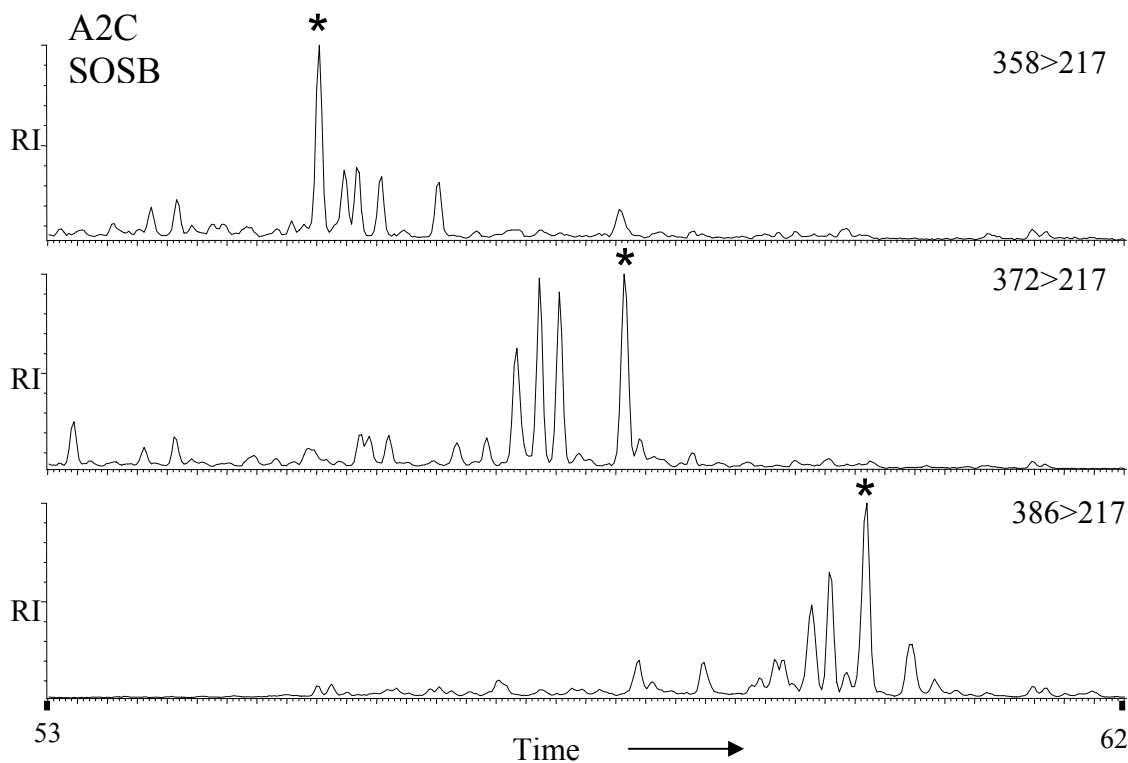


Figure 6. GC-MS MRM chromatograms of the full series of 21-norsteranes (marked with asterisks) from the A2C rock sample OMR 235 of Oman on a DB-1 column.

Experimental Procedures

Sampling.

Samples from Australia were collected from fully cored petroleum exploration and stratigraphic wells. Samples from the Lake Maurice West-1 (LMW1) and Karlaya-1 (K1) wells of the Officer Basin were selected at the Glenside Drill Core Storage Facility, which is managed and run by the Primary Industries and Resources South Australia. The samples from the Wallara-1 (W1) well of the Amadeus Basin were selected at the Northern Territory Geological Survey's core library in Alice Springs. The core samples were sectioned at the core facility and either placed in fabric bags or wrapped in aluminum foil pre-heated to 550°C and then placed into twist bags for transport to MIT and storage prior to analysis.

Rock (OMR) and oil (OMO) samples from the South Oman Salt Basin were collected and analyzed for biomarker parameters conventionally used for oil-source correlation (Grosjean et al., 2009). Neoproterozoic oils from Eastern Siberia (ES) and a suite of

Phanerozoic oils were provided by John Zumberge of Geomark Research, Houston, Texas. Sediment samples from the Chuar Group were contributed by Susannah Porter and Geoscience Australia. A collection of rocks and oils from major producing fields worldwide was also provided by Geoscience Australia. Two oils from the Jinxian Sag in China were provided by Lu Hong. Each sample's provenance, age, type and lithology are provided in Table 1 and 2.

Sample	Unit	Approx. Age (Ma)	Sample Type	Lith.
ES001	Kamov	700	oil	c
ES005	Kamov	700	oil	c
ES010	Kamov	700	oil	c
ES015	Kamov	700	oil	c
ES018	Kamov	700	oil	c
ES020	Kamov	700	oil	c
ES043	Parshino	598	oil	c
ES048	Byuk	598	oil	c
ES053	Byuk	598	oil	c
ES057	Katanga	588	oil	c
ES064	Tetere	568	oil	c
ES066	Tetere	568	oil	c
ES068	Tetere	568	oil	c
ES080	Usol'ye	561	oil	c
ES083	Usol'ye	561	oil	c
ES087	Usol'ye	561	oil	c
ES089	Usol'ye	561	oil	c
ES091	Bilir	561	oil	c
K1 1947	Tanana	589	rock	c
K1 1985	Tanana	589	rock	c
K1 2023	Tanana	589	rock	c
OMO005	A1C	547	oil	c
OMO006	A4C	542	oil	c
OMO015	A5C	540	oil	c
OMO016	A4C	542	oil	c
OMO031	A3C	543	oil	c
OMO033	A2C	545	oil	c
OMO034	A2C	545	oil	c
OMO035	A6C	539	oil	c
OMO036	A4C	542	oil	c
OMO038	A4C	542	oil	c
OMO039	A3C	543	oil	c
OMO040	A1C	547	oil	c
OMO041	A3C	543	oil	c
OMO043	A5C	540	oil	c
OMO051	A3C	543	oil	c
OMO052	A3C	543	oil	c
OMO053	A2C	545	oil	c
OMO054	A5C	540	oil	c
OMO055	A2C	545	oil	c
OMO056	A2C	545	oil	c
OMO057	A2C	545	oil	c
OMO058	A4C	542	oil	c

OMO059	A6C	539	oil	c
OMR002	Buah	550	rock	c
OMR017	Buah	550	rock	c
OMR020	Buah	550	rock	c
OMR028	A3C	543	rock	c
OMR029	A4C	542	rock	c
OMR030	A4C	542	rock	c
OMR031	A4C	542	rock	c
OMR032	A4C	542	rock	c
OMR033	A4C	542	rock	c
OMR034	A2C	545	rock	c
OMR035	A3C	543	rock	c
OMR036	A3C	543	rock	c
OMR037	A3C	543	rock	c
OMR038	A3C	543	rock	c
OMR039	A1C	547	rock	c
OMR040	A5C	540	rock	c
OMR041	A5C	540	rock	c
OMR042	A2C	545	rock	c
OMR149	Buah	550	rock	c
CA 203	Monterey Fm	8	oil	c
CA205	Monterey Fm	8	oil	c
CA247	Monterey Fm	8	oil	c
CA248	Monterey Fm	8	oil	c
CBO002	Canning Basin-Blina 1	383	oil	c
CBO008	Canning Basin-Sundown 2	323	oil	c
AGSO 3923	Svanbergfjellet	800	rock	c
PBO 004	Perth Basin	248	oil	c
CBO005	Canning Basin-Blina OD	383	oil	c
PBO 016	Perth Basin	248	oil	c
FL002	Florida/Sunniland	105	oil	c
AGSO 3499	Marla 3	528	rock	c
AGSO 5679	Georgina Lst	507	rock	c
GR0002	Prinos Greece	6	oil	c
SI0006	Coso Dissi Sicily	6	oil	c
SP0004	Amposta Spain	44	oil	c
CH0039	Jiangnan China	44	oil	c
SI0001	Ragusa Sicily	214	oil	c
RU0354	Iskrin Vogal/Ural	380	oil	c
RU0383	Kuzbaev Vogal/Ural	381	oil	c
MI067	Lee 9 Michigan	436	oil	c

Table 1. Identity, provenance, age, type and lithology of each carbonate sample. Carbonate lithology is denoted by c. The ES, K1, OMO, and OMR samples are used in all of the plots below, whereas the rest are only used in Figure 7 and 8. Dates for A5 and A6 samples are not known, but are approximated from the other Ara unit dates.

Sample	Unit	Approx. Age (Ma)	Sample Type	Lith.
ES022	Vanavara	605	oil	s
ES024	Vanavara	605	oil	s
ES026	Vanavara	605	oil	s
ES030	Kursov	605	oil	s
ES035	Vanavara	605	oil	s
W1 1450	Bitter Springs	925	rock	s
W1 1345	Areyonga	778	rock	s
W1 1306	Aralka	707	rock	s
W1 1272	Pioneer	589	rock	s
W1 1045	Pertatataka	589	rock	s
W1 853	Pertatataka	589	rock	s
W1 706	Arumbera	542	rock	s
LMW1 373	Dey Dey Mudstone	589	rock	s
LMW1 431	Dey Dey Mudstone	589	rock	s
OMO001	Q	537	oil	s
OMO012	Q	537	oil	s
OMO018	Q	537	oil	s
OMO019	Q	537	oil	s
OMO020	Q	537	oil	s
OMO021	Q	537	oil	s
OMR016	Masirah Bay	635	rock	s
OMR027	Masirah Bay	635	rock	s
OMR099	Shuram	570	rock	s
OMR150	Shuram	570	rock	s
OMR151	Shuram	570	rock	s
OMR152	Shuram	570	rock	s
OMR153	Masirah Bay	635	rock	s
OMR154	Shuram	570	rock	s
OMR155	Shuram	570	rock	s
OMR156	Shuram	570	rock	s

OMR157	Masirah Bay	635	rock	s
CH7	Shahejie Fm Zh7 2280m	173	oil	s
CH9	Kongdian Fm Zh9 2360-2390m	173	oil	s
Brazil 4438	Irati Shale	270	rock	s
SP-14-53-20	Walcott Mbr	750	rock	s
AK-10-60-3	Awatubi	760	rock	s
SP-12-53-12	Carbon Canyon	770	rock	s
NOSID 30	Brent Oil	654	oil	s
ICO 40	Lion Sand? Ivory coast	83	oil	s
CA223	Carneros (Temblor Fm)	20	oil	s
CA230	Wilhelm	4	oil	s
ICO 14	Lion Sand	105	oil	s
BS001	Scotland Gp	45	oil	s
AGSO 4193	Victor Bay	1200	rock	s
AGSO 4520	Nonesuch	1000	rock	s
AGSO 4536	Nonesuch	1000	rock	s
GA2000337	Green River Shale Gilsonite	45	rock	s
AGSO 1316	Currant Bush Lst	507	rock	s
AGSO 1361	Inca Fm	507	rock	s
SW0001	Gotland Sweden	487	oil	s
AGSO 5141	Walcott Mbr 4.01	750	rock	s
AGSO 5120	Walcott Mbr 31	750	rock	s
AGSO 5121	Walcott Mbr 34	750	rock	s
AGSO 5123	Walcott Mbr 57	750	rock	s
AGSO 5125	Walcott Mbr 79	750	rock	s
AGSO 5136	Walcott Mbr 90	750	rock	s
AGSO 5133	Walcott Mbr 271	750	rock	s

Table 2. Identity, provenance, age, type and lithology of each siliciclastic sample. Siliciclastic lithology is denoted by s. The ES, W1, LMW1, OMO, and OMR samples are used in all of the plots below, whereas the rest are only used in Figure 7 and 8. The age for Q oils is not known, but is approximated from the Ara unit dates.

General Procedure.

Organic free solvents from OmniSolv were used. Prior to use, all glassware and aluminum foil were fired at 550°C for 8h and glass wool; pipettes and silica gel were fired at 450°C for 8h.

Sediment samples were cleaned with de-ionised water, rinsed with methanol and dichloromethane and crushed manually with the sample wrapped in fired aluminum foil.

They were then ground to a fine powder in a SPEX 8510 Shatterbox fitted with an 8505 alumina ceramic puck mill that was carefully cleaned between samples with aqueous detergent, fired sand, and finally rinsed with distilled water, methanol, dichloromethane and hexane. Rock powders were extracted using an accelerated solvent extractor (Dionex ASE) using a 9:1 mixture of dichloromethane and methanol. The resultant extracts were carefully evaporated under nitrogen to a volume of approximately 2 mL whereupon activated Cu was added to remove elemental sulfur. The sample was then separated by liquid chromatography on a silica gel 60 (Merck, 230-400 mesh) column using hexane to elute the saturate fraction, 4:1 hexane/dichloromethane to elute the aromatic fraction, and 7:3 dichloromethane/methanol to elute the polar fraction. One milligram aliquots of the saturate fractions were then reduced to 0.1 mL and added to insert vials together with 50 ng of internal standard. The saturate fraction was analyzed by GC-MS using D4 (D₄- $\alpha\alpha\alpha$ -ethylcholestane, Chiron), an internal standard that served as an index of relative retention time and for quantification.

Gas Chromatography-Mass Spectrometry (GC-MS) was performed using a Micromass Autospec-Ultima instrument equipped with an Agilent 6890N Series gas chromatograph. Biomarkers in the saturated hydrocarbon fraction were analyzed by GC-MS with the Autospec operated in the metastable reaction monitoring (MRM) mode. A 60 m J&W Scientific DB-1 fused silica capillary column (0.25 mm i.d., 0.25 μ m film thickness) was used with helium at constant flow as carrier gas. Samples were injected in splitless mode. The oven was programmed 60°C, held for two minutes, ramped to 150°C at 10°C/min, then to 315°C at 3°C/min where it was held isothermal for 24 min. The source was operated in EI-mode at 70 eV ionization energy. Peak identification was based on retention time comparisons with the hydrocarbons present in a synthetic standard oil (AGSO Standard Oil) and abundances measured by comparing peak areas to the internal D₄ sterane standard without any adjustment for possible differential responses. Full scan analyses were acquired under the same GC conditions as described above and the scan rate was 0.80 s/decade over a mass range of 50 to 600 m/z with a total cycle time of 1.06s. Data were acquired and processed using MassLynx v4.0 software.

OMO 012, a sample of Q oil from the SOSB, was analyzed on a GC×GC-ToF-MS system that employed a dual stage cryogenic modulator (Leco, Saint Joseph, Michigan) installed in an Agilent 6890N gas chromatograph configured with a 7683B series split/splitless auto-injector, two capillary gas chromatography columns, and a time of flight mass spectrometer. The extract was injected in splitless mode and the purge vent was opened at 0.5 minutes. The inlet temperature was 300°C. The first-dimension column and the dual stage cryogenic modulator reside in the main oven of the Agilent 6890N gas chromatograph (Agilent, Wilmington, Delaware). The second-dimension column is housed in a separate oven installed within the main GC oven. With this configuration, the temperature profiles of the first-dimension column, dual stage thermal modulator and the second-dimension column can be independently programmed. The first-dimension column was a nonpolar Restek Rtx-1MS, (25m length, 0.2 mm I.D., 0.2 µm film thickness) that was programmed to remain isothermal at 45°C for 10 minutes and then ramped from 45 to 320°C at 1.5°C min⁻¹. Compounds eluting from the first dimension column were cryogenically trapped, concentrated, focused and re-injected (modulated) onto a second dimension column. The modulator cold jet gas was dry Nitrogen, chilled with liquid Nitrogen. The thermal modulator hot jet air was heated to 55°C above the temperature of the main GC oven (Thermal Modulator Temperature Offset = 55°C). The hot jet was pulsed for 0.75 second every 6 seconds with a 2.25 second cooling period between stages. Second-dimension separations were performed on a 50% phenyl polysilphenylene-siloxane column (SGE BPX50, 1.25 m length, 0.10 mm I.D., 0.1 µm film thickness) that was programmed to remain isothermal at 65°C for 10 minutes and then ramped from 70 to 340°C at 1.5°C min⁻¹. The carrier gas was helium at a constant flow rate of 1.1 mL min⁻¹. The Leco ToF-MS detector signal was sampled at 50 spectra per second. The transfer line from the second oven to the ToF-MS was deactivated fused silica (0.5 m length, 0.18 mm I.D.) which was held at a constant temperature of 280°C. The ToF source temperature was 225°C, the detector voltage was 1575 Volts, and the mass defect was manually set at 96.1milli-amu/100amu.

An isomerization experiment was performed on androstane, following the method of Rampen et al. (2009). 5α-androstane from Sigma (5 mg) was placed in a 6 mm diameter

pyrex tube with 0.5 mg Pd/C. The tube was evacuated and sealed, heated to 320°C for 36 hours and then cooled to room temperature. The contents were rinsed out with hexane and filtered on silica gel to remove the catalyst.

Results and Discussion

Distribution of compound C through time.

The relative abundance of C₁₉ norsterane (C₁₉C) is highest in oils reservoired in Ediacaran formations of Eastern Siberia, late Neoproterozoic to earliest Cambrian rocks and oils of the SOSB, and the Walcott Member of the Chuar Group of Arizona, as shown in a selection of GC-MS chromatograms in Figure 7. Trace amounts of compound C₁₉C were found in Phanerozoic rocks and oils, but its abundance was orders of magnitudes lower than that found in Neoproterozoic samples of similar lithologies. Figure 8 depicts the ratio C/ (A+B) plotted versus geological time, showing the predominance of C₁₉C in the Neoproterozoic to Early Cambrian, independent of the lithology of the source rock. The siliciclastic samples with high C/ (A+B) values around 800 Ma are from the Walcott Member of the Chuar Group, Arizona. The samples with high C/ (A+B) values near 540 Ma are Q oil samples from the SOSB. The source rock for these oils is not known but is thought to be siliciclastic and of Early Cambrian age (Grosjean et al., in prep.).

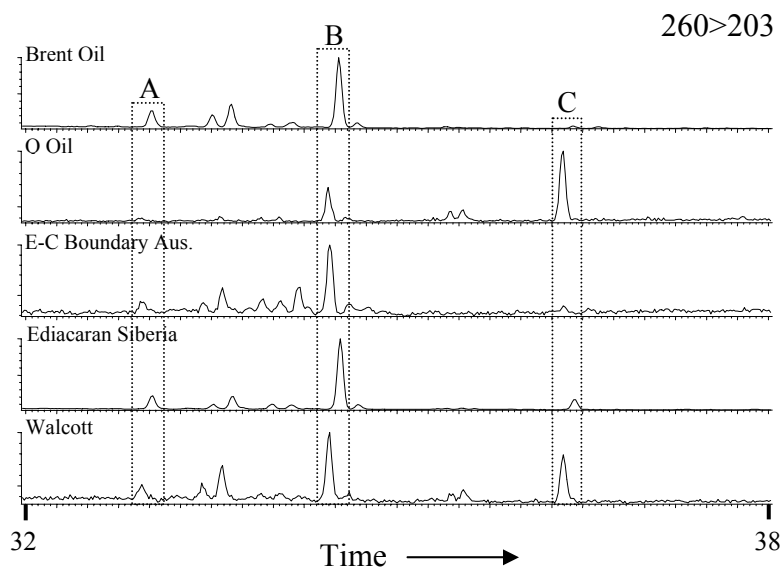


Figure 7. GC-MS MRM chromatograms showing the distributions of C₁₉ norsteranes in a selection of oils and rocks spanning the Neoproterozoic to Jurassic.

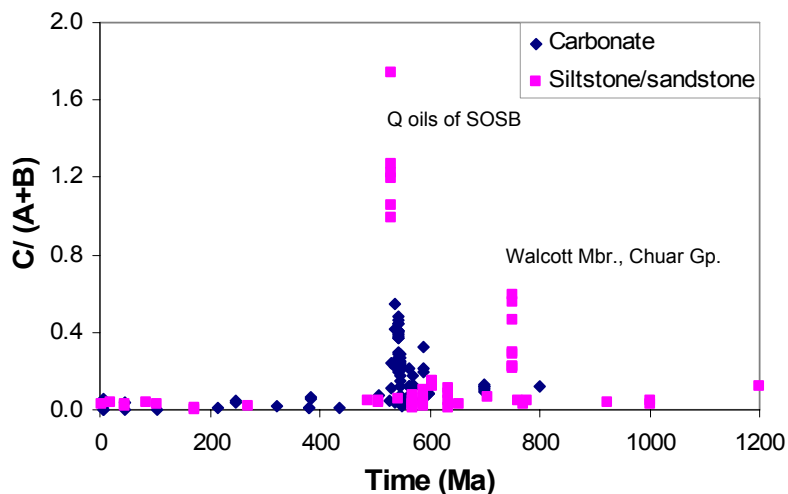


Figure 8. Cross-plot of $C_{19}C / (A+B)$ vs. geologic time showing the relative abundance of compound $C_{19}C$ in Neoproterozoic to Early Cambrian aged samples, independent of lithology.

These data show that the abundance of the $C_{19}C$ is highest in rocks of Neoproterozoic to Early Cambrian age, which suggests that the biological source(s) were particularly prominent in the later Neoproterozoic. We therefore propose that a high abundance of $C_{19}C$ may be used as an age indicator for Neoproterozoic to Early Cambrian samples. This is a particularly important indicator for oils, which can migrate.

Biomarker ratios that are known to vary with geological age include C_{28} to C_{29} regular and diasteranes, 24-nordiacholestanes to 27-nordiacholestanes and 24-isopropylcholestanes to 24-*n*-propylcholestanes. The observed increase in the $C_{28}/(C_{28}+C_{29})$ steranes ratio through the geological record may be associated with changes in the composition of phytoplankton assemblages through the Mesozoic Era (Grantham & Wakefield, 1988). Knoll et al. (2007) have directly attributed this to the rise to prominence of chlorophyll a + c containing phytoplankton (dinoflagellates, diatoms and coccolithophorids) that has been independently documented on the basis microfossil distributions. The ratio of $C_{28}/(C_{28}+C_{29})$ steranes in Paleozoic and Neoproterozoic oil samples is generally less than 0.4. Therefore, a ratio greater than 0.5 for bitumen from a Precambrian rock should be viewed with caution as it may be an indicator of contamination with younger hydrocarbons (Grantham & Wakefield, 1988; Schwark & Emt, 2006). It is important to note, however, that when studying individual rock

samples, as opposed to oils, the relative abundance of C₂₈ steranes has been shown to spike at extinctions events (Schwark & Emt, 2006). Similarly, some prasinophyte green algae biosynthesize a suite of sterols dominated by C₂₈ sterols (Kodner et al., 2008). Therefore, it is entirely possible that bitumens from individual Paleozoic or Proterozoic rock samples could have high C₂₈/ (C₂₈+C₂₉) steranes ratios.

Also of importance in this respect is the 24-nordiacholestanes ratio (Holba et al., 1998). The ratio of 24-nordiacholestanes/ (24-nordiacholestanes + 27-nordiacholestanes) increases roughly in accord with the diatom radiation in the Cenozoic and is therefore expected to be very low in the Ediacaran and Cambrian (Holba et al., 1998). It is important, however, to note that this ratio is entirely based on data from gathered from oil samples where the age of the source rocks is thought to be known quite well. Since there is no published database for the C₂₈/ (C₂₈+C₂₉) steranes ratio or the 24-nordiacholestanes/ (24-nordiacholestanes + 27-nordiacholestanes) ratio, the use of these in Paleozoic organic-rich rocks as indicators of contamination will remain subject to uncertainties. While steroids with the 24-norcholesterol structure have only been detected in extant diatoms and dinoflagellates (Rampen et al., 2007), it remains possible that their ancestors, or some other type of phytoplankton not yet analyzed for its natural products, produced compounds of this type in the past.

Neither of the above age biomarker ratios is useful for identifying rocks of Neoproterozoic to Cambrian age. The only age-diagnostic biomarker ratio known that can be applied to this respect is the ratio of 24-isopropylcholestanes to 24-*n*-propylcholestanes (24i/n) since it is only high in Neoproterozoic to Ordovician rock and oil samples (McCaffrey et al., 1994; Love et al., 2009). Sterols with an *n*-propyl side-chain substituent occur most prominently in marine chrysophyte algae (Moldowan et al., 1990). On the other hand, sterols bearing 24-isopropyl substituents occur most prominently in demosponges (McCaffrey et al., 1994; Love et al., 2009). Most phylogenies derived from 18S r-DNA and protein sequences identify demosponges as the most basal animal lineage (Sperling et al., 2007). One explanation for the very high 24i/n ratio for steranes that has been observed in Neoproterozoic to Cambrian oils and rocks is

that, as pioneering metazoans, demosponges (or their direct ancestors) enjoyed a relatively short period of ecological prominence with very little competition. As animal life continued to diversify, and predation and competition for space became the prime biological interactions for animal life, the relative importance of sponge biomass declined relative to other taxonomic groups. A decrease in the 24i/n ratio for steranes from the middle Cambrian to present is consistent with sponges occupying a comparatively minor ecological role throughout the Phanerozoic (McCaffrey et al., 1994; Love et al., 2009).

Distribution of C₁₉ norsterane C with lithology and depositional environment.

Figure 9 shows a correlation between C/ (A+B) and the gammacerane to hopane ratio (γ/H). The latter is an indicator of water column stratification and possibly hypersalinity (Sinninghe Damsté et al., 1995). Only sediment formations with high gammacerane to hopane values have a high abundance of C₁₉C, which suggests that the relative abundance of C₁₉C is controlled by similar factors that affect gammacerane. It also suggests that C₁₉C can also be used as a water stratification indicator.

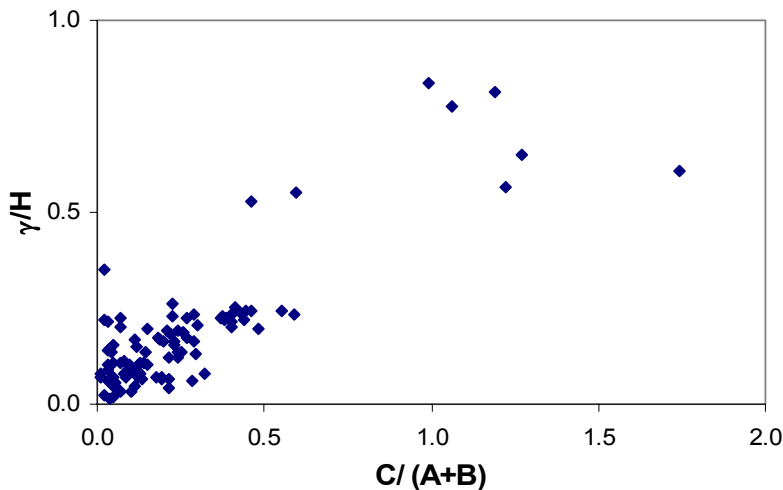


Figure 9. Cross-plot of C/ (A+B) with the gammacerane/ hopane (γ/H) ratio showing a positive correlation. The linear relationship has $R^2 = 0.72$.

Identity of C₁₉ norsterane C.

Three possibilities are immediately apparent as potential structures for a hydrocarbon molecule with the mass spectral features of the C₁₉ norsteranes. A prominent 260 to 203

transition suggests the possibility of A-norsteranes, 18-norsteranes or 19-norsteranes. A favored hypothesis is that the C₁₉ norsteranes are A-norsteranes, which is based on GC-MS MRM and full scan mass spectra and literature comparisons. A-norcholestanes and 19-norcholestanes have been synthesized in prior work (van Graas et al., 1982). Analyses of their mass spectra showed that the A-norcholestanes had a higher abundance of the 135 Da fragment compared to the 148 Da fragment whereas the reverse was true to the 19-norcholestanes. As can be seen in Figure 10, the abundance of the 135 Da fragment is greater than that of the 148 Da fragment for each of the three compounds. Using the known fragmentation pathways of cholestane as a reference, mass assignments for the fragmentation of three possible structures of the C₁₉ norsteranes are given in Figure 11.

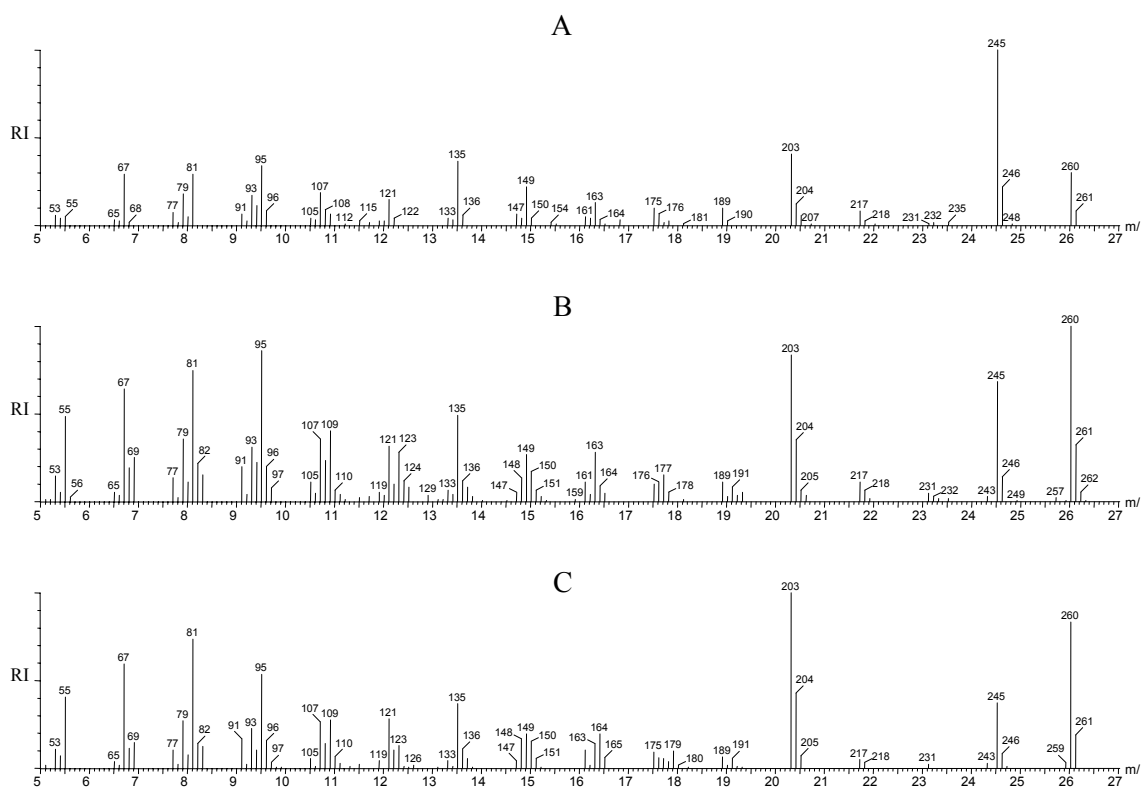


Figure 10. Spectra of C₁₉ norsteranes A, B, and C in Q oil sample OMO 001.

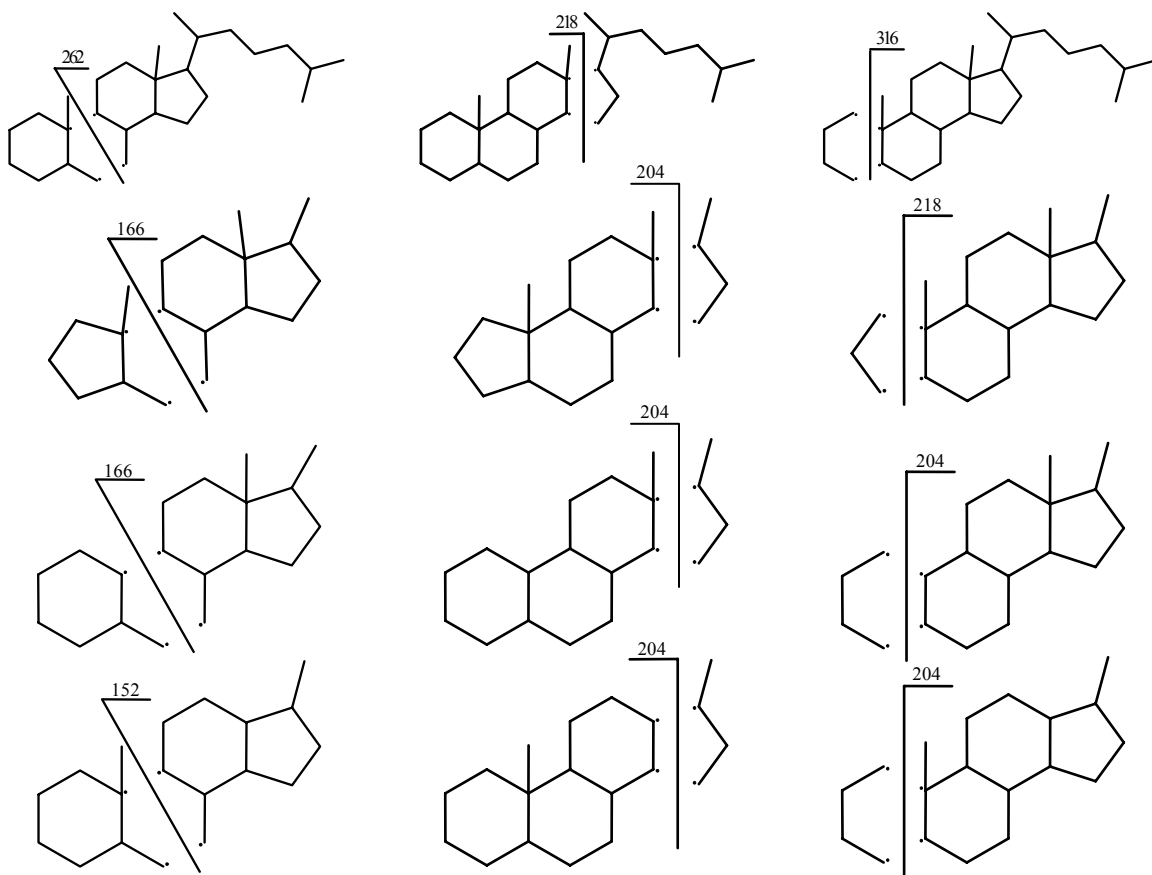


Figure 11. Fragmentation patterns used to identify the C₁₉ norsteranes.

To obtain more information on the structures of these compounds, two-dimensional gas chromatographic analysis (GCxGC) was conducted along with Time-of-Flight (TOF) mass spectrometric detection. Extending the chromatographic resolution to the second dimension reveals no added complexity for compounds C₁₉B and C₁₉C over that which was already evident in the conventional GC-MS approach, suggesting that these compounds are single isomers and pure compounds (Figure 12). The spectrum of compound C₁₉A was too weak to be able to discern properly. However, as expected, all three isomers eluted in the area diagnostic for compounds with 4 saturated hydrocarbon rings.

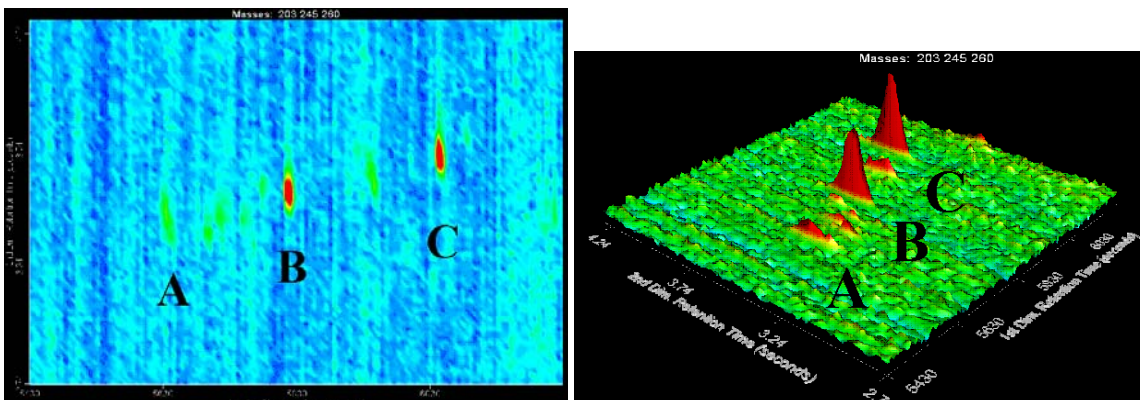


Figure 12. A GCxGC composite chromatogram of masses 203, 245, and 260 shown in two different views.

We also investigated the possibility that compound C₁₉C was the regular C₁₉ sterane 5 α , 14 α -androstane or another isomer of androstane. To accomplish this, we spiked a saturated hydrocarbon sample with a high abundance of C₁₉C with 5 α -androstane. This eluted just after compound C₁₉B, between C₁₉B, and C₁₉C, and had a mass spectrum that was distinct from C₁₉A, C₁₉B, and C₁₉C. An isomeric mixture of androstanes was then prepared via a high-temperature sealed-tube reaction using Pd/C as catalyst to promote rearrangement reactions. This reaction produced small amounts of new compounds with spectra consistent with the structure of androstane isomers. By GC-MS analysis, all of the neoformed compounds eluted earlier than 5 α -androstane and did not coelute with C₁₉A, C₁₉B, or C₁₉C (Figure 13). The GCxGC analysis of these androstane isomers is ongoing.

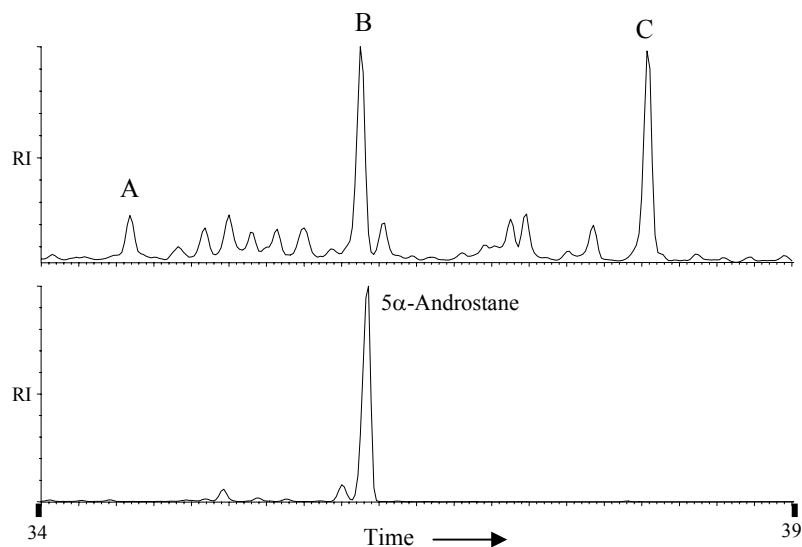


Figure 13. GC-MS chromatogram for a Q oil OMO 021 showing $C_{19}A$, $C_{19}B$, $C_{19}C$, and the isomers of androstane produced by sealed-tube isomerization. The data were collected in full scan mode on a DB-1 column with C_{19} compounds visualized through the 260 m/z selected ion chromatogram.

Mass spectral data suggest the most likely structures for the three isomers $C_{19}A$, $C_{19}B$, and $C_{19}C$ are A-norsteranes with different stereochemistries. Although the peaks elute seemingly too far apart to have closely similar structures, it is possible that different ring conformations result in bigger differences in retention time than one might expect. The difference in retention time is likely too small for $C_{19}A$ to be a diastereane form of $C_{19}B$ or $C_{19}C$. We are endeavoring to determine the precise structures of $C_{19}A$, $C_{19}B$, and $C_{19}C$ through chemical synthesis of authentic standards. This work is being conducted in collaboration with Professor J Rullkötter, University of Oldenburg. An attempt to isolate these compounds from SOSB sediments in order to determine the structure using NMR spectroscopy is also underway.

A-norsteranes have a contracted A-ring (i.e. five instead of six carbon atoms). C_{26} - C_{28} A-norsteranes with $5\beta(H)$ - and $5\alpha(H)$ - configurations have been previously identified in Cretaceous black shales by mass spectroscopy (van Graas et al., 1982). However, to the best of our knowledge, no analogous compounds lacking side-chains have been reported. In more recent studies of late Neoproterozoic rocks and oils from the South Oman Salt Basin (SOSB), three isomeric C_{19} norsteranes (A, B, and C) were identified as components of saturated hydrocarbon fractions (Grosjean et al., 2009). A potential

precursor molecule would most likely be a sterol with a hydroxymethyl group at the 3 position on the A ring and possibly one or two double bonds elsewhere in the structure. Such structures exist in nature (Minale & Sodano, 1974a; Kanazawa et al., 1979; Bohlin et al., 1980; Kitagawa et al., 1983; Djerassi & Silva, 1991). Through diagenesis, the hydroxymethyl functionality on such a compound could be oxidized and lost through decarboxylation. It has also been suggested that A-norsteranes in sediments are derived from A-norsterols, or that they may be diagenetic products of cholesterol (Kerr & Baker, 1991). The only organisms known to date that synthesize A-norsteroids are sponges (Minale & Sodano, 1974a; Kanazawa et al., 1979; Bohlin et al., 1980; van Graas et al., 1982; Kitagawa et al., 1983; Djerassi & Silva, 1991), which synthesize them from dietary sterols (De Rosa et al., 1975a). These include 3-hydroxymethyl-A-norsteranes with C₈-C₁₀ side chains (Minale & Sodano, 1974a; Kanazawa et al., 1979; Bohlin et al., 1980), 3-hydroxymethyl-A-norsterenes with C₈-C₁₀ side chains (Kanazawa et al., 1979; Bohlin et al., 1980; Teshima et al., 1980), and 3-hydroxymethyl-A-norgorgostane (Bohlin et al., 1980).

An 18-norsterane lacks the angular methyl group normally at carbon 13. No compounds of this type have previously been identified in the rock record. The only known potential precursor molecules, 18-norsteroids, known to date are the 18-norpregane derivative fukujusonorone, which was extracted from Japanese pheasant eyes (Shimizu et al., 1969; Solomon et al., 1974) and veralkamine, which was extracted from the angiosperm *Veratrum album* (Tomko et al., 1967).

A 19-norsterane lacks the angular methyl group normally found at carbon 10. As yet, no compounds of this type have been identified in the rock record. However, possible precursor 19-norsteroids have been found in nature and the sources include gorgonians (Popov et al., 1976; Popov et al., 1983), a sponge (Minale & Sodano, 1974b), soft coral (Huang, 2008), and fungi (Barrero et al., 1998; Nieto & A., 2008). Though a 19-norcholesta-5,7,9(10)-trien-3 β -ol has been detected in blood plasma and faeces of humans with Smith-Lemli-Opitz syndrome (Batta et al., 1995), it may have been formed during the analyses as a conversion product of cholesta-5,8-dien-3 β -ol (Ruan et al.,

1996). The fungal 19-norsterol is neoergosterol, but it is not as likely to be a precursor to a saturated 19-norsterane because its B ring is aromatized and this would likely remain so through diagenesis. It has been shown that the sponge *Axinella polypoides* synthesizes 19-norsteroids via modification of a regular dietary steroid precursor (De Rosa et al., 1975b). Another group of molecules that could lead to 19-norsteranes in the rock record are 19-OH sterols. These compounds have been isolated from soft corals (Bortolotto et al., 1976; Iguchi et al., 1989; Wang et al., 1992; Duh et al., 1998; Rao et al., 1999; Huang, 2008) and a sponge (Gunasekera & Schmitz, 1983). Again, the hydroxymethyl group is more readily oxidized than a simple methyl substituent and can then be lost via decarboxylation.

The other interesting feature of the C₁₉ norsteranes presented, besides the unusual nucleus, is the shortened side chain. Only a few types of organisms are known to dealkylate sterol side chains. Those able to dealkylate at C₂₄ are mollusks (Collignon-Thiennot et al., 1973; Saliot & Barbier, 1973; Khalil & Idler, 1976; Teshima et al., 1979), crustaceans (Teshima & Kanazawa, 1971; Kanazawa et al., 1976), a cnidarian (Saliot & Barbier, 1973), sponges (Malik et al., 1988; Kerr et al., 1990), nematodes (Chitwood, 1999 and refs within), and insects (Clark & Bloch, 1959; Robbins et al., 1962; Ikekawa et al., 1966). This process may be more widespread, however, as the last step in this dealkylation has been shown in a green alga (Giner & Djerassi, 1992).

Side chains shorter than C₈ have also been identified in a gorgonian (Popov et al., 1983). 24-norsteranes are likely formed by 24-norsterols which are probably sterols alkylated at C₂₄ and then C₂₆ and C₂₇ are removed. Organisms that synthesize 24-norsterols include bivalves (Goad, 1981). A sponge makes a 19, 24-dinorsterol (Minale & Sodano, 1974b).

Though A-norsteranes have been suggested to be sponge biomarkers (van Graas et al., 1982), they were encountered in sediments of the Walcott Member of the Chuar Group, which is between ~800 and 742 Ma (Karlstrom et al., 2000). This may, or may not, be older than the evolution of sponges as it is older than the ~713 Ma Sturtian glacial (Bowring et al., 2007) and the current earliest evidence for sponges is just before the

Marinoan glacial around 650 Ma (Love et al., 2009). Of the organisms known to shorten sterol side chains today, none have been shown to have evolved by the early Neoproterozoic where we clearly see C₁₉ norsteranes in sediments, however these metazoans had unicellular ancestors. Novel steroids could reasonably be predicted to have arisen in these lineages.

Distribution of 21-norsteranes with lithology and depositional environment.

21-Norsteranes have been proposed to occur in high concentration in hypersaline environments of relatively immature rocks and oils generated in the early oil window (Bao & Li, 2001; Grosjean et al., 2009). As shown in Figure 14, the 21-norcholestane and 21-norstigmastane ratios follow expected trends, broadly correlating with gammacerane to hopane ratios. The abundance of 21-norstigmastane is measured relative to the closely-eluting 5 α ,14 β ,17 β -20R isomer of ergostane. It has been shown that 21-norsteranes are susceptible to input from thermal cracking of other steroids in rocks and oils of high thermal maturity (Moldowan et al., 1991). The ratio of 18 α -22,29,30-trisnorneohopane (Ts) relative to C₃₀ hopane is a well-known as maturity indicator useful for post-mature samples (Volkman et al., 1983). If we remove the samples from the gammacerane to hopane plot with a Ts/ C₃₀ hopane ratio greater than 1.5, which are the most likely to have an additional input from thermal cracking, we obtain a more linear trend, as shown in Figure 15.

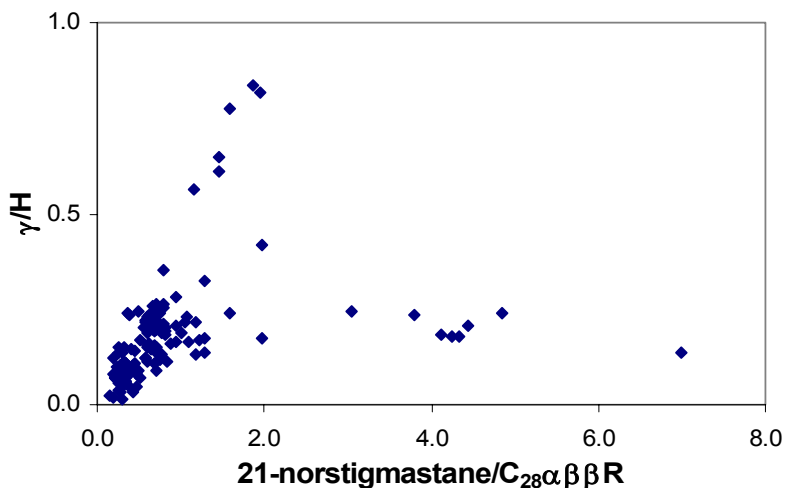


Figure 14. Crossplot of γ/H vs. $21\text{-norstigmastane}/C_{28}\alpha\beta\beta R$ showing a weak positive correlation.

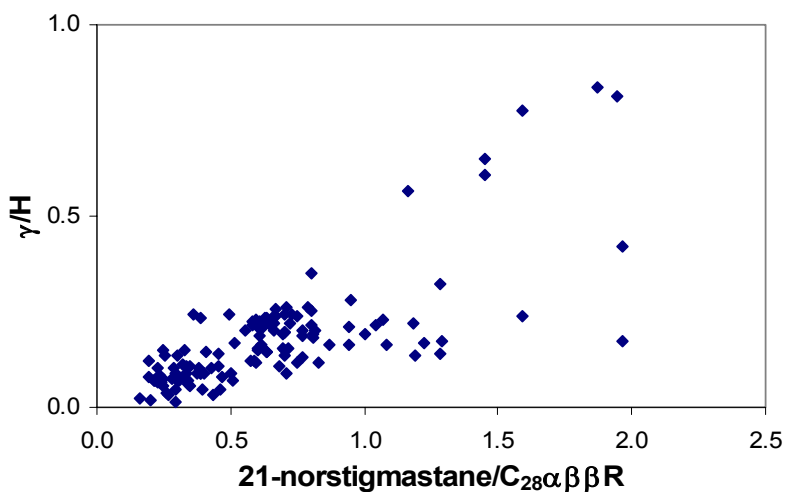


Figure 15. Crossplot of γ/H vs. $21\text{-norstigmastane}/C_{28}\alpha\beta\beta R$ without post-mature samples, showing a positive correlation. The linear relationship has $R^2 = 0.56$.

Despite the fact that a few oils in our study were clearly of high thermal maturity and Moldowan et al. (1991) have shown that of C_{26} steranes, 21-norsteranes are the most thermally stable, there is likely only a small contribution of these compounds to the sediments that derives from the thermal cracking of higher molecular weight steroids. Hydropyrolysis experiments have produced 21-norsteranes directly from kerogen hydropyrolysates, which suggests that their precursors were most likely incorporated into the kerogen during the earliest stages of diagenesis (Farrimond et al., 2003; Love, 2008). Figure 16 compares chromatograms for the saturated bitumen extract vs. the kerogen

hydropyrolysis product of the Oman sample OMR 235 of the A2C unit of the Ara Formation. The 21-norsteranes are in high abundance in all cases where this experiment was carried out, suggesting that the compounds were present as 21-norsterols (or possibly also functionalized at C₂₁) in the sedimentary environment and incorporated into the kerogen during the earliest stages of diagenesis.

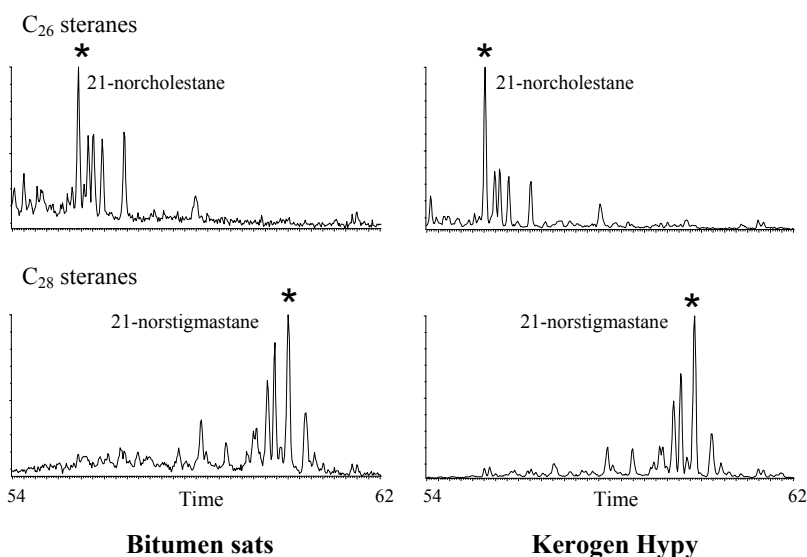


Figure 16. GC-MS data showing the C₂₆ and C₂₈ 21-norsterane abundances in bitumen and kerogen hydropyrolysate of rock sample OMR 235 of the A2C from Oman. Data from G. Love.

Although the structures of the 24-methyl and 24-ethyl homologues of the 21-norsteranes have yet to be proven, we can be confident that their relative retention times and specific mass spectroscopic fragmentations are entirely consistent with this assignment. Also, the relative abundances in the different families of SOSB oils support this identification. In the Huqf and carbonate stringer oil families where C₂₉ steranes are dominant, 21-norstigmastane is the most prominent homologue. In the Q oil family where C₂₇ steranes are dominant, 21-norcholestane is the most prominent homologue. The correlation between cholestane to 21-norcholestane and stigmastane to 21-norstigmastane is shown in Figure 17. This uneven distribution in the rock record also supports the suggestion that they are not diagenetic products since these processes would affect all of the steranes similarly. It is more likely that a specific organism assimilated conventional sterols and subsequently altered them to yield compounds that then degraded to 21-norsteranes.

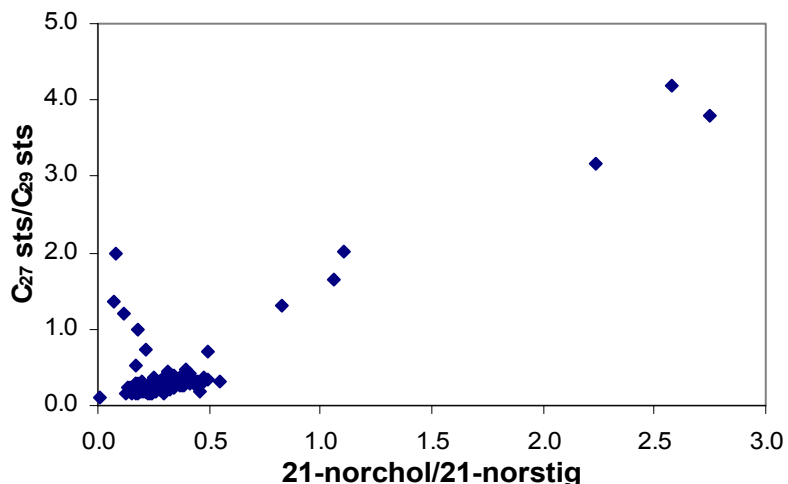


Figure 17. Crossplot of C₂₇ steranes/ C₂₉ steranes vs. 21-norcholestanol/ 21-norstigmastane showing a positive correlation. The linear relationship has R² = 0.78.

21-Norsteranes lack the methyl group that is attached to C₂₀ in a conventional steroid. These may be derived from 21-norsterols or a sterol with a functionalized C₂₁ that is easily removed through oxidation. It is not known, if they even exist, how 21-norsterols are synthesized. It may be through a simple excision of C₂₁ or it may be through the common conversion of cholesterol to a hormone with a C₂₁-pregnane skeleton hydroxylated at C₂₀ followed by transmethylation reactions by S-adenosylmethionine to build up the rest of the side chain (Goad, 1981).

Conclusions

Three isomers of a C₁₉ norsterane have been recognized in SOSB oils and rocks. One isomer (C₁₉C) is potentially useful as an indicator of water column stratification for rocks and oils of Neoproterozoic to Early Cambrian age. Compound C₁₉B is usually the dominant isomer. Analysis of their mass spectra suggests that all are A-norsterane isomers. Although the source organism(s), and more importantly the function, of compound C₁₉C remain unknown, it is quite useful as an age marker and water column stratification indicator.

The origins of the 21-norcholestanes are also enigmatic. However, it appears that the molecules in this series are also useful as indicators of water column stratification. For

samples of the middle oil window or of relatively higher maturity it may be difficult to resolve their diagenetic versus biological sources (Moldowan et al., 1991), however from the hydrolysis results it is clear that these steranes are formed in early diagenesis. This suggests that though there is also a possible contribution due to thermal maturation, there is likely a strong biological contribution. In immature to moderately thermally mature sediments 21-norsteranes are most abundant in samples from stratified depositional environments suggesting a biological source that is hypersaline or redox tolerant. The parent compounds may have been sterols functionalized at C₂₁, allowing facile oxidation and cleavage in early diagenesis.

Acknowledgements

The author wishes to thank Gordon Love for the hydrolysis experiment and Robert Nelson and Christopher Reddy for GCxGC experiment (run by Dr. Nelson in the Reddy lab).

References

- Anbar, A. D.; Knoll, A. H. **2002**. Proterozoic ocean chemistry and evolution: A bioinorganic bridge? *Science* **297**, 1137-1142.
- Bao, J.; Li, M. **2001**. Unprecedented occurrence of novel C₂₆-C₂₈ 21-norcholestanes and related triaromatic series in evaporitic lacustrine sediments. *Org. Geochem.* **32**, 1031–1036.
- Barrero, A. F.; Oltra, J. E.; Poyatos, J. A.; Jiménez, D.; Oliver, E. **1998**. Phycomysterols and other sterols from the fungus *Phycomyces blakesleeanus*. *J. Nat. Prod.* **61**, 1491-1496.
- Batta, A. K.; Salen, G.; Tint, G. S.; Shefer, S. **1995**. Identification of 19-nor-5,7,9(10)-cholestatrien-3 β -ol in patients with Smith-Lemli-Opitz syndrome. *J. Lipid Res.* **36**, 2413-2418.
- Bohlin, L.; Gehrken, H. P.; Scheuer, P. J.; Djerassi, C. **1980**. Minor and trace sterols in marine invertebrates XVI. 3 ξ -Hydroxymethyl-A-nor-5 α -gorgostane, a novel sponge sterol. *Steroids* **35**, 295-304.
- Bortolotto, M.; Braekman, J. C.; Daloz, D.; Losman, D.; Tursch, B. **1976**. Chemical studies of marine invertebrates. XXIII. A novel polyhydroxylated sterol from the soft coral *Litophyton viridis* (coelenterata, octocorallia, alcyonacea). *Steroids* **28**, 461-466.
- Bowring, S. A.; Grotzinger, J. P.; Condon, D. J.; Ramezani, J.; Newall, M. J.; Allen, P. A. **2007**. Geochronologic constraints on the chronostratigraphic framework of the Neoproterozoic Huqf Supergroup, Sultanate of Oman. *Am. J. Sci.* **307**, 1097-1145.

- Canfield, D. E.; Teske, A. **1996**. Late Proterozoic rise in atmospheric oxygen concentration inferred from phylogenetic and sulphur-isotope studies. *Nature* **382**, 127-132.
- Chitwood, D. J. **1999**. Biochemistry and function of nematode steroids. *Crit. rev. biochem. mol. biol.* **34**, 273-284.
- Clark, A. J.; Bloch, K. **1959**. Conversion of ergosterol to 22-dehydrocholesterol in *Blattella germanica*. *J. Biol. Chem.* **234**, 2589-2594.
- Cloud, P. E. Jr. **1968**. Atmospheric and hydrospheric evolution on the primitive Earth. *Science* **160**, 729-736.
- Collignon-Thiennot, F.; Allais, J.-P.; Barbier, M. **1973**. Existence de deux voies de biosynthèse du cholestérol chez un mollusque: la Patelle *Patella vulgate* L., (Gastéropodes, Prosobranches, Archéogastéropodes). *Biochimie* **55**, 579-582.
- De Rosa, M.; Minale, L.; Sodano, G. **1975a**. Metabolism in Porifera IV. Biosynthesis of the 3 β -hydroxymethyl-A-nor-5 α -steranes from cholesterol by *Axinella verrucosa*. *Experientia* **31**, 408-410.
- De Rosa, M.; Minale, L.; Sodano, G. **1975b**. Metabolism in Porifera-V. Biosynthesis of 19-nor-stanols: conversion of cholesterol into 19-nor-cholestanols by the sponge *Axinella polypoides*. *Experientia* **31**, 758-759.
- Derry, L. A.; Kaufman, A. J.; Jacobsen, S. B. **1992**. Sedimentary cycling and environmental change in the Late Proterozoic: Evidence from stable and radiogenic isotopes. *Geochim. et Cosmochim. Acta* **56**, 1317-1329.
- Des Marais, D. J.; Strauss, H.; Summons, R. E.; Hayes, J. M. **1992**. Carbon isotope evidence for the stepwise oxidation of the Proterozoic environment. *Nature* **359**, 605-609.
- Djerassi, C. & Silva, C. J. **1991**. Sponge sterols: Origin and biosynthesis. *Acc. Chem. Res.* **24**, 371-378.
- Duh, C.-Y.; Wang, S.-K.; Chu, M.-J.; Sheu, J.-H. **1998**. Cytotoxic sterols from the soft coral *Nephthea erecta*. *J. Nat. Prod.* **61**, 1022-1024.
- Farrimond, P.; Love, G. D.; Bishop, A. N.; Innes, H. E.; Watson, D. F.; Snape, C. E. **2003**. Evidence for the rapid incorporation of hopanoids into kerogen. *Geochim. Cosmochim. Acta* **67**, 1383-1394.
- Fike, D. A.; Grotzinger, J. P.; Pratt, L. M.; Summons, R. E. **2006**. Oxidation of the Ediacaran ocean. *Nature* **444**, 744-747.
- Giner, J. L.; Djerassi, C. **1992**. Evidence for sterol side-chain dealkylation in *Chlamydomonas reinhardtii*. *Phytochemistry* **31**, 3865-3867.
- Goad, L. J. **1981**. Sterol biosynthesis and metabolism in marine invertebrates. *Pure & Appl. Chem.* **51**, 837-852.
- Grantham, P. J.; Wakefield, L. L. **1988**. Variations in the sterane carbon number distributions of marine source rock derived crude oils through geological time. *Org. Geochem.* **12**, 61-73.
- Grosjean, E.; Love, G. D.; Stalvies, C.; Fike, D. A.; Summons, R. E. **2009**. Origin of petroleum in the Neoproterozoic-Cambrian South Oman Salt Basin. *Org. Geochem.* **40**, 87-110.
- Grosjean, E.; Love, G. D.; Kelly, A. E.; Summons, R. E. In prep. Clues to the origin of the 'Q' oils and condensates of North Oman: Geochemical evidence for an Early Cambrian origin of the 'Q' oils and condensates of North Oman.

- Gunasekera, S. P.; Schmitz, F. J. **1983**. Marine natural products: $9\alpha,11\alpha$ -epoxycholest-7-ene- $3\beta,5\alpha,6\beta,19$ -tetrol 6-acetate from a sponge, *Dysidea* sp. *J. Org. Chem.* **48**, 885-886.
- Holba, A. G.; Tegelaar, E. W.; Huizinga, B. J.; Moldowan, J. M.; Singletary, M. S.; McCaffrey, M. A.; Dzou, L. I. P. **1998**. 24-norcholestanes as age-sensitive molecular fossils. *Geology* **26**, 783-786.
- Huang, Y.-C. **2008**. Chemical constituents and anti-inflammatory activity studies of Formosan soft coral *Nephthea chabrolii*. Master's thesis, National Sun Yat-sen University.
- Iguchi, K.; Saitoh, S.; Yamada, Y. **1989**. Novel 19-oxygenated sterols from the Okinawan soft coral *Litophyton viridis*. *Chem. Pharm. Bull.* **37**, 2553-2554.
- Ikekawa, N.; Suzuki, M.; Kobayashi, M.; Tsuda, K. **1966**. Studies on the sterol of *Bombyx mori* L. IV. Conversion of the sterol in the silkworm. *Chem. Pharm. Bull.* **14**, 834-836.
- Kanazawa, A.; Guary, J.-C. B.; Ceccaldi, H. J. **1976**. Metabolism of [^{14}C] β -sitosterol injected at various stages of the molting cycle in prawn *Penaeus japonicus* bate. *Comp. Biochem. Physiol.* **54B**, 205-208.
- Kanazawa, A.; Teshima, S.-I.; Hyodo, S.-I. **1979**. Sterols of the sponges (Porifera class Demospongiae). *Comp. Biochem. Physiol.* **62B**, 521-525.
- Karlstrom, K. E.; Bowring, S. A.; Dehler, C. M.; Knoll, A. H.; Porter, S. M.; Des Marais, D. J.; Weil, A. B.; Sharp, Z. D.; Geissman, J. W.; Elrick, M. B.; Timmons, J. M.; Crossey, L. J.; Davidek, K. L. **2000**. Chuar Group of the Grand Canyon: Record of breakup of Rodinia, associated change in the global carbon cycle, and ecosystem expansion by 740 Ma. *Geology* **28**, 619-622.
- Kerr, R. G.; Baker, B. J. **1991**. Marine Sterols. *Nat. Prod. Rep.* **8**, 465-497.
- Kerr, R. G.; Baker, B. J.; Kerr, S. L.; Djerassi, C. **1990**. Biosynthetic studies of marine lipids-XXIX. Demonstration of sterol side chain dealkylation using cell-free extracts of marine sponges. *Tetrahedron Lett.* **31**, 5425-5428.
- Khalil, M. W.; Idler, D. R. **1976**. Steroid biosynthesis in the whelk, *Buccinum undatum*. *Comp. Biochem. Physiol.* **55B**, 239-242.
- Kitagawa, I.; Kobayashi, M.; Kitanaka, K.; Kido, M.; Kyogoku, Y. **1983**. Marine natural products. XII. On the chemical constituents of the Okinawan marine sponge *Hymeniacidon aldis*. *Chem. Pharm. Bull.* **31**, 2321-2328.
- Knoll, A. H.; Carroll, S. B. **1999**. Early animal evolution: Emerging views from comparative biology and geology. *Science* **284**, 2129-2137.
- Knoll, A.H.; Summons, R. E.; Waldbauer, J.; Zumberge, J. **2007**. The geological succession of primary producers in the oceans. In: The Evolution of Primary Producers in the Sea. (P. Falkowski & A.H. Knoll, eds.), Elsevier, Burlington, pp. 133-163.
- Kodner, R. B.; Pearson, A.; Summons, R. E.; Knoll, A. H. **2008**. Sterols in red and green algae: quantification, phylogeny, and relevance for the interpretation of geologic steranes. *Geobiology* **6**, 411-420.
- Lambert, I. B.; Walter, M. R.; Wenlong, Z.; Songnian, L.; Guogan, M. **1987**. Palaeoenvironment and carbon isotope stratigraphy of Upper Proterozoic carbonates of the Yangtze Platform. *Nature* **325**, 140-142.
- Love, G. D. **2008**. pers. comm.

- Love, G. D.; Grosjean, E.; Stalvies, C.; Fike, D. A.; Grotzinger, J. P.; Bradley, A. S.; Kelly, A. E.; Bhatia, M.; Meredith, W.; Snape, C. E.; Bowring, S. A.; Condon, D. J.; Summons, R. E. **2009**. Fossil steroids record the appearance of Demospongiae during the Cryogenian Period. *Nature* **457**, 718-721.
- Malik, S.; Kerr, R. G.; Djerassi, C. **1988**. Biosynthesis of marine lipids. 19. Dealkylation of the sterol side chain in sponges. *J. Am. Chem. Soc.* **110**, 6895-6897.
- McCaffrey, M. A.; Moldowan, J. M.; Lipton, P. A.; Summons, R. E.; Peters, K. E.; Jeganathan, A.; Watt, D. S. **1994**. Paleoenvironmental implications of novel C₃₀ steranes in Precambrian to Cenozoic age petroleum and bitumen. *Geochim. Cosmochim. Acta* **58**, 529-532.
- McFadden, K. A.; Huang, J.; Chu, X.; Jiang, G.; Kaufman, A. J.; Zhou, C.; Yuan, X.; Xiao, S. **2008**. Pulsed oxidation and biological evolution in the Ediacaran Doushantuo Formation. *Proc. Natl. Acad. USA* **105**, 3197-3202.
- Minale, L.; Sodano, G. **1974a**. Marine sterols: Unique 3 β -hydroxymethyl-A-nor-5 α -steranes from the sponge *Axinella verrucosa*. *J. C. S. Perkin I* 2380-2384.
- Minale, L.; Sodano, G. **1974b**. Marine sterols: 19-Nor-stanols from the sponge *Axinella polypoides*. *J. C. S. Perkin I* 1888-1892.
- Moldowan, J. M.; Fago, F. J.; Lee, C. Y.; Jacobson, S. R.; Watt, D. S.; Slougui, N.-E.; Jeganathan, A.; Young, D. C. **1990**. Sedimentary 24-*n*-propylcholestanes, molecular fossils diagnostic of marine algae. *Science* **247**, 309-312.
- Moldowan, J. M.; Lee, C. Y.; Watt, D. S.; Jeganathan, A.; Slougui, N.-E.; Gallegos, E. J. **1991**. Analysis and occurrence of C₂₆-steranes in petroleum and source rocks. *Geochim. Cosmochim. Acta* **55**, 1065-1081.
- Nieto, I. J.; A., C. C. **2008**. Triterpenoids and fatty acids identified in the edible mushroom *Pleurotus sajor-caj*ú. *J. Chil. Chem. Soc.* **53**, 1515-1517.
- Popov, S.; Carlson, R. M. K.; Wegmann, A.-M.; Djerassi, C. **1976**. Occurrence of 19-nor cholesterol and homologs in marine animals. *Tetrahedron Lett.* **39**, 3491-3494.
- Popov, S.; Carlson, R. M. K.; Djerassi, C. **1983**. Occurrence and seasonal variation of 19-norcholes-4-en-3-one and 3 β -monohydroxy sterols in the Californian gorgonian *Muricea californica*. *Steroids* **41**, 537-548.
- Porter, S. H. **2004**. The fossil record of early eukaryotic diversification. *Paleontological Society Papers* **10**, 35-50.
- Rampen, S. W.; Schouten, S.; Abbas, B.; Panoto, F. E.; Muyzer, G.; Campbell, C. N.; Fehling, J.; Sinninghe Damsté, J. S. **2007**. On the origin of 24-norcholestanes and their use as age-diagnostic biomarkers. *Geology* **35**, 419-422.
- Rampen, S. W.; Schouten, S.; Hopmans, E. C.; Abbas, B.; Noordeloos, A. A.M.; Geenevasen, J. A.J.; Moldowan, J. M.; Denisevich, P.; Sinninghe Damsté, J. S. **2009**. Occurrence and biomarker potential of 23-methyl steroids in diatoms and sediments. *Org. Geochem.* **40**, 219-228.
- Rao, M. R.; Venkatesham, U.; Venkateswarlu, Y. **1999**. Two new 19-oxygenated polyhydroxy steroids from the soft coral *Nephthea chabroli*. *J. Nat. Prod.* **62**, 1584-1585.
- Robbins, W. E.; Dutky, R. C.; Monroe, R. E.; Kaplanis, J. N. **1962**. The metabolism of H³- β -sitosterol by the German cockroach. *Ann. Entomol. Soc. Am.* **55**, 102-104.
- Ruan, B.; Pang, J.; Wilson, W. K.; Schroepfer, Jr., G. J. **1996**. Concerning the thermolability of cholesta-5,8-dien-3 β -ol, a sterol that accumulates in blood and

- tissues in a human genetic developmental disorder. *Bioorg. Med. Chem. Lett.* **6**, 2421-2424.
- Saliot, A.; Barbier, M. **1973**. Stérols en solution dans l'eau de mer: Leur utilisation par les invertébrés marins. *J. exp. mar. Biol. Ecol.* **13**, 207-214.
- Schwark, L.; Empt, P. **2006**. Sterane biomarkers as indicators of palaeozoic algal evolution and extinction events. *Palaeogeogr. palaeoclimatol. palaeoecol.* **240**, 225-236.
- Shimizu, Y.; Sato, Y.; Mitsuhashi, H. **1969**. Isolation and characterization of fukujusonorone, a 18-norpregnane derivative from *Adonis amurensis* Regel et Radd. *Experientia* 1129-1130.
- Sinninghe Damsté, J. S.; Kenig, F.; Koopmans, M. P., Köster, J.; Schouten, S.; Hayes, J. M.; de Leeuw, J. W. **1995**. Evidence for gammacerane as an indicator of water-column stratification. *Geochim. Cosmochim. Acta* **59**, 1895-1900.
- Solomon, P. H.; Nakanishi, K.; Fallon, W. E.; Shimizu, Y. **1974**. Confirmation of 18-norsteroidal structure of "fukujusonorones." sensitivity of CMR to configurational changes. *Chem. pharm. bull.* **22**, 1671-1673.
- Sperling, E. A.; Pisani, D.; Peterson, K. J. **2007**. Poriferan paraphyly and its implications for Precambrian palaeobiology. In: *The Rise and Fall of the Ediacaran Biota*. (P. Vickers-Rich & P. Komarower, eds.), The Geological Society of London, Special Publications 286, London, pp. 355-368.
- Teshima, S.-I.; Kanazawa, A. **1971**. Bioconversion of the dietary ergosterol to cholesterol in *Artemia salina*. *Comp. Biochem. Physiol.* **38B**, 603-607.
- Teshima, S.-I.; Kanazawa, A.; Miyawaki, H. **1979**. Metabolism of β -sitosterol in the mussel and the snail. *Comp. Biochem. Physiol.* **63B**, 323-328.
- Teshima, S.-I.; Kanazawa, A.; Hyodo, S.-I. **1980**. 3 β -Hydroxymethyl-24-methylene-A-nor-5 α -cholestane from the sponge. *Bull. Jpn. Soc. Sci. Fish.* **46**, 1517-1520.
- Tomko, J.; Vassová, A.; Adam, G.; Schreiber, K.; Höhne, E. **1967**. Veralkamine, a novel type of steroidal alkaloid with a 17 β -methyl-18nor-17-isocholestane carbon skeleton. *Tetrahedron Lett.* **40**, 3907-3911.
- van Graas, G.; de Lange, F.; de Leeuw, J. W.; Schenck, P. A. **1982**. A-nor-steranes, a novel class of sedimentary hydrocarbons. *Nature* **296**, 59-61.
- Volkman, J. K.; Alexander, R.; Kagi, R. I.; Woodhouse, G. W. **1983**. Demethylated hopanes in crude oils and their applications in petroleum geochemistry. *Geochim. Cosmochim. Acta* **47**, 785-794.
- Wang, G. S.; Li, F. Y.; Zeng, L. M.; Ma, L. B.; Tu, G. Z. **1992**. Structure determination of Nepalsterol A and B with 19-hydroxy group from soft coral *Nephthea*. *Chem. J. Chin. Univ.* **13**, 623-627.

4. C-Isotopic Studies of Hydrocarbons in Neoproterozoic to Cambrian Samples

Abstract

The Neoproterozoic Era marks the first appearance of animals in the fossil record. Much research has been focused on the ventilation of the global ocean in the Neoproterozoic as it is considered a primary factor in the diversification of life at this time. One of the most interesting features of the Neoproterozoic record is the presence of large excursions in the $\delta^{13}\text{C}$ of carbonates, with little to no corresponding change in the $\delta^{13}\text{C}$ of the coeval organic carbon. To delve into what was happening in the organic carbon cycle, we chose to study two series of organic compounds using compound-specific carbon isotope analysis of samples from Oman, Eastern Siberia and Australia. This chapter describes a widespread reversal in isotopic patterns in the Ediacaran and the implications of this change. In rocks and oils older than ~550 Ma, *n*-alkanes are enriched in ^{13}C relative to the acyclic isoprenoids pristane and phytane. In younger sediments, the *n*-alkanes are depleted compared to these isoprenoids, with the possible exception of those deposited during Phanerozoic oceanic anoxic events. In Oman, this transition coincides with the termination of the Shuram Excursion, an interval when marine carbonates show very negative $\delta^{13}\text{C}$ values with no corresponding shift in the isotopic composition of co-occurring organic carbon. Several hypotheses for the cause(s) of this isotopic switch will be examined and the possible relationship to the radiation of metazoans will be addressed. The most likely cause is the availability of oxygen. This work uses an independent means to examine the ocean redox changes of the Neoproterozoic, corroborating previous data showing ventilation of at least shallow marine regions by ~550 Ma. The data also show that though the bulk $\delta^{13}\text{C}$ of organics during this time period does not change markedly, a large community reorganization may have occurred.

Introduction

Much of recent Neoproterozoic research has been focused on understanding the timing and extent of the ventilation of the global ocean. Recently, carbon and sulfur isotopes have been used to suggest ventilation of the water column by ~550 Ma (Fike et al., 2006; McFadden et al., 2008). Molybdenum concentration data support these results (Scott et

al., 2008). The work presented here concerns the timing and global nature of this phenomenon using an independent form of measurement, compound specific $\delta^{13}\text{C}$ isotopes of hydrocarbon isoprenoids and *n*-alkanes. It has been hypothesized that the change in isotopic fractionation between these molecules is related to the oxidation state of the ocean (Logan et al., 1995). To obtain a more global perspective we studied a range of rocks and oils from individual basins in Oman, Eastern Siberia and Australia. We also analyzed the relationship of these compound specific isotopes to the bulk isotopic changes in Oman, where we have the best lithographic and age constraints.

Recent work has shown that though there are large excursions in the carbonate isotope record, the $\delta^{13}\text{C}$ of the corresponding organics was quite stable in the Ediacaran (Fike et al., 2006; McFadden et al., 2008). Since there is little change in the bulk organic signal in the Ediacaran, we chose to study the isotopic compositions of specific organic compound classes for further information: molecules derived from primary producers, isoprenoids, and from primary producers and heterotrophs, *n*-alkanes.

The main isoprenoids of interest are pristane and phytane, which are primarily derived from the phytol side chain of chlorophyll a (Blumer et al., 1963; Blumer & Snyder 1965; Didyk et al., 1978). The ester side chain of chlorophyll a is easily hydrolyzed, producing phytol, which, in oxic environments, is subsequently oxidized and decarboxylated to yield pristane. In reducing environments, it yields phytane (Didyk et al., 1978). Much less specific biomarkers are *n*-alkanes, which are derived from the lipids of diverse autotrophic and heterotrophic organisms, including both protists and bacteria. Thus, to a first approximation, pristane and phytane can be considered to represent input from primary producers, whereas *n*-alkanes can be considered to represent the input from both primary producers and heterotrophs.

Consider the food chain in Figure 1, where primary producers use inorganic carbon with an isotopic composition of δ_a to biosynthesize isoprenoids with an isotopic composition of δ_1 and *n*-alkanes with an isotopic composition of δ_{2p} . These primary producers are then consumed by heterotrophs that biosynthesize *n*-alkanes with an isotopic composition of

δ_{2h} . An important value that will be referred to from this point forward is Δ , which is $\delta_2 - \delta_1$, where δ_1 is the average $\delta^{13}\text{C}$ of the isoprenoids pristane and phytane in a sample, and δ_2 is the average $\delta^{13}\text{C}$ of the *n*-alkanes *n*-C₁₇ and *n*-C₁₈ in a sample that were biosynthesized by both the primary producers and heterotrophs. The absolute values of δ_1 and δ_2 and their ordering with respect to each other are not the focus. Rather, the importance lies in the trend of Δ . In the Neoproterozoic, an unconventional relationship exists between isoprenoids and *n*-alkanes where Δ is positive, whereas in latest Ediacaran and most of Phanerozoic rocks Δ is negative. A negative Δ is considered conventional because it is consistent with the ordering imposed by the isoprenoidal and acetogenic biosynthetic pathways for most marine organisms.

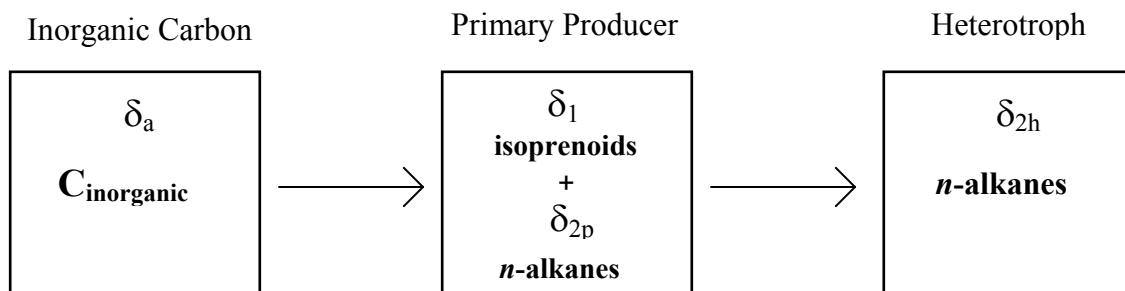


Figure 1. Food chain with appropriate δ labels. Dissolved, inorganic carbon is taken up by primary producers that use it to biosynthesize isoprenoids with a $\delta^{13}\text{C}$ of δ_1 and *n*-alkanes with a $\delta^{13}\text{C}$ of δ_{2p} . The heterotrophs then eat the primary producers and, using this biomass, biosynthesize *n*-alkanes with a $\delta^{13}\text{C}$ of δ_{2h} . This food chain continues ad infinitum to the right as larger and larger heterotrophs eat the smaller ones before them, biosynthesizing $\delta_{2h'}$, $\delta_{2h''}$, $\delta_{2h'''}$, etc.

Figure 2 represents a compilation of the work of Hoering, Logan, Brocks and others, providing average isotopic compositions for *n*-alkanes and isoprenoids in the Proterozoic and Phanerozoic oceans. In line with the established biosynthetic relationships of the dominant marine organisms, Phanerozoic sediments contain *n*-alkanes that are depleted in ^{13}C compared to pristane and phytane, a conventional relationship where Δ is negative, with the possible exception of those deposited during Phanerozoic oceanic anoxic events (e.g., Grice et al., 2005). In the Proterozoic, however, further reflecting the anomalous nature of C-isotopic data from that time, isoprenoids are more depleted in ^{13}C than *n*-alkanes; there is an inverted relationship amongst the hydrocarbons where Δ is positive

(e.g., Logan et al., 1995). Logan et al. (1995) showed that this phenomenon is evident in different, co-eval sedimentary basins. They did not, however, look at the change over time in individual basins.

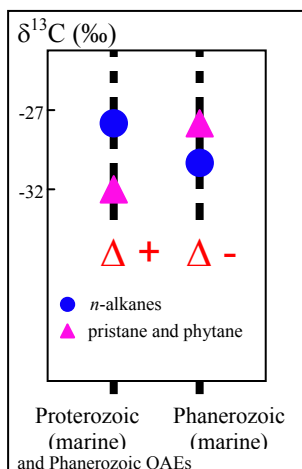


Figure 2. Isotopic ordering of isoprenoids vs. *n*-alkanes in Proterozoic and Phanerozoic marine systems showing a positive Δ for Proterozoic sediments and a negative Δ for Phanerozoic sediments, modified from Brocks et al., 2003a.

Experimental

Sampling.

Samples from the South Oman Salt Basin were collected and analyzed for biomarker parameters conventionally used for oil-source correlation (Grosjean et al., 2009). Eastern Siberian samples were selected from an oil collection provided by John Zumberge of Geomark Research, Houston, Texas. Samples from Australia were collected from fully cored petroleum exploration and stratigraphic wells. The samples from the Wallara-1 well of the Amadeus Basin were selected at the Northern Territory Geological Survey's core library in Alice Springs. These core samples were sectioned at the core facility, wrapped in aluminium foil pre-heated to 550°C and then placed into twist bags for transport to MIT and storage prior to analysis.

General Procedure.

Organic free solvents from OmniSolv were used. Prior to use, all glassware and aluminum foil were fired at 550°C for 8h and glass wool; pipettes and silica gel were fired at 450°C for 8h.

Sediment samples were cleaned with deionised water, rinsed with methanol and dichloromethane and crushed manually with the sample wrapped in fired aluminum foil. They were then ground to a fine powder in a SPEX 8510 Shatterbox fitted with an 8505 alumina ceramic puck mill that was carefully cleaned between samples with aqueous detergent, fired sand and finally rinsed with distilled water, methanol, dichloromethane and hexane. Rock powders were extracted using an accelerated solvent extractor (Dionex ASE) using a 9:1 mixture of dichloromethane and methanol. The resultant extracts were carefully evaporated under nitrogen to a volume of approximately 2 mL whereupon activated Cu was added to remove elemental sulfur. The sample was then separated by liquid chromatography on a silica gel 60 (Merck, 230-400 mesh) column using hexane to elute the saturate fraction, 4:1 hexane/dichloromethane to elute the aromatic fraction, and 7:3 dichloromethane/methanol to elute the polar fraction. The saturate fraction was further separated using 5 Å molecular sieves to trap the *n*-alkanes. The sieves were first combusted at 350°C for 16 hrs and stored in airtight jar at 120°C. The saturated fraction was dissolved in cyclohexane and transferred into a 3 mL vial. For every 10-20 mg of saturates 0.5 g of sieves were added to the vial, which was filled with cyclohexane up to ~2 mL. The vial was heated at 80°C over night after which it was cooled and filtered. The sieves were washed with several small portions of cyclohexane and air dried. The *n*-alkanes were then recovered from the sieves using HF and extracting the solution four times with 1 mL pentane. Where there was enough sample, the isoprenoids were further isolated from the branched/ cyclic fraction using a thiourea adduction performed according to the methods of Rubinstein & Strausz (1979).

Compound-specific isotope results for lipids were obtained with a ThermoFinnigan TraceGC equipped with a J&W DB-1MS column (60 m x 32 mm, 0.25 mm film). Chromatographic conditions were initially 60°C for 3 minutes, ramped from 60 - 180°C at 10°C/min, then 180 - 320°C at 4°C/min, and finally held at 320°C for 40 min. The GC was coupled to a combustion furnace interfaced to a Finnigan MAT DeltaPlus XP isotope ratio monitoring mass spectrometer operated with Isodat 2.0. Precision of isotope results were measured with standards and found to be better than 0.3‰ vs. VPDB, and sample replicates produced average errors of ~ 0.7‰ vs. VPDB.

Results and Discussion

The South Oman Salt Basin (SOSB) comprises a carbonate platform and a deeper Athel Sub-basin (Figure 3). Figure 4 shows the compound specific isotope data for the SOSB carbonate platform region. The y axis is stratigraphic height, also showing radiometric age constraints from U-Pb analysis of zircons (Bowring et al., 2007); the x-axis is the Δ value. Below the red dotted line is the inverted relationship between the hydrocarbons, while above it is the conventional relationship. The switch occurs somewhere within the Buah Formation or A1 units of the Ara Formation, giving an age range of ~550-545 Ma for the change (Bowring et al., 2007). The Ara Formation records shallow water conditions, which would be fully oxidized rapidly with increasing atmospheric oxygen levels, and has, on average, a negative Δ . We also looked at the A4 unit equivalents in the deeper Athel Sub-basin (Figure 5). From oldest to youngest these are the U shale, Silicilyte and Thuleilat shale units. The A4 unit of the Ara Formation and the U Formation are considered to be coeval due to stratigraphic position and the presence of uranium enrichment in both (Schröder & Grotzinger, 2007). The U and Thuleilat shale units are from deep marine settings, while the Silicilyte unit is more restricted (Schröder & Grotzinger, 2007). As seen in Figure 5, on average, the U shale unit shows a positive value for Δ while the two younger units give the same relationship as the A4 unit, a negative value of Δ . The switch occurred later, in the Athel Sub-basin, which is more easily seen in Figure 6. If correlations are correct, this would date the switch in the Athel Sub-basin to ~542 Ma (Bowring et al., 2007). This pattern may follow oxygen availability. It may have taken an extra ~8 Ma for the deeper Athel Sub-basin to be fully oxidized. The data for both sub-basins are given in Table 1.

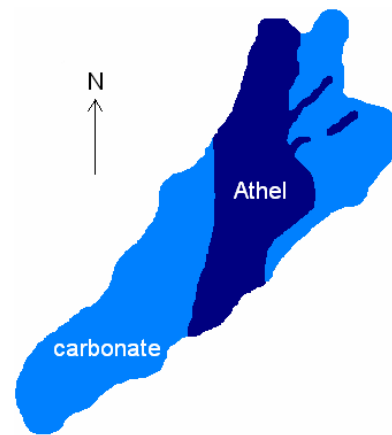
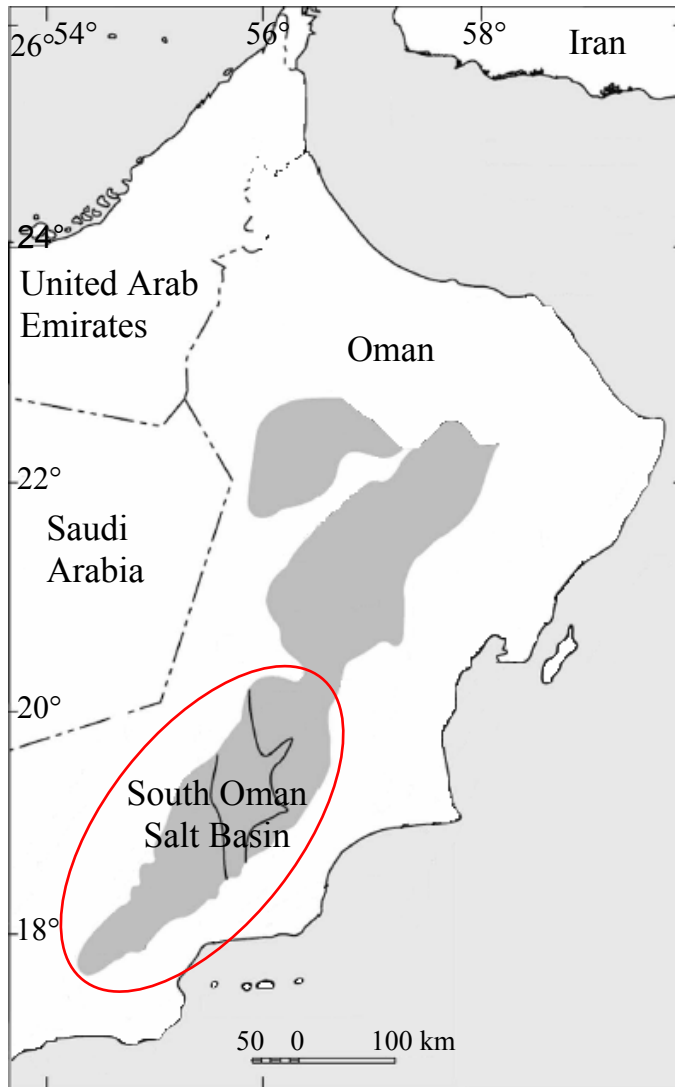


Figure 3. On the left is the South Oman Salt Basin (SOSB), modified from Grosjean et al., 2009. On the right is detail of the region, showing that it is comprised of carbonate platforms to the north and south of the deeper Athel Sub-basin, modified from Bowring et al., 2007.

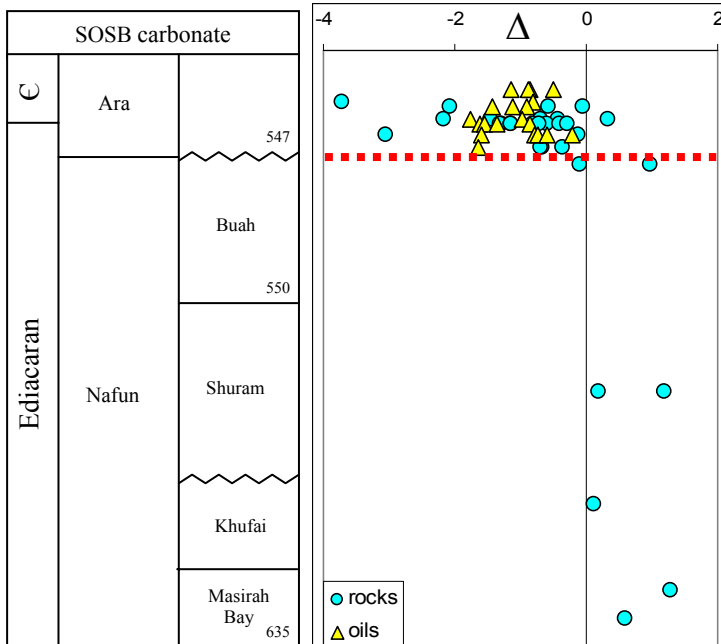


Figure 4. Compound specific isotopic data from the carbonate platform of the SOSB showing a significant change in Δ in the Buah Formation. The teal circles are rock data and the yellow triangles are from oils. The oil data are from a proprietary report to the Petroleum Development of Oman. As the origin of the Q oil is yet unknown, it is grouped with the Ara Formation in this figure.

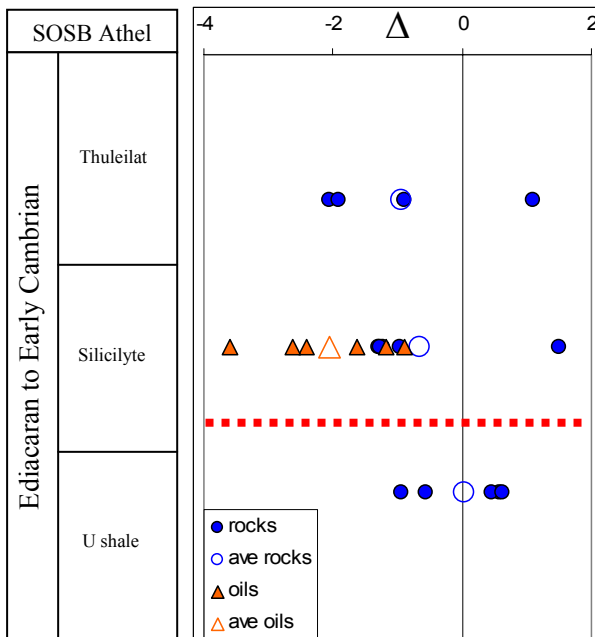


Figure 5. Compound specific isotopic data from the Athel Sub-basin of the SOSB showing a small but significant change in Δ in the U shale or Silicilyte units. The blue circles are rock data and the orange triangles are from oils. The open symbols represent the averages for each unit.

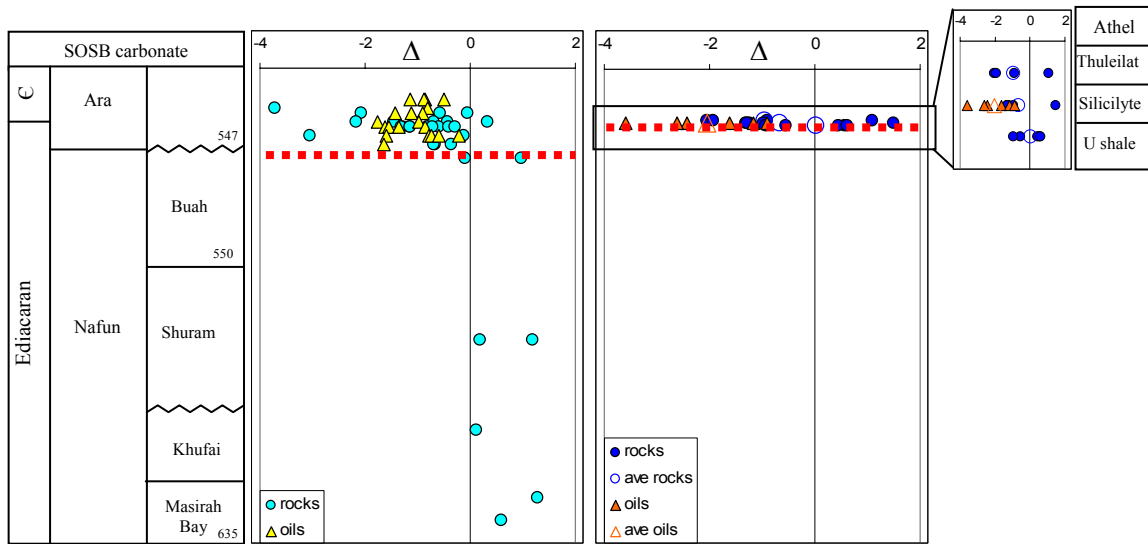


Figure 6. Compound specific isotope data for the entire SOSB, showing that the shift occurs later in the deeper Athel Sub-basin.

South Oman Salt Basin			
Carbonate Platform			
Sample ID	Formation	Age	Δ
OMO 012	Q	537	-1.15
OMO 018	Q	537	-0.86
OMO 019	Q	537	-0.88
OMO 020	Q	537	-0.49
OMO 035	A6C	539	-0.80
OMO 054	A5C	540	-0.90
OMO 043	A5C	540	-1.13
OMO 037	A5C	540	-1.42
OMO 036	A4C	542	-0.98
OMO 038	A4C	542	-1.76
OMO 039	A3C	543	-1.62
OMO 041	A3C	543	-1.55
OMO 051	A3C	543	-1.35
OMO 052	A3C	543	-0.86
OMO 053	A2C	545	-0.79
OMO 049	A2C	545	-0.73
OMO 055	A2C	545	-0.23
OMO 056	A2C	545	-0.59
OMO 057	A2C	545	-1.60
OMO 040	A1C	547	-1.64
OMR 272	A6S	539	-3.73
OMR 040	A5C	540	-0.05
OMR 041	A5C	540	-0.56
OMR 219	A5C	540	-2.07
OMR 030	A4C	542	-0.68
OMR 031	A4C	542	-2.17
OMR 029	A4C	542	0.33
OMR 032	A4C	542	-0.42
OMR 033	A4C	542	-1.46
OMR 036	A3C	543	-0.61
OMR 038	A3C	543	-1.29
OMR 028	A3C	543	-0.82
OMR 035	A3C	543	-0.40
OMR 037	A3C	543	-0.27
OMR 220	A3C	543	-1.31

OMR 222	A3C	543	-1.14
OMR 232	A3C	543	-1.15
OMR 233	A3C	543	-0.73
OMR 034	A2C	545	-3.04
OMR 042	A2C	545	-0.12
OMR 039	A1C	547	-0.67
OMR 229	A1C	547	-0.69
OMR 231	A1C	547	-0.36
OMR 017	Buah	550	0.98
OMR 020	Buah	550	-0.10
OMR 010	Shuram	590	1.20
OMR 026	Shuram	590	0.20
MQ1 4000	Khufai	610	0.13
MQ1 4200	Masirah Bay	625	1.28
MQ1 4244	Masirah Bay	630	0.60
Athel Sub-basin			
Sample ID	Formation	Age	Δ
OMO 025	Silicylite	542	-1.63
OMO 029	Silicylite	542	-1.17
OMO 030	Silicylite	542	-2.42
OMO 044	Silicylite	542	-0.90
OMO 048	Silicylite	542	-2.62
OMO 050	Silicylite	542	-3.59
OMR 011	Thuleilat	541.5	-2.05
OMR 021	Thuleilat	541.5	-1.92
OMR 022	Thuleilat	541.5	1.10
OMR 003	Thuleilat	541.5	-0.90
OMR 012	Silicylite	542	1.50
OMR 013	Silicylite	542	-1.30
OMR 004	Silicylite	542	-1.23
OMR 023	Silicylite	542	-1.27
OMR 024	Silicylite	542	-0.97
OMR 006	U shale	542.5	-0.55
OMR 014	U shale	542.5	0.57
OMR 025	U shale	542.5	0.45
OMR 005	U shale	542.5	-0.94
OMR 007	U shale	542.5	0.63

Table 1. Δ data for the SOSB with sample IDs, formations, and approximate ages.

This signal is also seen in samples from Eastern Siberian basins and the Amadeus Basin in Australia. Unfortunately, the age constraints are weak for both of these sections. The Eastern Siberian oil data are shown in Figure 7. Unfortunately, there are no corresponding well-dated rocks, so the ages are unconstrained except for the approximate ages of the reservoir rocks. The change in sign for Δ occurs very roughly in the

Ediacaran. Although the ages here are poorly defined, the high abundance of 24-isopropylcholestanes in the oils corroborates the suggestion that the switch occurs in the Ediacaran in Eastern Siberia (Love et al., 2009; Chapter 2). The data are given in Table 2.

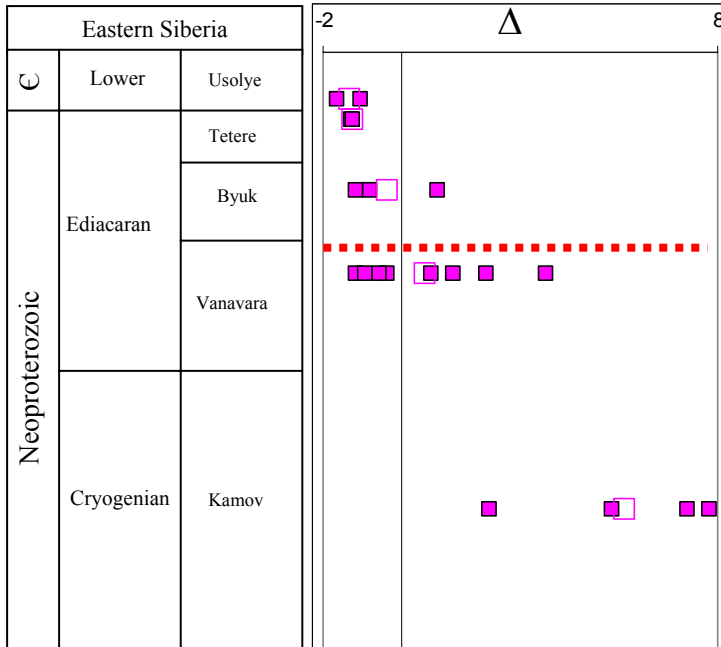


Figure 7. Compound specific isotopic data from Eastern Siberia showing a significant change in Δ within the Vanavara Formation. The larger, unfilled squares are the averages for each formation. The Vanavara Formation stands for the Vanavara Formation and its equivalents, the Kursov, Nepa and Parshino Formations. The Byuk Formation stands for the Byuk Formation and its equivalent, the Katanga Formation.

Eastern Siberia			
Sample ID	Formation	Age	Δ
ES 083	Usol'ye	562	-1.03
ES 080		562	-1.65
ES 068	Tetere	567	-1.25
ES 064		567	-1.28
ES 057	Katanga	585	-1.18
ES 053	Byuk	585	0.93
ES 048		585	-0.80
ES 043	Parshino	606	-0.92
ES 040	Nepa	606	-0.55
ES 036		606	-1.15
ES 035	Vanavara	606	2.13
ES 030	Kursoy	606	-0.38
ES 026	Vanavara	606	0.76
ES 024		606	1.29
ES 022		606	3.65
ES 020	Kamov	665	2.21
ES 018		665	5.33
ES 015		665	7.23
ES 010		665	7.80

Table 2. Δ data for Eastern Siberia with sample IDs, formations, and approximate ages.

The Australian rock samples studied are from the Amadeus Basin of the Centralian Superbasin. In Figure 8 are the compound specific isotope data for this region. The switch here occurs somewhere between 580 and 542 Ma, though the age constraints are largely uncertain as there are no zircon dates, but only geological correlations (Walter et al., 2000). The data are given in Table 3.

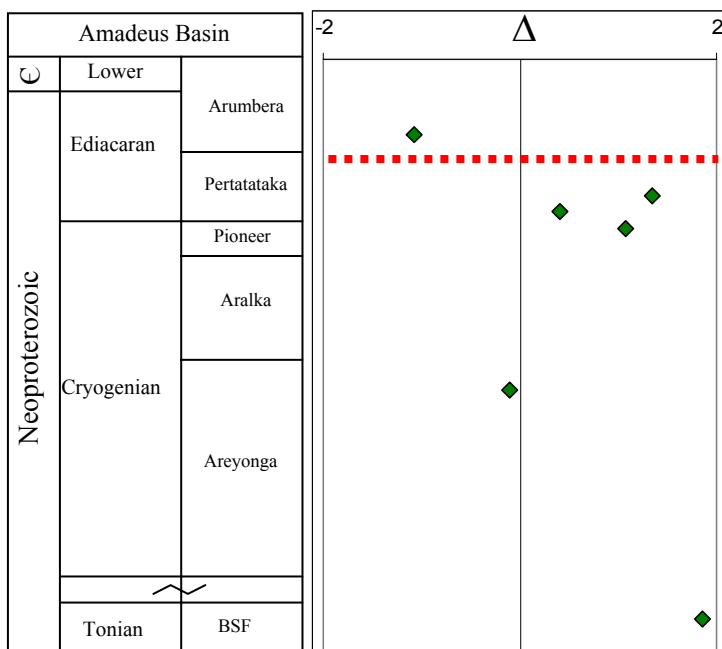


Figure 8. Compound specific isotopic data from the Amadeus Basin of the Centralian Superbasin in Australia, showing a significant change in Δ in the upper Pertatataka Formation or lowest Arumbera Formation.

Amadeus Basin, Australia			
Sample ID	Formation	Age	Δ
W1 544	Arumbera	544	-1.08
W1 580	Pertatataka	580	1.35
W1 590	Pertatataka	590	0.40
W1 600	Pioneer	600	1.08
W1 695	Areyonga	695	-0.10
W1 830	Bitter Springs	830	1.85

Table 3. Δ data for the Amadeus Basin of the Centralian Superbasin in Australia with sample IDs, formations, and approximate ages.

In order to better understand the relationship of these compound specific isotopes to the bulk isotopic changes in the Ediacaran, we further analyzed the samples from the carbonate platform of the SOSB where we have the best lithographic and age constraints. The change from visibly decoupled to coupled $\delta^{13}\text{C}$ of carbonate and of organics in the SOSB, shown in Figure 9 with a grey line, is close in time to the reorganization of isotopic values of the organic classes *n*-alkanes and isoprenoids (Figure 9). This suggests that they may have had a common trigger.

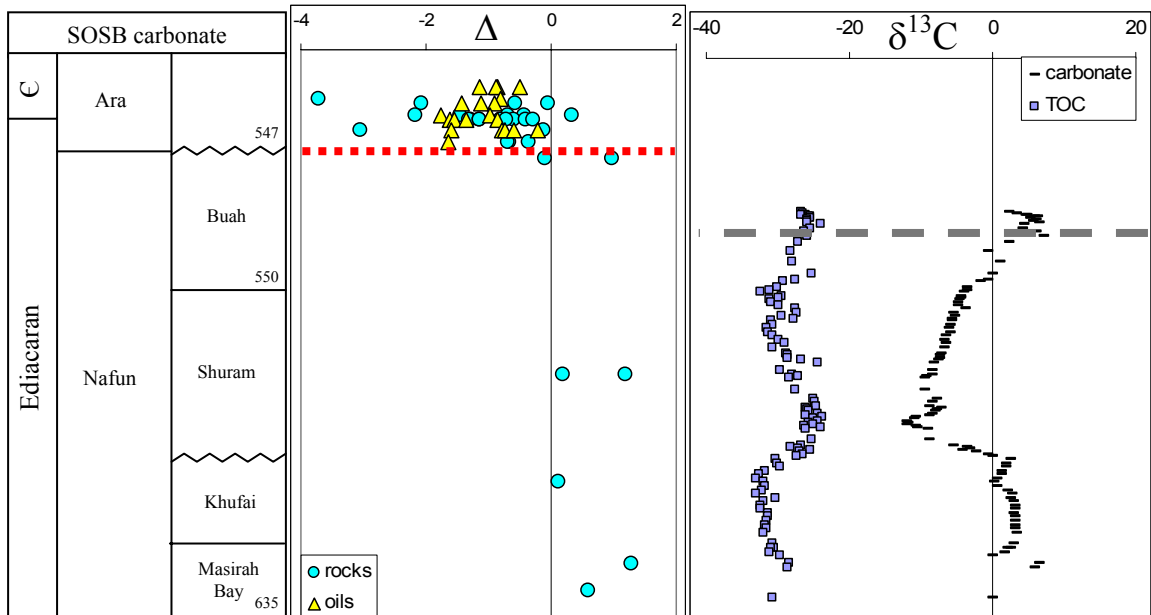


Figure 9. Compound specific isotopic data from Oman with bulk δ_a and δ_o data from Fike et al., 2006, showing that where Fike et al. (2006) see a visibly correlated coupling between bulk δ_a and δ_o data in the Buah Formation (grey line) is roughly the same point in time where we observe a significant change in Δ (red line). Vertical positions of Δ data for Nafun Group are unknown within each formation with respect to the bulk isotope data.

To understand all of these changes, it is necessary to understand the basics of the carbon cycle and mass balance. The carbon cycle can give information about the environmental conditions of the Neoproterozoic Era. Organic carbon is linked with oxygen via the reversible reaction: $\text{CO}_2 + \text{H}_2\text{O} \leftrightarrow \text{CH}_2\text{O} + \text{O}_2$, where CH_2O is representative of organic carbon. Autotrophs drive the reaction to the right while heterotrophs drive the reaction to the left. When organic carbon is buried or otherwise escapes this loop, oxygen is released.

Isotopic measurements are valuable since they may be preserved well through time (Hayes et al., 1987; Knoll et al., 1986). All of the data are based on delta notation. $\delta^{13}\text{C} = 1000[(R-R_{\text{std}})/R_{\text{std}}]$ where R is the $^{13}\text{C}/^{12}\text{C}$ of a sample and R_{std} is the abundance $^{13}\text{C}/^{12}\text{C}$ ratio for the standard, Pee Dee Belemnite. The $\delta^{13}\text{C}$ value for crustal carbon is around -5‰ (Holser et al., 1988). This is the isotopic composition of carbon entering the global system. The carbon exits the system as buried inorganic and organic carbon. The $\delta^{13}\text{C}_{\text{organic}}$ (δ_o) is equal to the $\delta^{13}\text{C}_{\text{carbonate}}$ (δ_a) minus a fractionation factor, ϵ . Using isotopic mass balance, $\delta_{\text{in}} = \delta_{\text{out}} = f_a\delta_a + f_o\delta_o$, where f_a is the fraction of carbon buried as

carbonate, f_o is the fraction of carbon buried as organic carbon and $f_a = 1 - f_o$. This is valid if the system is in steady state, but the ocean is not always in steady state. For example, δ_{in} may not be -5‰ if there is another carbon source like dissolved organic carbon or methane that is affecting it.

In the Phanerozoic, where the carbon cycle has generally been in a steady state, dissolved inorganic carbon (DIC) is the main carbon pool in the ocean. Marine primary producers fix this carbon, producing organic carbon with $\delta^{13}C$ values offset from the inorganic carbon isotopic composition by a biological fractionation, ϵ . This yields $\delta^{13}C$ isotopic signals in the sedimentary record where δ_a and δ_o are visibly coupled and therefore co-evolve in a predictable manner. In the middle to late Neoproterozoic, there is a lack of obvious coupling between δ_a and δ_o . Rothman et al. (2003) calculated that from ~738 to 555 Ma, f_o is approximately 1 and go through an elegant mathematical explanation of why this is a reflection of dynamic change in a non-steady state carbon cycle.

Fike et al. (2006) performed a detailed chemostratigraphic study of sections in Oman which is shown in Figure 10. There are three areas of different carbon cycling patterns. In the Khufai Formation and older rocks, there is no visible coupling of the carbonate record and the paired organic carbon isotopic record, indicating a dynamic carbon cycle. During the Shuram excursion, which is circled in red, δ_a and δ_o are anti-correlated. Because they appear somewhat coupled, this may be explained by an initial quasi-steady state in the carbon cycle where f_o was constant but ϵ was changing. Just after the excursion, in the blue circle, the δ_a and δ_o do visibly couple and correlate, indicating a change to a carbon cycle in steady state.

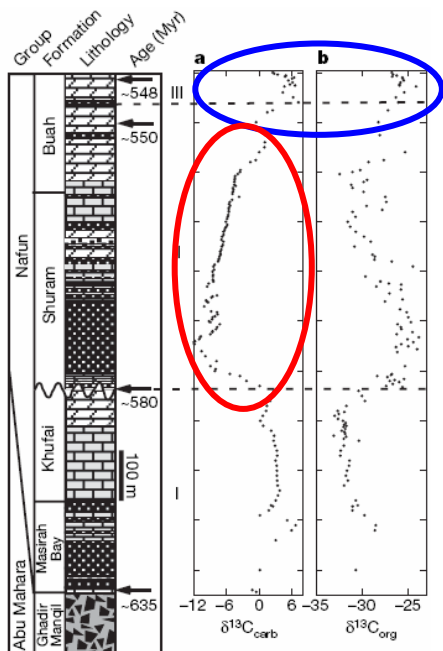


Figure 10. Inorganic and organic carbon isotope signatures of the carbonate platform of the SOSB, adapted from Fike et al., 2006. In the red circle is the Shuram excursion and the blue circle shows where the organic and carbonate signatures visibly correlate.

As can be seen in Figure 10 and especially in McFadden et al. (2008), there is little change in the bulk δ_o signal in the Neoproterozoic, so we chose to study certain organic compound classes for further information. Compound-specific isotope data give more specific information that may provide insight to the complexity of the food chain and thereby give clues about changing trophic structures leading up to the Cambrian explosion (Hayes et al., 1987). In this chapter we identified two classes of organic carbon to study: molecules derived from primary producers, isoprenoids, and from primary producers and heterotrophs, *n*-alkanes.

The main isoprenoids of interest are pristane and phytane, which are primarily derived from the phytol side chain of chlorophyll a (Blumer et al., 1963; Blumer & Snyder 1965; Didyk et al., 1978). Other potential sources of these isoprenoids include zooplankton (Blumer et al., 1963), tocopherols (Goosens et al., 1984), methyltrimethyltridecylchromans (Li et al., 1995), and archeal ether lipids (Chappe et al., 1982). There is, however, good geochemical evidence that these are minor contributors. Firstly, pristane is likely present in zooplankton because of the chlorophyll in the phytoplankton they eat, so it is still a primary isotopic signal. Also, not only is tocopherol of minor abundance with

respect to chlorophyll (Bucke et al., 1966), it is formed by the same biosynthetic pathway as chlorophyll and would have the same isotopic composition (Li et al., 1995). Methyltrimethyltridecylchromans are likely formed by a reaction of phytol with phenols, and again likely retain the primary isotopic signature (Li et al., 1995; Koopmans et al., 1999). Possible archaeal inputs will be discussed below, however archaeal lipids predominantly degrade to phytane, not pristane (e.g., Brassell et al., 1981; Chappe et al., 1982) and in an analysis of 300 crude oils, which range in age from the Devonian to the Tertiary, Li et al. (1995) found that only two samples did not contain $\delta^{13}\text{C}$ isotopically equivalent pristane and phytane. This suggests that in the vast majority of samples, pristane and phytane have the same source, limiting the possibility of significant archaeal input to phytane.

Isoprenoids in sediments are derived solely from compounds produced by primary producers, but the *n*-alkanes come from compounds produced by both primary producers and heterotrophs. Heterotrophs, however, produce *n*-alkanes that are relatively enriched in ^{13}C because the carbon retained by organisms is more enriched than the carbon respired by around 1‰ (DeNiro & Epstein, 1978; McConnaughey & McRoy, 1979). This 1‰ compounds as the food chain lengthens.

Throughout most of the Phanerozoic Eon, *n*-alkanes are isotopically depleted in ^{13}C relative to isoprenoids, which leads to a negative Δ (Hayes, 2001). In the Proterozoic isoprenoids are more depleted in ^{13}C than *n*-alkanes; there is an inverted relationship amongst the hydrocarbons where Δ is positive (e.g., Logan et al., 1995). Three main hypotheses have been put forward to explain the anomalous Δ signals in the late Neoproterozoic and the change to Phanerozoic-like Δ values in the late Ediacaran. These are: there was an added source of light carbon to the ocean which was DOM or methane, or we are simply seeing a shift from a prokaryotic dominated ocean to a eukaryotic dominated ocean. It will not be possible to fully evaluate these hypotheses until we analyze the compound specific isotopic signals in the early Neoproterozoic and older rocks.

Rothman et al. (2003) proposed that in the Neoproterozoic the balance of carbon pools in the ocean must have been different. Since δ_a varied substantially while δ_o varied very slowly, they suggest that the organic carbon reservoir was somehow buffered. They hypothesize that the dissolved organic carbon (DOC) was two to three orders of magnitude larger in size than in the Phanerozoic and thus a much larger contributor to the oceanic carbon pool (note: use of the term DOC is not meant to distinguish between dissolved and suspended colloidal or fine particulate organic carbon). In this model, the DOC pool would have allowed for intense heterotrophy. Heterotrophs use DOC, not DIC, as their carbon and energy source so the isotopic signal of the heterotrophic biomass may have masked the coupled signal of primary producers to produce sedimentary δ_a and δ_o that are not visibly coupled. In this case, a large change in the carbonate signature would not necessarily lead to a corresponding effect in the organic signature.

Therefore the change in sign of capital delta may have occurred because of the varying inputs from primary producers versus heterotrophs. In the middle to late Neoproterozoic, the proposed large amount of DOC in the ocean would have allowed intense heterotrophy, driving up the isotopic composition of *n*-alkanes, resulting in a positive Δ (Logan et al., 1995). When this organic matter was buried, heterotrophy declined and DIC became the major carbon pool. The signal of light *n*-alkanes from carbon fixation by primary producers with a negative Δ would then become dominant. Looking back at the Fike et al. (2006) data in Figure 10, during the Shuram excursion heterotrophs would be using DOC, swamping the primary producer signal. Around 548 Ma, when the Shuram excursion ends, the δ_a and δ_o do visibly couple, indicating a change to a carbon cycle in steady state where DIC was the main carbon source. In the compound specific data at this time we see the light *n*-alkane signal from primary producers (which yields a negative Δ), suggesting their ecological dominance at that time. The large DOC pool would have been depleted, allowing for a significant rise in atmospheric oxygen, which would have likely aided the radiation of metazoans in the late Ediacaran to Early Cambrian.

Figure 11 provides an interpretation of the Rothman hypothesis. The relative sizes of the boxes are drawn to scale. Today, the DIC in the ocean is $\sim 2000 \mu\text{mol/kg}$, and the DOC is

~100 $\mu\text{mol/ kg}$. According to Rothman et al. (2003) this means that the DOC concentration of the Neoproterozoic was around 10,000 $\mu\text{mol/ kg}$. Hotinski et al. (2004) utilize a model, developed by Broecker & Peng (1982), in which the DIC concentration increases as the square root of the atmospheric levels of CO_2 increase. This puts the Ediacaran DIC values in the range of 1-7 times that of today, around 8000 $\mu\text{mol/ kg}$. This calculation assumes that the concentration of calcium was the same in the Neoproterozoic as it is today, but this is reasonable.

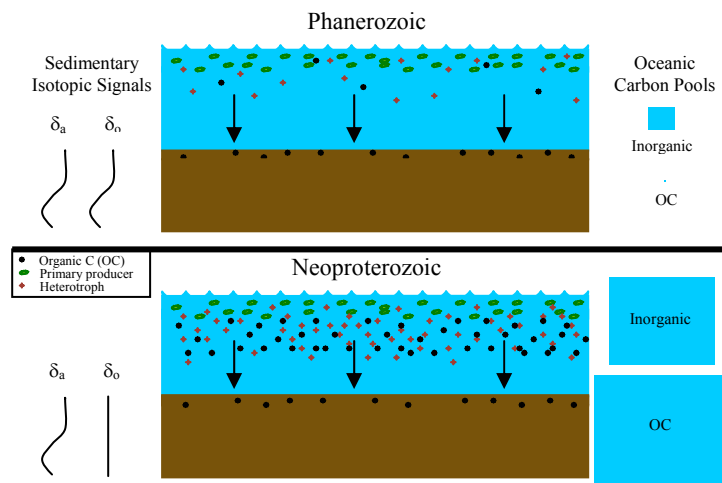


Figure 11. Depiction of the Phanerozoic ocean vs. the hypothesized Neoproterozoic ocean, involving the changes in the size of marine carbon pools and the effect of this on the ocean communities and the δ_a and δ_o signatures.

If the DOM hypothesis is correct, the abnormal Δ signature would only appear once the DOM built up enough and it would end as the DOC pool was removed by respiration or burial. A burial of DOM may lead to the increase of oxygen and thus of metazoan diversity. Although this theory fits the data, a mechanism for the formation and sustainability of such a staggeringly large pool of DOC for tens if not hundreds of millions of years has not been established. However, if the oceans at this time were ferruginous (Canfield et al., 2008), there would be little to no oxygen or sulfate available for the remineralization of organic carbon. So, perhaps remineralization was suppressed compared to the modern ocean and DOC had a longer residence time, potentially leading to a high DOC ocean.

A number of biological/ ecological explanations for the change in the sign of Δ have been proposed with the general idea that DOM must be removed from the system via burial. For example, the evolution of algae with recalcitrant biopolymers would have kept some of the organic carbon from being quickly recycled and made it easier to bury. Also, the proliferation of Ediacara and sponge fauna present at this time in the ocean likely filtered and trapped dissolved and particulate organic matter. Ediacara likely only consumed particulate and/ or dissolved organic matter due to their small size and likely benthic habit (Sperling et al., 2007). Though significantly later than the first appearance of sponges (Love et al., 2009), the timing of the Shuram excursion correlates well with the hypothesized ecological dominance of sponges (Sperling et al., 2007). This theory may also suggest that we would see increased TOC in the sediments around this time, which is true for the SOSB and Eastern Siberia, but not for Australia. However, the Australian rocks may have been high in TOC, but they are simply too mature now to be able to tell. Assuming DOM was being depleted in the Ediacaran, the shortening of food chains is also a plausible explanation for the change in Δ . As food chains shorten, the 'plus one per mil' effect diminishes. This would happen if the start of the food chain was a large phytoplankton, as opposed to the smallest phytoplankton that can successfully utilize DOM.

This change could have also occurred through the advent of animals with guts which could then create fecal pellets and enhance the export of DOM from the water column, however macrozooplankton with fecal pellets big enough to sink likely evolved around 520 Ma (Chen & Zhou, 1997; Vannier & Chen, 2000; Peterson et al., 2005). Biomineralization may have also provided ballast for organic matter. Cloudina first appeared around 549 Ma, but they were most likely benthic, allowing for little ballasting (Grotzinger et al., 1995).

There are theories founded on geologic processes as well. The earth was tectonically active during this time period, which may have created large depocenters, enhancing the burial of organic carbon and other reductants. Similarly, clays have been proposed to absorb organic carbon, and an increased flux of clays at this time could have helped bury

organic carbon (Kennedy et al., 2006). This clay factory hypothesis is less substantiated as Ediacaran shales are not especially organic rich, which would be expected if clays adsorbed the organic carbon in the water column and buried them. Additionally, recent work has found that ‘the deposition of pedogenic clays has remained broadly constant over Proterozoic time and into the Early Cambrian,’ which is incompatible with the clay factory hypothesis (Tosca et al., 2008).

Alternatively, the extra source of light carbon buffering the system may have been methane. By around 800 Ma the oceans may have returned to a ferruginous state (Canfield et al., 2008), so the sulfur cycle was not likely very active. With low oxygen concentrations and sulfide being stripped out of the water column by Fe^{2+} , sulfate may have been depleted before all of the organic carbon was remineralized. In this circumstance, methanogenesis would be a thermodynamically favored process, providing an additional source of light carbon. If this theory is correct, one should see the inception of anomalous Δ values as oceans become ferruginous and the signal should end as the concentration of any oxidants with higher metabolic energy yields rise, either in the ocean as a whole in the Ediacaran to Cambrian, or in individual basins throughout the Proterozoic where the local environment has been characterized as euxinic or oxic. One must be careful in these interpretations, however, as a basin designated as being euxinic may merely have a euxinic lens above a ferruginous water column. If methanogenic archaea were active, the phytane $\delta^{13}\text{C}$ values would likely be depleted relative to the $\delta^{13}\text{C}$ pristane values, for which we see no evidence. Methanogenic lipids predominantly degrade to phytane (e.g., Brassell et al., 1981; Chappe et al., 1982), so an input from methanogens would lead to phytane $\delta^{13}\text{C}$ values that are depleted with respect to the pristane values (Murray et al., 1998). However, the values in our data and the Archean data of Brocks et al. (2003a, 2003b) show no statistical difference between $\delta^{13}\text{C}$ values of pristane and phytane. Additionally, with the presence of methanogenesis, there would likely be methanotrophy, so methanotrophic biomarkers would be expected to be higher in strata with abnormal Δ values. The biomarker 3-methylhopane, likely derived from hopanoids of methanotrophic bacteria (Collister et al., 1992; Farrimond et al., 2004), has not been found to vary with the Δ values in the sediments studied. This hypothesis cannot

be fully assessed, however until we collect compound specific isotope data on rocks or oils older than 550 Ma that have been shown to be euxinic, but even then it may not be conclusive.

Recently, another theory has been put forward, suggesting that the compound specific isotopic shift is due to a change in the dominant marine communities from a prokaryotic dominated ocean to a eukaryotic dominated ocean (Close et al., 2008). This is supported by the observation that in the modern Pacific Ocean small (0.2 – 0.5 μm) particulate matter, assumed to be from picoplankton, is enriched relative to the larger particulate matter, assumed to be eukaryotic. If this theory is correct, this signal should be seen throughout the Proterozoic until non-picoplankton eukaryotes clearly become ecologically dominant. For the simplified case of a change from a prokaryote dominated ocean to a eukaryote dominated ocean, in terms of biomarkers, the abnormal Δ signal should be seen wherever hopane abundances are strongly dominant over sterane abundances, which has yet to be indicated. Again, we must be careful with this interpretation as not all bacteria biosynthesize hopanoids and most of those found to have the ability are aerobic (Rohmer et al., 1984). Another concern is that though eukaryotic algae have been shown to produce acetogenic lipids that are depleted in ^{13}C relative to the phytol (Schouten et al., 1998), prokaryotes have not universally shown the reverse relationship (Hayes, 2001). The relative $\delta^{13}\text{C}$ of these compounds are determined by the metabolism of the organism, not by where they fall on the tree of life. For example, *Chlorobium limicola*, which uses the reverse tricarboxylic acid cycle, biosynthesizes fatty acids that are more enriched than its isoprenoids (van der Meer et al., 1998), while *Synechocystis*, which has a C_3 metabolism, produces acetogenic lipids that are more depleted than phytol (Sakata et al., 1997). Organisms that use the reverse tricarboxylic acid cycle are not considered to have ever been dominant in the ocean (Knoll et al., 2007).

Conclusions

We have shown a relative change in the carbon isotopic relationship of *n*-alkanes vs. isoprenoids in individual basins in Oman, Eastern Siberia and Australia so this

phenomenon appears to be roughly global in the Ediacaran. The change from *n*-alkanes being enriched in ^{13}C relative to isoprenoids to being depleted relative to isoprenoids appears to occur in the Ediacaran, the best age constraint being ~ 550 Ma from the carbonate platform of the SOSB, coincident with the end of the Shuram Excursion, but it is not necessary for the change to be globally synchronous. This point is best seen in Oman where we see the change in the deeper Athel Basin occurring ~ 8 Ma after the carbonate platform. This corroborates previous studies that show full ventilation of shallow, marine regions by 550 Ma.

The change in the sign of Δ shows a community restructuring as the chemocline moves deeper. When it becomes negative in the SOSB, this suggests that the water column in this area was ventilated. However, this was a relatively shallow area. Perhaps all of the negative isotope excursions in the Cambrian are due to further oxidation events as the chemocline is pushed even deeper, and finally settles in the sediment. This gives ample time for the turnover of DOC to occur without depleting the available oxidants. If the data from Fike et al. (2006) is actually signifying the removal of DOC from just the slopes, that is much less than the DOC of the entire ocean and makes the DOC ocean more physically feasible. It may take until the late Cambrian for full oxygenation of the global deep waters to occur.

The fact that the change from decoupled to coupled $\delta^{13}\text{C}$ of carbonate and of organics and changes in Δ both occur in the Ediacaran suggests that they may have had the same trigger. Both the DOC and methane hypotheses reasonably explain this. The theory that we are simply seeing a shift from a prokaryotic dominated ocean to a eukaryotic dominated ocean may explain the compound specific changes seen, but the bulk isotopic changes cannot be explained by this simple community shift. However, these changes could all be effects of the same environmental trigger; the community shift does not necessarily have to cause both bulk and compound specific isotopic changes. The three hypotheses are all plausible with the current data.

Acknowledgements

The author wishes to thank Roger Summons, Emmanuelle Grosjean and Sean Silva for the compound specific carbon isotope data for the oils of the carbonate platform of the SOSB, which were in the proprietary report to the Petroleum Development of Oman.

References

- Blumer, M.; Snyder, W. D. **1965**. Isoprenoid hydrocarbons in recent sediments: Presence of pristane and probably absence of phytane. *Science* **150**, 1588-1589.
- Blumer, M.; Mullin, M. M.; Thomas, D. W. **1963**. Pristane in zooplankton. *Science* **140**, 974.
- Bowring, S. A.; Grotzinger, J. P.; Condon, D. J.; Ramezani, J.; Newall, M. J.; Allen, P. A. **2007**. Geochronologic constraints on the chronostratigraphic framework of the Neoproterozoic Huqf Supergroup, Sultanate of Oman. *Am. J. Sci.* **307**, 1097-1145.
- Brassell, S. C.; Wardroper, A. M. K.; Thomson, I. D.; Maxwell, J. R.; Eglinton, G. **1981**. Specific acyclic isoprenoids as biological markers of methanogenic bacteria in marine sediments. *Nature* **290**, 693-696.
- Brocks, J. J.; Buick, R.; Summons, R. E.; Logan, G. A. **2003a**. A reconstruction of Archean biological diversity based on molecular fossils from the 2.78 to 2.45 billion-year-old Mount Bruce Supergroup, Hamersley Basin, Western Australia. *Geochim. Cosmochim. Acta* **67**, 4321-4335.
- Brocks, J. J.; Buick, R.; Logan, G. A.; Summons, R. E. **2003b**. Composition and syngeneity of molecular fossils from the 2.78 to 2.45 billion-year-old Mount Bruce Supergroup, Pilbara Craton, Western Australia. *Geochim. Cosmochim. Acta* **67**, 4289-4319.
- Broecker, W. S.; Peng, T. H. **1982**. Tracers in the Sea: Palisades, New York, Lamont-Doherty Geological Observatory, p. 690.
- Bucke, C.; Leech, R.; Hallaway, M.; Morton, R. **1966**. The taxonomic distribution of plastoquinone and tocopheroquinone and their intercellular distribution in leaves of *Vicia Faba L.* *Biochim. Biophys. Acta* **112**, 19-34.
- Canfield, D. E.; Poulton, S. W.; Knoll, A. H.; Narbonne, G. M.; Ross, G.; Goldberg, T.; Strauss, H. **2008**. Ferruginous conditions dominated later Neoproterozoic deep-water chemistry. *Science* **321**, 949-952.
- Chappe, B.; Albrecht, P.; Michaelis, W. **1982**. Polar lipids of archaebacteria in sediments and petroleum. *Science* **217**, 65-66.
- Chen, J.; Zhou, G.-Q. **1997**. Biology of the Chenjiang fauna. In: The Cambrian Explosion and the fossil record. (J. Chen, Y. N. Cheng & H. V. Iten, eds.), Bulletin of the National Museum of Natural Science, Vol. 10, Taichung, pp. 11-105.
- Close, H. G.; Diefendorf, A. F.; Freeman, K. H.; Pearson, A. **2008**. A modern analogue for Proterozoic inverse carbon isotope signatures. *Eos Trans. AGU* **89**, Fall Meet. Suppl., Abstract PP14A-07.
- Collister, J. W.; Summons, R. E.; Lichtfouse, E.; Hayes, J. M. **1992**. An isotopic biogeochemical study of the Green River oil shale. *Org. Geochem.* **19**, 265-276.
- DeNiro, M. J.; Epstein, S. **1978**. Influence of diet on the distribution of carbon isotopes in

- animals. *Geochim. Cosmochim. Acta* **42**, 495-506.
- Didyk, B. M.; Simoneit, B. R. T.; Brassell, S. C.; Eglinton, G. **1978**. Organic geochemical indicators of palaeoenvironmental conditions of sedimentation. *Nature* **272**, 216-222.
- Farrimond, P.; Talbot, H. M.; Watson, D. F.; Schulz, L. K.; Wilhelms, A. **2004**. Methylhopanoids: Molecular indicators of ancient bacteria and a petroleum correlation tool. *Geochim. Cosmochim. Acta* **68**, 3873-3882.
- Fike, D. A.; Grotzinger, J. P.; Pratt, L. M.; Summons, R. E. **2006**. Oxidation of the Ediacaran Ocean. *Nature* **444**, 744-747.
- Goosens, H.; de Leeuw, J. W.; Schenck, P. A.; Brassell, S. C. **1984**. Tocopherols as likely precursors of pristane in ancient sediments and crude oils. *Nature* **312**, 440-442.
- Grice, K.; Cao, C.; Love, G. D.; Böttcher, M. E.; Twitchett, R. J.; Grosjean, E.; Summons, R. E.; Turgeon, S.C.; Dunning, W.; Jin, Y. **2005**. Photic zone euxinia during the Permian-Triassic superanoxic event. *Science* **307**, 706-709.
- Grosjean, E.; Love, G. D.; Stalvies, C.; Fike, D. A.; Summons, R. E. **2009**. Origin of petroleum in the Neoproterozoic-Cambrian South Oman Salt Basin. *Org. Geochem.* **40**, 87-110.
- Grotzinger, J. P.; Bowring, S. A.; Saylor, B. Z.; Kaufman, A. J. **1995**. Biostratigraphic and geochronologic constraints on early animal evolution. *Science* **270**, 598-604.
- Hayes, J. M. **2001**. Fractionation of the isotopes of carbon and hydrogen in biosynthetic processes. In: Stable Isotope Geochemistry, Reviews in Mineralogy and Geochemistry. (J. W. Valley & D. R. Cole, eds.), Mineralogical Society of America, Washington, DC, pp. 225-278.
- Hayes, J. M.; Takigiku, R.; Ocampo, R.; Callot, H. J.; Albrecht, P. **1987**. Isotopic compositions and probable origins of organic molecules in the Eocene Messel shale. *Nature* **329**, 48-51.
- Holser, W. T.; Schidlowski, M.; Mackenzie, F. T.; Maynard, J. B. **1988**. In: Chemical Cycles in the Evolution of the Earth. (C. B. Gregor, R. M. Garrels, F. T. Mackenzie & J. B. Maynard, eds.), Wiley, New York, pp. 105-173.
- Hotinski, R. M.; Kump, L. R.; Arthur, M. A. **2004**. The effectiveness of the Paleoproterozoic biological pump: A $\delta^{13}\text{C}$ gradient from platform carbonates of the Pethei Group (Great Slake Lake Supergroup, NWT). *GSA Bull.* **116**, 539-554.
- Kennedy, M.; Droser, M.; Mayer, L. M.; Pevear, D.; Mrofka, D. **2006**. Late Precambrian oxygenation; inception of the clay mineral factory. *Science* **311**, 1446-1449.
- Knoll, A. H.; Hayes, J. M.; Kaufman, A. J.; Swett, K.; Lambert, I. B. **1986**. Secular variation in carbon isotope ratios from Upper Proterozoic successions of Svalbard and East Greenland. *Nature* **321**, 832-838.
- Knoll, A.H.; Summons, R. E.; Waldbauer, J; Zumberge, J. **2007**. The geological succession of primary producers in the oceans. In: The Evolution of Primary Producers in the Sea. (P. Falkowski & A.H. Knoll, eds.), Elsevier, Burlington, pp. 133-163.
- Koopmans, M. P.; Rijpstra, W. I. C.; Klapwijk, M. M.; de Leeuw, J. W.; Lewan, M. D.; Sinninghe Damsté, J. S. **1999**. A thermal and chemical degradation approach to decipher pristane and phytane precursors in sedimentary organic matter. *Org. Geochem.* **30**, 1089-1104.
- Li, M.; Larter, S. R.; Taylor, P.; Jones, D. M.; Bowler, B.; Bjorøy, M. **1995**. Biomarkers

- or not biomarkers? A new hypothesis for the origin of pristane involving derivation from methyltrimethyltridecylchromans (MTTCs) formed during diagenesis from chlorophyll and alkylphenols. *Org. Geochem.* **23**, 159-167.
- Logan, G. A.; Hayes, J. M.; Hieshima, G. B.; Summons, R. E. **1995**. Terminal Proterozoic reorganization of biogeochemical cycles. *Nature* **376**, 53-56.
- Love, G. D.; Grosjean, E.; Stalvies, C.; Fike, D. A.; Grotzinger, J. P.; Bradley, A. S.; Kelly, A. E.; Bhatia, M.; Meredith, W.; Snape, C. E.; Bowring, S. A.; Condon, D. J.; Summons, R. E. **2009**. Fossil steroids record the appearance of Demospongiae during the Cryogenian Period. *Nature* **457**, 718-721.
- McConnaughey, T.; McRoy, C. P. **1979**. Food-web structure and the fractionation of carbon isotopes in the Bering Sea. *Mar. Biol.* **53**, 257-262.
- McFadden, K. A.; Huang, J.; Chu, X.; Jiang, G.; Kaufman, A. J.; Zhou, C.; Yuan, X.; Xiao, S. **2008**. Pulsed oxidation and biological evolution in the Ediacaran Doushantuo Formation. *Proc. Natl. Acad. USA* **105**, 3197-3202.
- Murray, A. P.; Edwards, D.; Hope, J. M.; Borehan, C. J.; Booth, W. E.; Alexander, R. A.; Summons, R. E. **1998**. Carbon isotope biogeochemistry of plant resins and derived hydrocarbons. *Org. Geochem.* **29**, 1199-1214.
- Peterson, K. J.; McPeck, M. A.; Evans, D. A. D. **2005**. Tempo and mode of early animal evolution: inferences from rocks, Hox, and molecular clocks. *Paleobiology* **31**, 36-55.
- Rohmer, M. Bouvier-Nave, P.; Ourisson, G. **1984**. Distribution of hopanoid triterpenes in prokaryotes. *J. Gen. Microbio.* **130** 1137-1150.
- Rothman, D. H.; Hayes, J. M.; Summons, R. E. **2003**. Dynamics of the Neoproterozoic carbon cycle. *Proc. Natl. Acad. USA* **100**, 8124-8129.
- Rubinstein, I.; Strausz, O. P. **1979**. Geochemistry of the thiourea adduct fraction from an Alberta petroleum. *Geochim. cosmochim. Acta* **43**, 1387-1392.
- Sakata, S.; Hayes, J. M.; McTaggart, A. R.; Evans, R. A.; Leckrone, K. J.; Togasaki, R. K. **1997**. Carbon isotopic fractionation associated with lipid biosynthesis by a cyanobacterium: Relevance for interpretation of biomarkers. *Geochim. Cosmochim. Acta* **61**, 5379-5389.
- Schouten, S.; Klein Breteler, W. C. M.; Blokker, P.; Schogt, N.; Rijpstra, I. C.; Grice, K.; Baas, M.; Sinninghe Damsté, J. S. **1998**. Biosynthetic effects on the stable carbon isotopic compositions of algal lipids: Implications for deciphering the carbon isotopic biomarker record. *Geochim. Cosmochim. Acta* **62**, 1397-1406.
- Schröder, S.; Grotzinger, J. P. **2007**. Evidence for anoxia at the Ediacaran-Cambrian boundary: the record of redox-sensitive trace elements and rare earth elements in Oman. *J. Geol. Soc.* **164**, 175-187.
- Scott, C.; Lyons, T. W.; Bekker, A.; Shen, Y.; Poulton, S. W.; Chu, X.; Anbar, A. D. **2008**. Tracing the stepwise oxygenation of the Proterozoic ocean. *Nature* **452**, 456-459.
- Sperling, E. A.; Pisani, D.; Peterson, K. J. **2007**. Poriferan paraphyly and its implications for Precambrian palaeobiology. In: *The Rise and Fall of the Ediacaran Biota*. (P. Vickers-Rich & P. Komarower, eds.), The Geological Society of London, Special Publications 286, London, pp. 355-368.
- Tosca, N. J.; Johnston, D. T.; Mushegian, A.; Rothman, D. H.; Knoll, A. H. **2008**. Clay mineralogy and organic carbon burial in Proterozoic basins. *Eos Trans. AGU* **89**,

- Fall Meet. Suppl., Abstract PP21B-1412.
- Van der Meer, M. T. J.; Schouten, S.; Sinninghe Damsté, J. S. **1998**. The effect of the reversed tricarboxylic acid cycle on the ^{13}C contents of bacterial lipids. *Org. Geochem.* **28**, 527-533.
- Vannier, J.; Chen, J.-Y. **2000**. The Early Cambrian colonization of pelagic niches exemplified by *Isoxys* (Arthropoda). *Lethaia* **33**, 295-311.
- Walter, M. R.; Veevers, J. J.; Calver, C. R.; Gorjan, P.; Hill, A. C. **2000**. Dating the 840-544 Ma Neoproterozoic interval by isotopes of strontium, carbon, and sulfur in seawater, and some interpretative models. *Precambrian Res.* **100**, 371-433.

5. Neoproterozoic Rocks with Confounding Biomarker Signatures: Novel Environmental Signals or Contamination?

Abstract

In biomarker studies of ancient rocks, one of the prime issues to establish is that the compounds under investigation are indigenous and syngenetic. Neoproterozoic to Cambrian aged rocks from Ukraine, China, Canada, Russia and Australia were extracted and the compositions of these bitumens were evaluated for biomarkers indicative of geological age, thermal maturity, and biological sources. Most of the studied samples contained low percentages of bitumens (~ 0.01%) and exhibited biomarker signals atypical for Neoproterozoic to Cambrian samples. The anomalous features were high $C_{28}/(C_{28} + C_{29})$ steranes ratios, high 24-nordiacholestanes ratios, low thermal maturities, differences in C_{28} and C_{29} $\alpha\alpha\alpha$ 20S/ (S + R) values, odd over even predominance in the higher carbon *n*-alkanes, bimodal *n*-alkane distributions, and/ or large UCMs. Some of these signals may be indicative of novel Neoproterozoic organisms or depositional environments, but for many of the samples the likelihood of contamination appears to be quite high.

Introduction

Considerable concern surrounds the integrity of bitumens isolated from ancient rock samples (e.g., McKirdy, 1974; Hayes et al., 1983; Hoering & Navale, 1987; Summons & Walter, 1990; Brocks et al., 2008; Waldbauer et al., 2009). The problem is particularly acute with respect to very old rocks, but applies in one form or another to all analyses of ancient rocks. This chapter examines the compositions of bitumens from rock samples from multiple locations (Ukraine, China, Canada, Russia and Australia) and identifies features that are atypical of Neoproterozoic to Cambrian aged rocks in order to provide an assessment of what these anomalies might mean. The end-member hypotheses to distinguish are that these are signatures for novel microbial communities and their depositional environments or that they are entirely due to contamination. There also might be an intermediate situation where the bitumens comprise mixtures of hydrocarbons from multiple sources. Contamination may have occurred after sediment deposition as younger oils migrated through the rock, or more recently during drilling,

sampling, handling, or storage. It is important to address age-sensitive parameters, maturity parameters, *n*-alkane patterns, the type of sample (hand sample vs. core), geological considerations, and other considerations in order to fully evaluate the significance of these signatures.

Age-sensitive biomarkers and their limitations.

As an age parameter, the ratio of $C_{28}/(C_{28} + C_{29})$ steranes was originally identified as something that varied systematically with the geological age of petroleum source rocks (Grantham and Wakefield, 1988). The increase in this ratio through the geological record may be associated with the diversification of phytoplankton assemblages through the Mesozoic, so a ratio greater than 0.3 for bitumen from a Precambrian rock may be an indicator of contaminated samples or an inappropriate age for the host rock (Grantham & Wakefield, 1988; Schwark & Empt, 2006). Knoll et al. (2007) attribute the trend to the evolution of chlorophyll *c* algae. In some studies of individual rock samples, as opposed to oils, the abundances of C_{28} steranes were observed to be elevated during the Kacak, Upper and Lower Kellwasser extinction events of the Devonian and Carboniferous (Schwark & Empt, 2006). An alternative interpretation for high $C_{28}/(C_{28} + C_{29})$ steranes ratios in ancient sediments may be an increase in contribution from prasinophytes, which appear to be resilient to oxygen depleted environments (Schwark & Empt, 2006), some of which are known to biosynthesize C_{28} sterols (Volkman, 1986; Kodner et al., 2008).

Also of use is the 24-nordiacholestanes ratio (Holba et al., 1998). The ratio of 24-nordiacholestanes/ (24-nordiacholestanes + 27-nordiacholestanes) roughly follows diatom evolution and is therefore expected to be very low, less than 0.25, in the Ediacaran and Cambrian (Holba et al., 1998). For each of the nordiacholestanes, the $\beta\alpha S$ and $\beta\alpha R$ isomers are summed. This hypothesis was updated due to the identification of 24-norsterols in a diatom and a dinoflagellate by Rampen et al., (2007) who suggest that the ratio is affected by the evolution of both diatoms and dinoflagellates. This revised hypothesis is supported by other findings of 24-norsterols in dinoflagellates (Goad & Withers, 1982; Kokke & Spero, 1987; Thomson et al., 2004). It is essential, however, to note that this ratio is based on data solely from oils. All of the oil samples studied met

these criteria and are presented in Chapter 2. Oils give average values for a basin. It may be the case that the rocks presented in this chapter that did not meet these conditions are merely indicating unique conditions that, while not usual for the Neoproterozoic as a whole, may truly be the conditions in a local area for a period of time in the Neoproterozoic.

Maturity parameters and use.

As all of the sediments are over half a billion years old, they are expected to be thermally mature. The sterane 20S/ (20S + 20R) values were used to assess maturity. Values at or near 0.55 indicate oil-mature samples (Seifert & Moldowan, 1986). It is important, however, that these values be very similar in each series of steranes. In this study, we consider the 20S/ (S + R) ratios for C₂₈ and C₂₉ steranes. If these biomarkers are both indigenous to the original rock, the values of these ratios should be very close as they would have seen the same thermal history. A large difference in the two ratios suggests multiple sources of different maturities, and likely age. If, for example, the C₂₈ steranes have a lower ratio, then it is likely that they are younger than the indigenous bitumen and that the sample has been compromised.

Another maturity parameter is hopane stereochemistry. The biological form is 17βH, 21βH, while the geological forms are αβ (hopanes) and βα (moretanes). Hopane is more thermodynamically stable than moretane, so high C₃₀ hopane/ moretane ratios are also indicative of oil-mature samples (Seifert & Moldowan, 1980). It is not expected that Neoproterozoic rocks would still have the biological form in a pristine sample. Due to the higher expected maturities, one also does not expect to see high abundances of hopanes or steranes. Thus, usually, these signals should not be visible in the full scan of the saturate fraction.

Patterns of normal alkanes (n-alkanes).

The pattern of *n*-alkanes in an uncontaminated Neoproterozoic sample should be consistent with what is known about the prevailing biology. Normal alkanes are derived from biomolecules made by algae, bacteria, and land plants. An odd over even preference

in the intensities of *n*-alkanes, particularly nC_{27} , nC_{29} and nC_{31} , suggests the presence of land-plant input (Peters et al., 2005). Current fossil and genomic data suggest that land plants originated in the mid-Ordovician (Qiu et al., 2006), so this odd over even preference in high numbered alkanes may be seen as contamination in Neoproterozoic samples. Studies of the saturate fractions of oils (Grosjean et al., 2009; Chapter 2) mainly show a signal that rises quickly in relative intensity and then declines smoothly in abundance with carbon number. The *n*-alkane pattern is most reliable when it is unimodal. A bimodal pattern, though not necessarily indicative of contamination, creates the possibility that one distribution is of a more recent contribution to the bitumen. Lastly, biodegradation is, along with other factors, indicated by loss of light *n*-alkanes and generation of an unknown complex mixture (UCM) or hump in the spectrum (Peters et al., 2005). Biodegradation indicates that organisms later came and consumed some of the original organics, leading to signal decay, and may have even contributed some of their own to the rock, introducing younger biomarkers.

General issues.

As a general principal, and provided clean drilling techniques were employed, sediment core samples are preferable to outcrop samples. Outcrop samples are exposed to weathering which both alters organic material and aids its degradation, lowering the concentration of biomarkers (Peters et al., 2005). A useful way to minimize contamination from outcrop samples is to saw off the outside sections of a rock. This was possible for the Chinese and Canadian samples. Unfortunately, the Ukrainian and Russian outcrop samples were all too small for this to be useful.

In either case, however, there are numerous ways for inadvertent contamination to occur between collection and analysis. A recent study found contamination of samples could be due to storage in plastic bags, presence of sunscreen on hands used to handle samples, and use of lubricants (Grosjean & Logan, 2007). These contaminants included fatty acid amides, chemical antioxidants, UV absorbers, branched alkanes with quaternary carbon atoms, alkyl cyclohexanes and alkyl cyclopentanes.

Whatever the type of sample, it is preferable to focus on rocks containing in excess of 1% TOC. With low TOC samples (< 1%) even low levels of contaminants can overwhelm the original biomarker signatures. One important factor for this requirement is low thermal maturity. If the rock has been through extensive metamorphism it is unlikely that any biomarkers will have survived the associated thermal history.

Unavoidable corruption of sediments can occur during burial when basinal fluids containing younger hydrocarbons migrate through porous rock intervals. In this case, maturity-sensitive and age-sensitive biomarkers become quite useful. Another possible way to distinguish this is to look at the 20S/ (S + R) ratios for C₂₈ and C₂₉ steranes, as described above.

Experimental

Sampling.

Samples from Ukraine, which were provided by Dr. Dima Grazhdankin, were collected from tributaries of the Dnester River and stored in cloth sample bags until analysis. Samples from China, which were provided by Dr. Shuhai Xiao, had been stored in polypropylene sample bags. Sediment core samples from the Coppercap Formation in Canada were provided by Dr. Rigel Lustwerk and had been stored in cloth sample bags. Outcrop and core samples from Russia were provided by Dr. Mikhail Fedonkin in Moscow and had been stored in cardboard boxes. Samples from Australia were collected from fully cored petroleum exploration and stratigraphic wells. Samples from the Lake Maurice West-1 (LMW1) and Karlaya-1 (K1) wells of the Officer Basin and Mount James-1 (MJ1) of the Stuart Shelf were selected at the Glenside Drill Core Storage Facility which is managed and run by the Primary Industries and Resources South Australia. The samples from the Wallara-1 (W1) well of the Amadeus Basin were selected at the Northern Territory Geological Survey's core library in Alice Springs. These core samples were sectioned at the core facility, wrapped in aluminium foil pre-heated to 550°C and then placed into twist bags for transport to MIT and storage prior to analysis. Further details of the sampled strata are given in Table 1.

Area and Strata	Type	Age	Lithology	Depositional setting	TOC	Fossils	Key References
Ukraine: Podolia region of the East European Platform							
<i>Rovno Horizon</i>							
Khmelnitsky Fm.	outcrop	Cambrian	argillite and siltstone				Iosifidi et al., 2005
Okunets Fm.	outcrop	Cambrian	argillite and siltstone				Iosifidi et al., 2005
<i>Kotlin Horizon</i>							
Studenitsa Fm.	outcrop	Ediacaran	sandstone, siltstone and argillite				Iosifidi et al., 2005
Krushanovka Fm.	outcrop	Ediacaran	sandstone, siltstone and argillite				Iosifidi et al., 2005
Zhamovka Fm.	outcrop	Ediacaran	sandstone, siltstone and argillite				Iosifidi et al., 2005
Danilovka Fm.	outcrop	Ediacaran	siltstone and argillite				Iosifidi et al., 2005
<i>Redkino Horizon</i>							
Nagoryany Fm.	outcrop	Ediacaran	sandstone, siltstone and argillite				Iosifidi et al., 2005
Yaryshev Fm.	outcrop	Ediacaran	sandstone, siltstone and argillite				Iosifidi et al., 2005
China							
Xiuning: Hetang Fm.	outcrop	530 to 520 Ma	black shale/mudstone	marginal platform to deep shelf	high, up to 24 wt. %	small shelly fossils, sponge spicules, hexactinellid sponges, trilobites, small bilaterians	Yuan et al., 2002; Steiner et al., 2003; Xiao et al., 2005a
Yangtze Gorges: Dengying Fm., Shibantan Mbr	outcrop	551 to 538 Ma (Dengying)	dolomite	subtidal	high	Ediacaran body fossils, microbial structures, <i>Vendotaenia antiqua</i>	Xiao et al., 2005b
Weng'an: Doushantuo Fm.	outcrop	635-551 Ma	phosphatic shale with minor carbonate and shale	shallow to open marine	high	multicellular algae, acritarchs, fossil embryos, small bilaterians	Xiao et al., 1998; Chen et al., 2004; Condon et al., 2005
Canada							
Coppercap Fm.		Cryogenian	carbonate				Kaufman et al., 1997

Russia							
<i>Arkangelsk</i>							
Yorga	outcrop	Ediacaran	siltstone, sandstone, mudstone	delta plain to marine		dominated by <i>Leiosphaeridia</i> Eis., abundant fine filamentous algae	Grazhdankin, 2004; Grazhdankin et al., 2005
Zimny Gory	core	Ediacaran, 555.3 +/- 0.3 Ma near base	mainly mudstone and silty mudstone-sandstone	lower to upper shoreface, marine		filamentous forms and thin-walled <i>Leiosphaeridia</i> sp., abundant filamentous algae and plant films, colonial cyanobacteria	Sokolov & Fedonkin, 1990; Sokolov & Iwanowski, 1990; Martin et al., 2000; Ragozina et al., 2003; Grazhdankin, 2004
Verkhovka	outcrop	Ediacaran, base 558 +/- 1 Ma	mudstone with interbeds of siltstone	middle to upper shoreface, marine		diverse leiosphaerids	Sokolov & Iwanowski, 1990; Grazhdankin, 2003, 2004; Grazhdankin et al., 2005
Arkhangelsk	core	Ediacaran	mainly mudstone and silty mudstone	coastal marine		diverse leiosphaerids	Sokolov & Fedonkin, 1990; Sokolov & Iwanowski, 1990
Lyamtsa	outcrop	Ediacaran	siltstone-mudstone	lower through upper shoreface, marine		Thick walled <i>Leiosphaeridia</i> Eisenach	Sokolov & Fedonkin, 1990; Sokolov & Iwanowski, 1990; Grazhdankin, 2003, 2004
<i>St. Petersburg</i>							
Kotlin Horizon: Laminarite Fm.	outcrop	Ediacaran	clay shale	shallow marine	high	dominated by <i>Leiosphaeridia</i> Eisenach, abundant fine filamentous algae	Sokolov & Fedonkin, 1990; Sokolov & Iwanowski, 1990

Australia							
<i>Centralian Superbasin</i>							
Officer Basin: Tanana Fm.	core	Ediacaran		shelf to slope	low	Diverse acanthomorphic acritarchs	Grey et al., 2003; McKirdy et al., 2006
Karlaya Limestone	core	Ediacaran	micritic carbonate	shelf	low	Diverse acanthomorphic acritarchs	Grey et al., 2003; McKirdy et al., 2006
Dey Dey Mudstone	core	Ediacaran	mudstone with turbidites	deep water up to slope	low	Lower has leiospheres, upper has diverse acanthomorphic acritarchs	Grey et al., 2003; McKirdy et al., 2006
Amadeus Basin: Arumbera Sandstone	core	Ediacaran to Cambrian	sandstone with minor siltstone, conglomerate, shale and carbonate		low	Ediacaran fauna and diverse trace fossils	Zang & Walter, 1989; Walter et al., 1995
Pertatataka Fm.	core	Ediacaran	siltstone and shale with minor turbidite and sandstone	foreland-basin to marine outer shelf		stromatolites, acritarchs	Zang & Walter, 1989; Walter et al., 1995; Logan et al., 1997; Grey, 2005
Pioneer Sandstone Fm.	core	Cryogenian (635-850 Ma)					
Aralka Fm	core	Cryogenian (635-850 Ma)	siltstones and shales				Walter et al., 1995
Areyonga Fm.	core	Cryogenian (635-850 Ma)	tillite and phosphatic sediments				Walter et al., 1995
Bitter Springs Fm.	core	Tonian (850-1000 Ma)	carbonate and evaporite	shallow marine to lacustrine		stromatolites, acritarchs	Walter et al., 1995
<i>Stuart Shelf</i>							
Wonoka Fm.	core	Ediacaran	limestone, calcareous mudstone, sandstone	shelf		stromatolites, Ediacara-like megafossils	Haines, 2000; Walter et al., 2000

Table 1. Information on areas and strata studied including their collection type, age, lithology, depositional setting, total organic carbon (TOC), and fossils.

General Procedure.

Organic free solvents from OmniSolv were used. Prior to use, all glassware and aluminum foil were fired at 550°C for 8h and glass wool; pipettes and silica gel were fired at 450°C for 8h.

For each of the samples from the Hetang Formation, Doushantuo Formation and Shibantan Member of the Dengying Formation of China and Coppercap Formation of

Canada, the outer 5 mm were removed with a diamond saw and the inner and outer portions of each rock were analyzed separately or set aside, respectively. Sediment samples were cleaned with de-ionised water, rinsed with methanol and dichloromethane and crushed manually with the sample wrapped in fired aluminum foil. They were then ground to a fine powder in a SPEX 8510 Shatterbox fitted with an 8505 alumina ceramic puck mill that was carefully cleaned between samples with aqueous detergent, fired sand and finally rinsed with distilled water, methanol, dichloromethane and hexane. Rock powders were extracted using an accelerated solvent extractor (Dionex ASE) using a 9:1 mixture of dichloromethane and methanol. The resultant extracts were carefully evaporated under nitrogen to a volume of approximately 2 mL whereupon activated Cu was added to remove elemental sulfur. The sample was then separated by liquid chromatography on a silica gel 60 (Merck, 230-400 mesh) column using hexane to elute the saturate fraction, 4:1 hexane/dichloromethane to elute the aromatic fraction, and 7:3 dichloromethane/methanol to elute the polar fraction. One milligram aliquots of the saturate fractions were then reduced to 0.1 mL and added to insert vials with an internal standard. The saturate fraction was run on the Autospec with the following standards: 50 ng D₄ (D₄- $\alpha\alpha\alpha$ -ethylcholestane, Chiron) or 50 ng D₄ (D₄- $\alpha\alpha\alpha$ -ethylcholestane, Chiron) + 1 μ g *ai*-C₂₂ (3-methylheneicosane, ULTRA Scientific).

Gas Chromatography-Mass Spectrometry (GC-MS) was performed using a Micromass Autospec-Ultima instrument equipped with an Agilent 6890N Series gas chromatograph. Biomarkers in the saturated hydrocarbon fraction were analyzed by GC-MS with the Autospec operated in the metastable reaction monitoring (MRM) mode. A 60 m J&W Scientific DB-1 fused silica capillary column (0.25 mm i.d., 0.25 μ m film thickness) was used with helium at constant flow as carrier gas. Samples were injected in splitless mode. The oven was programmed 60°C, held for two minutes, ramped to 150°C at 10°C/min, then to 315°C at 3°C/min where it was held isothermal for 24 min. The source was operated in EI-mode at 70 eV ionization energy. Peak identification was based on retention time comparisons with the hydrocarbons present in a synthetic standard oil (AGSO Standard Oil) and abundances measured by comparing peak areas to the internal D₄ sterane standard without any adjustment for possible differential responses. Full scan

analyses were acquired under the same GC conditions as described above and the scan rate was 0.80 s/decade over a mass range of 50 to 600 m/z with a total cycle time of 1.06s. Data were acquired and processed using MassLynx v4.0 software.

Results and Discussion

A summary of age-sensitive and maturity-sensitive biomarker parameters for each studied sample is given in Table 2.

Area	Formation	Sample	% bitumen	C ₂₈ / (C ₂₈ +C ₂₉) Sts	24- Nordiachol. ratio	C ₃₀ Hopane/ moretane	C ₂₉ St ααα S/ (S+R)	C ₂₈ St ααα S/ (S+R)
Ukraine								
Rovno	Khmelnitsky	UKR 15	0.00	0.58	ND	11.81	0.46	0.35
	Okunets	UKR 13	0.01	0.52	ND	9.35	0.52	0.44
Kotlin	Studenitsa	UKR 12	0.01	0.58	ND	6.54	0.43	0.35
		UKR 19	0.00	0.51	ND	2.45	0.45	0.35
		UKR 5	0.01	0.57	0.47	11.30	0.46	0.35
	Krushanovka	UKR 9	0.00	0.52	ND	2.85	0.44	0.35
		UKR 11	0.00	0.58	ND	9.59	0.47	0.34
	Zharnovka	UKR 4	0.02	0.58	0.49	8.98	0.39	0.34
	Danilovka	UKR 6	0.01	0.51	0.45	4.35	0.39	0.34
		UKR 3	0.12	0.57	0.47	6.35	0.43	0.36
Redkino	Nagoryany	UKR 16	0.02	0.30	0.35	6.14	0.45	0.40
		UKR 2	ND	0.23	ND	ND	0.46	0.50
		UKR 17	0.05	0.27	0.17	5.49	0.50	0.47
	Yaryshev	UKR 7	0.00	0.52	0.31	14.36	0.45	0.41
		UKR 1	ND	0.33	ND	ND	0.45	0.47
		UKR 10	0.11	0.28	0.12	6.14	0.58	0.52
		UKR 14	0.00	0.54	0.41	6.67	0.36	0.30
		UKR 8	0.00	0.47	0.28	10.49	0.47	0.36
UKR 18	0.00	0.56	0.40	4.52	0.46	0.42		
China								
	Hetang	inside	0.00	0.54	ND	9.29	0.56	0.33
		outside	0.00	0.53	ND	13.75	0.50	0.32
	Shibantan	inside	0.00	0.48	ND	11.52	0.49	0.49
		outside	0.00	0.54	ND	13.48	0.36	0.38
	Doushantuo (WB)	inside	0.00	0.47	ND	10.26	0.53	0.43
		outside	0.00	0.56	ND	12.51	0.56	0.29
Canada								
	Copper cap	CCC1	0.00	0.50	0.31	14.01	0.49	0.41
		CCC2	0.05	0.52	0.35	12.39	0.50	0.42
		CCC3	0.03	0.50	0.36	13.61	0.44	0.41
		CCC4	0.01	0.51	0.37	14.28	0.48	0.40
Russia								
Arkangelsk core	Zimny Gory	M8	0.01	0.50	0.29	3.26	0.42	0.45
		M7	0.01	0.18	0.22	2.54	0.25	0.32
		M6	0.01	0.14	0.26	3.74	0.37	0.38
		M5	0.01	0.51	0.24	7.31	0.36	0.46
	lower Arkhangelsk beds	M4	0.01	0.42	0.35	2.94	0.44	0.32
	Riphean	M3	0.01	0.48	0.24	12.57	0.47	0.36
	Riphean	M2	0.00	0.46	0.24	13.90	0.50	0.36
Riphean	M1	0.00	0.46	0.24	13.07	0.49	0.45	
Arkangelsk outcrop	Yorga	65	0.02	0.26	0.32	3.06	0.12	0.12
	Verkovka	62	0.02	0.12	0.21	4.00	0.07	0.09
		63	0.01	0.21	0.41	2.64	0.11	0.10
		64	0.01	0.12	0.26	2.57	0.11	0.20
	Lyamza	61	0.02	0.22	0.20	3.04	0.20	0.28
St. Petersburg	Laminarite	66	0.09	0.23	0.21	5.69	0.06	0.07
		67	0.06	0.23	0.16	3.53	0.06	0.06
		68	0.01	0.25	0.16	6.98	0.09	0.10

Australia								
Officer Basin	Tanana	K1 1737	0.00	0.50	0.42	14.88	0.40	0.45
		K1 1814	0.00	0.51	0.37	7.35	0.42	0.52
		K1 1851	0.00	0.54	0.42	12.36	0.43	0.40
		K1 1947	0.00	0.37	0.54	1.65	0.48	0.41
		K1 1985	0.00	0.35	0.51	2.33	0.57	0.65
	K1 2023	0.00	0.18	0.09	4.25	0.47	0.52	
	Karlaya Limestone	K1 2089	0.00	0.45	0.57	3.68	0.45	0.39
	Dey Dey Mudstone	LMW1 319	0.00	0.05	0.34	ND	0.28	0.24
		LMW1 373	0.00	0.14	0.27	1.98	0.30	0.29
		LMW1 431	0.00	0.53	0.26	10.47	0.30	0.65
Amadeus Basin	Arumbera	W1 706.0	0.00	0.49	0.26	26.19	0.60	0.66
		W1 852.8	0.00	0.35	0.25	33.09	0.57	0.45
	Pertatataka	W1 1045.4	0.00	0.35	0.27	10.82	0.50	0.66
		W1 1250.8	0.00	0.50	0.31	13.70	0.61	0.51
		W1 1272.3	0.00	0.43	0.25	14.91	0.51	0.50
	Pioneer Sandstone	W1 1279.5	0.00	0.48	0.30	17.60	0.64	0.57
		W1 1286.6	ND	ND	ND	16.78	ND	ND
	Aralka	W1 1296.5	ND	ND	ND	21.02	ND	ND
		W1 1306.1	ND	0.44	ND	26.17	0.42	0.59
		W1 1324.3	0.00	0.49	0.31	22.59	0.59	0.48
	Areyonga	W1 1345.8	0.00	0.36	0.15	22.66	0.54	0.48
		W1 1368.1	0.00	0.45	0.30	21.07	0.58	0.46
		W1 1387.4	0.01	0.52	0.33	27.85	0.56	0.46
		W1 1407.2	0.00	0.44	0.29	21.18	0.60	0.47
		W1 1450.2	0.00	0.37	0.26	30.28	0.54	0.50
	Bitter Springs	W1 1658.3	0.00	0.46	0.28	26.52	0.53	0.51
		W1 1728.3	0.00	0.49	0.31	23.18	0.50	0.52
		W1 1826.8	0.00	0.45	0.29	28.03	0.49	0.53
		W1 1862.7	0.00	0.48	0.32	35.54	0.49	0.48
		W1 1904.9	0.00	0.47	0.29	27.41	0.48	0.51
		W1 1981.6	0.00	0.40	0.37	29.51	0.46	0.43
		W1 2000.8	0.00	0.44	0.39	31.81	0.46	0.51
	Stuart Shelf	Wonoka	MJ1 32.8	0.00	0.57	0.46	14.45	0.53
MJ1 106			0.00	0.45	0.46	13.03	0.42	0.37
MJ1 216			0.00	0.52	0.51	14.01	0.29	0.46
MJ1 285			0.00	0.54	0.49	12.60	0.26	0.40

Table 2. Key age and maturity parameters. St stands for steranes. The 24-nordiacholestanes ratio is 24-nordiacholestanes/ (24-nordiacholestanes + 27-nordiacholestanes). K1, LMW1, W1 and MJ1 are abbreviations for the well names Karlaya-1, Lake Maurice West-1, Wallara-1 and Mount James-1, respectively. Values that raise caution flags are in red, either because the value itself is out of the expected range for Neoproterozoic bitumen or, as in the case of the S/ S + R values, because they are markedly different between two homologues.

Age-sensitive biomarkers.

The samples from the Ukraine, China, Canada, many of the samples from the Arkhangelsk region of Russia, and most of the Australian samples have $C_{28}/(C_{28} + C_{29})$ steranes ratios and/ or 24-nordiacholestanes ratios that are incongruent with a Neoproterozoic age with average values for all of the samples being 0.42 and 0.32,

respectively. For the samples from Australia with the most reliable age biomarkers, a more complete story is provided in Appendix 1.

Maturity-sensitive parameters.

In most of the samples from Ukraine, China, Canada and Australia, the maturity parameters are consistent with a Neoproterozoic age of the bitumen. However, the C_{28} and C_{29} $\alpha\alpha\alpha$ $20S / (S + R)$ values are markedly different to each other (~ 0.1). In the standard AGSO oil run, the difference between C_{28} and C_{29} $\alpha\alpha\alpha$ $20S / (S + R)$ values was on average 0.02.

Maturity parameters are surprisingly low for some of the samples from the Arkhangelsk and St. Petersburg regions of Russia, with sterane $S / S + R$ ratios around 0.1. For the St. Petersburg samples, in the hopane traces, the $\beta\beta$ or biological form can be clearly identified, as is shown in Figure 1. Though such low thermal history is a concern for Neoproterozoic rock, evidence of a very low thermal history is corroborated by paleontological studies. The rocks from St. Petersburg have very light yellow microfossils and rocks of the Ediacaran White Sea outcrops have light orange microfossils (Knoll, 2009). A more thorough investigation of the samples from Russia is given in Appendix 2.

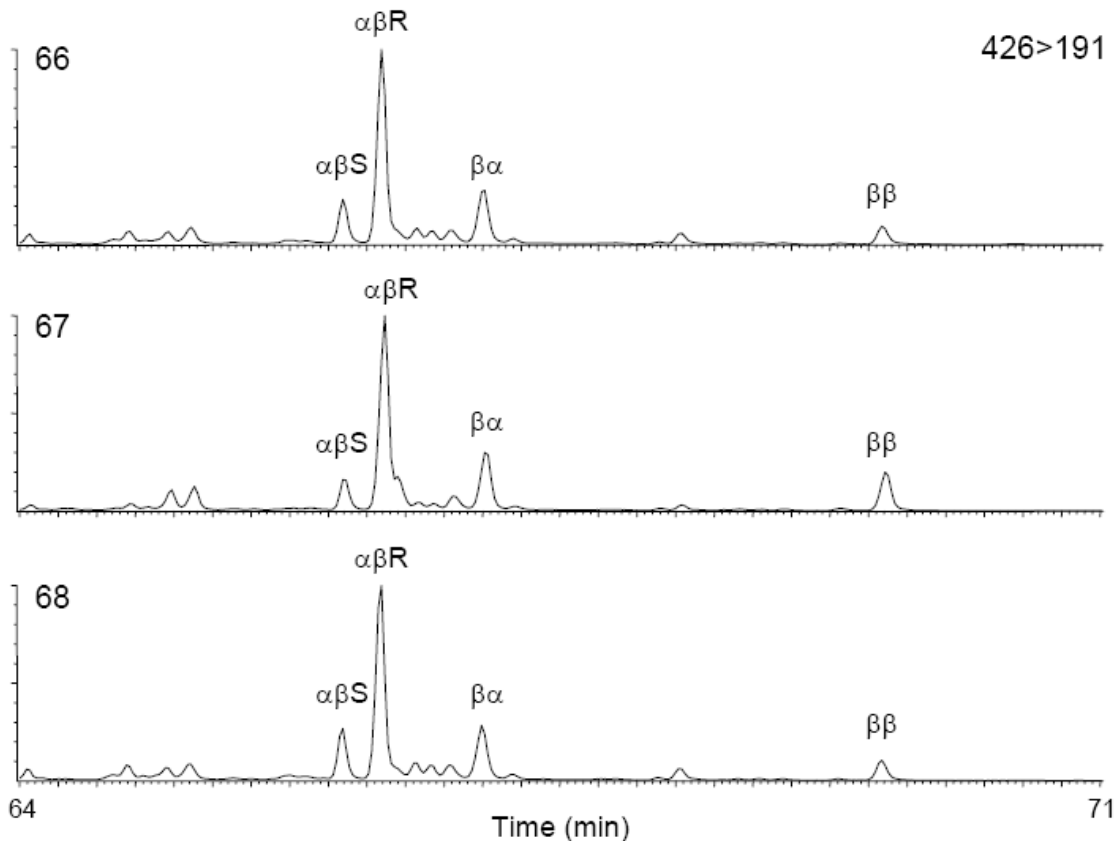


Figure 1. C₃₁ hopane distributions in saturate fractions of samples from St. Petersburg collected by GC-MS MRM showing the anomalously immature patterns with $\beta\beta$ isomers present and high 22R/ 22S + 22R ratios.

Patterns of n-alkanes.

The work on the outcrop samples from China demonstrated that these rocks had been subject to surficial contamination as all of the biomarkers found were only present in the outer layers. The full scan for the upper Doushantuo Formation (WB) inside, outside, Hetang (H) inside, outside, and Shibantan (S) inside and outside portion is shown from left to right in Figure 2. The only true peak seen in the inside samples is the standard *ai*-C₂₂ peak.

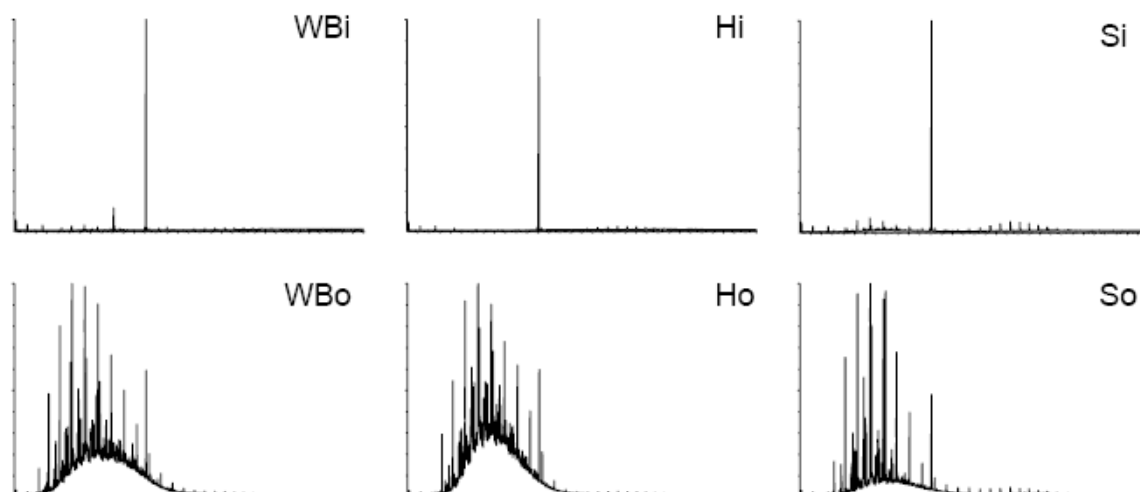


Figure 2. GC-MS full scans of the saturate fractions of samples from China showing that the only biomarkers are found on the outside of the samples, not the interior sections. The interior sections are denoted with an i and the outer sections are denoted with an o.

Total ion current chromatograms from the full scan GC-MS data for the outcrop samples from the Arkhangelsk region in Russian are shown in Figure 3 where steranes and hopanes are visible in samples 62 - 65, with a clear odd over even predominance in high carbon *n*-alkanes in sample 63, a feature also seen in many of the samples from Ukraine, the Amadeus Basin and St. Petersburg (Figure 4).

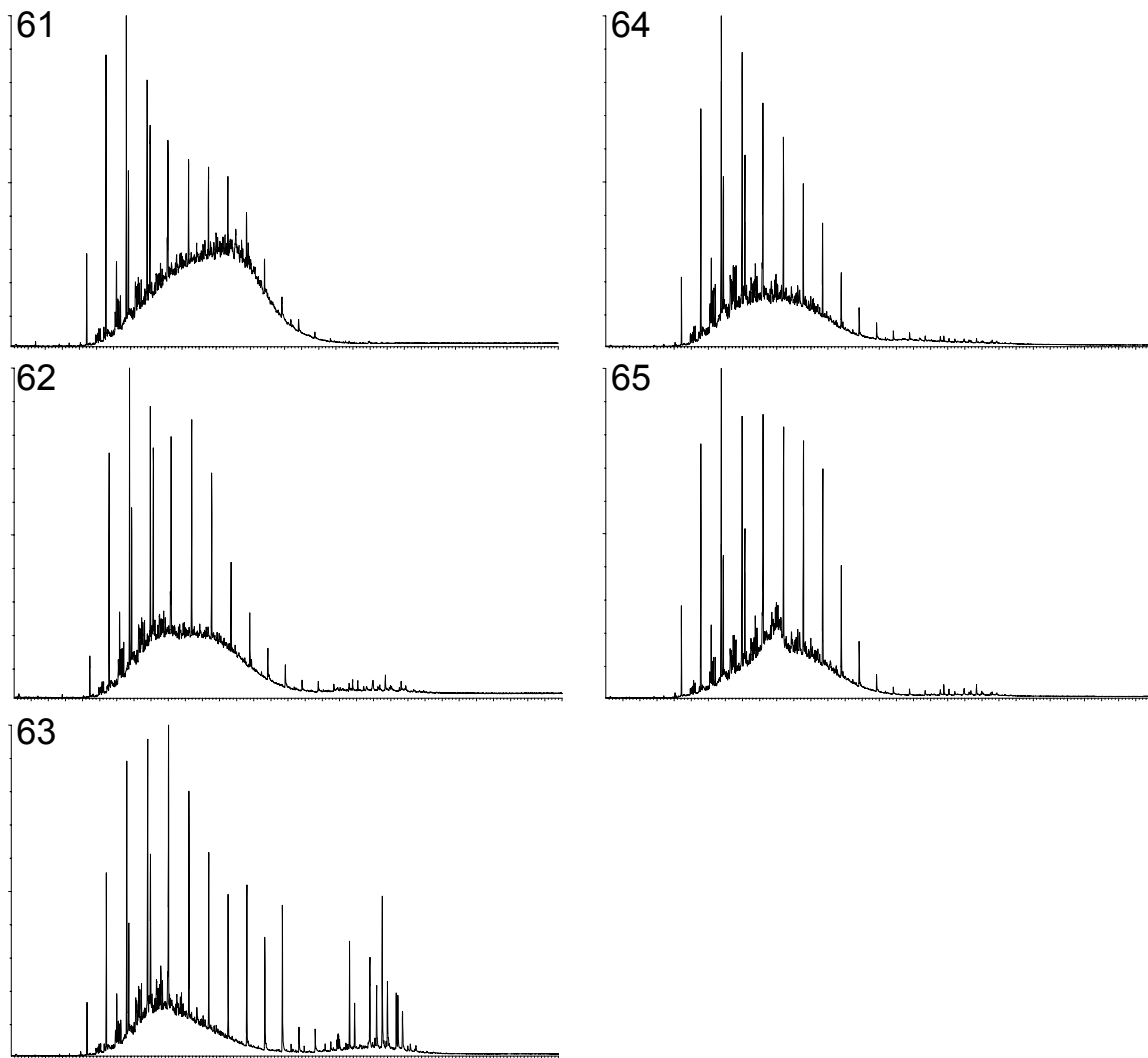


Figure 3. GC-MS full scan data for the saturate fractions of outcrop samples from Arkhangelsk showing an anomalously high abundance of steranes and hopanes and an even over odd predominance in the *n*-alkanes.

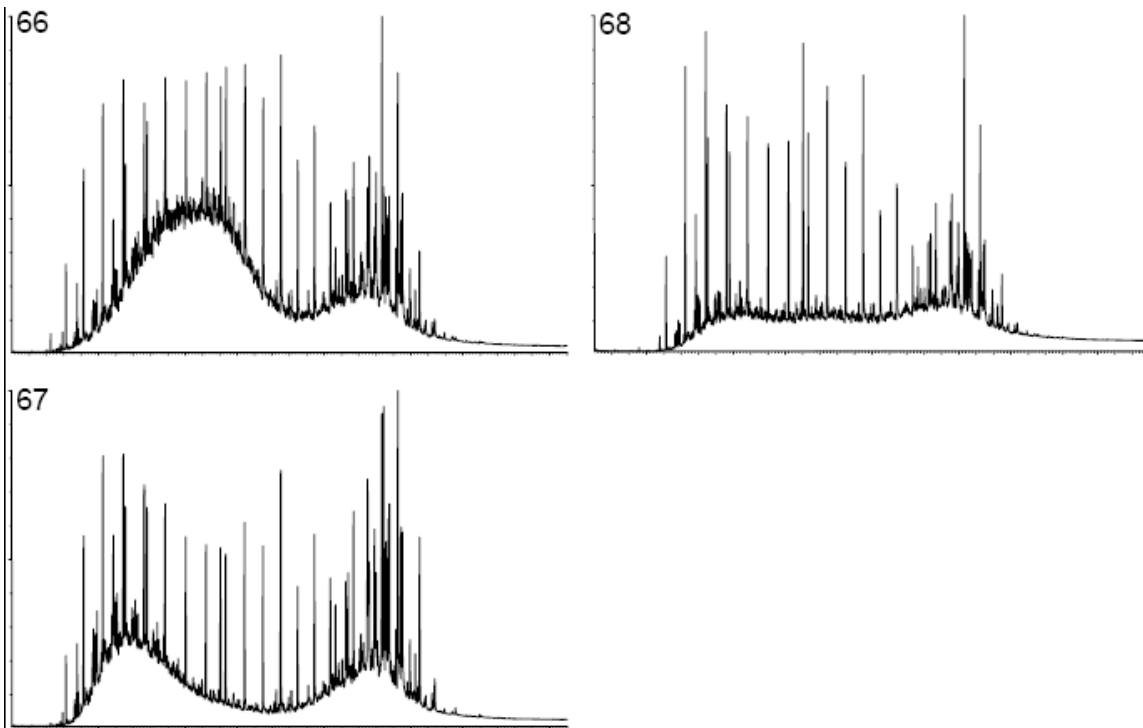


Figure 4. GC-MS full scan data for the saturate fractions of outcrop samples from St. Petersburg showing an odd over even predominance in the *n*-alkanes and a bimodal signal, suggesting the presence of land plants and multiple sources, respectively.

Also evident in the total ion chromatograms for the St. Petersburg samples in Figure 4 are bimodal *n*-alkane signatures that may be evidence for multiple contributions. This feature is also seen in the samples from Ukraine, Amadeus Basin and possibly Wonoka Formation (Figure 5).

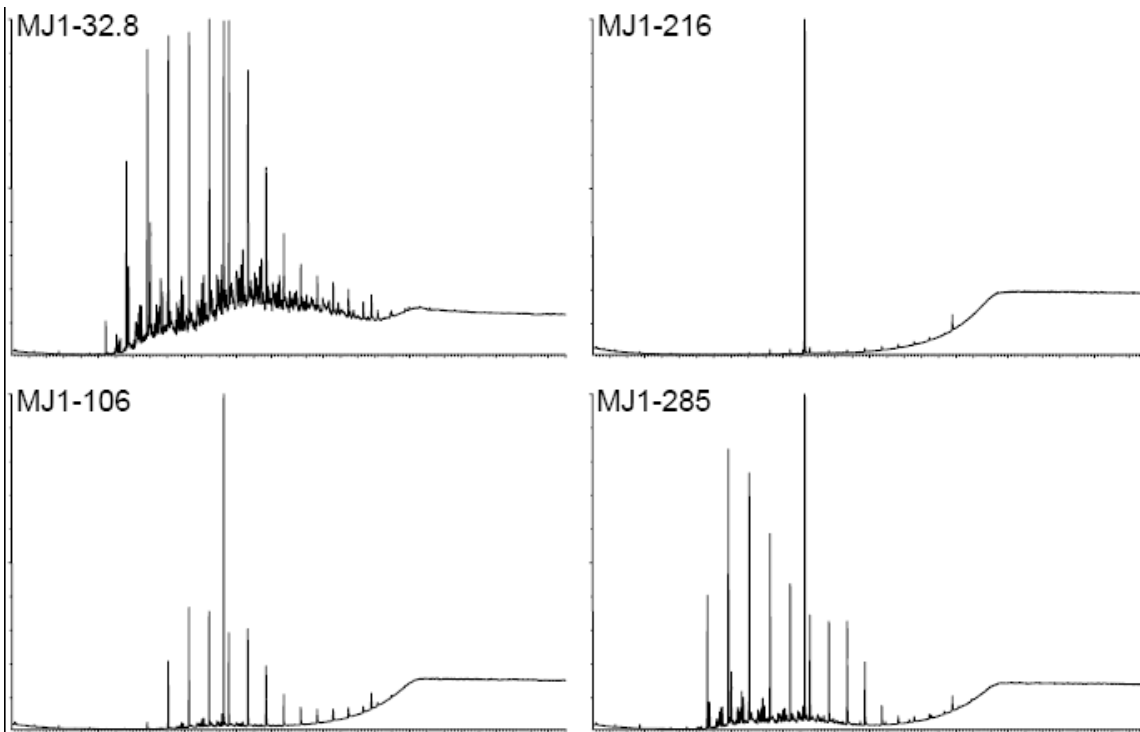


Figure 5. GC-MS full scan data for the saturate fractions of samples from the Wonoka Formation showing abnormal distributions, possibly indicating the presence of organic matter from multiple sources. The large peak that stands out is the standard *ai*-C₂₂.

For the samples from Coppercap Formation, Canada, the full scans for the saturated hydrocarbon fractions shown in Figure 6 show a lack of *n*-alkanes and a giant UCM in samples CCC2 - 4, suggesting that these bitumens have been biodegraded.

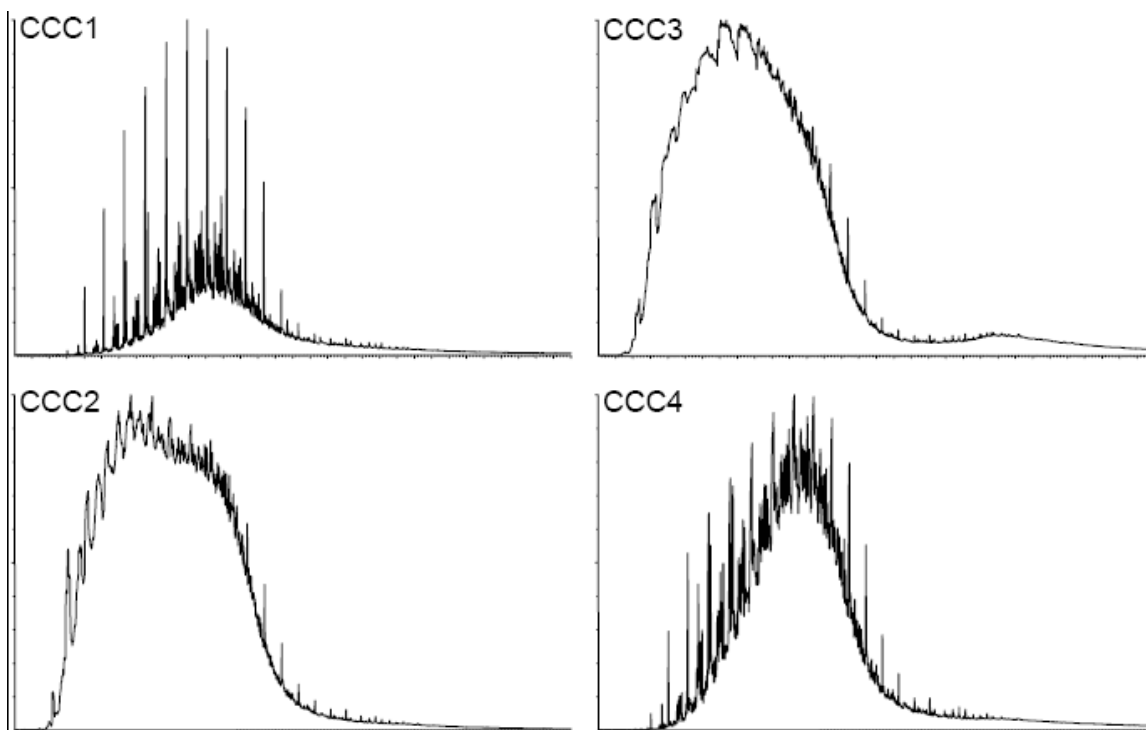


Figure 6. GC-MS full scan data for the saturate fractions of samples from the Coppercap Formation showing prominent UCMs likely indicative of biodegradation.

General issues.

The geology of the surrounding region must always be considered when analyzing samples. The samples from Ukraine are outcrop samples from the Podolia region of the East European Platform. Here, the Ediacaran sediments are overlain by Cretaceous (Albian-Cenomanian) sediments. Rb-Sr and K-Ar isotopic evidence suggest that there was extensive epigenetic alteration of the Redkino, Kotlin, and Rovno horizons in the Central East European Platform (Vinogradov et al., 2003), where our samples originate. Previous studies have shown that in the Devonian there was a tectonic episode (Leonov, 1976) that activated groundwater migration. This may have affected the state of the biomarkers preserved within these rocks, leading to a contamination of biomarkers or a washing of the indigenous biomarkers out of the rock, leading to low percentages of bitumens. There is also a possibility that these rocks were then contaminated by biomarkers from the much younger overlying rocks.

The high metamorphism in the Adelaide Rift Complex allows for the possibility of loss of the primary organic signal in the Wonoka samples of the Stuart Shelf, which is

adjacent to the Adelaide Rift Complex. The thermal history of rocks in this area increases the chance that any biomarkers present were destroyed.

Conclusions

The majority of the samples analyzed in this study have hydrocarbon patterns atypical for rocks of Neoproterozoic to Cambrian age. This may be due to novel environmental signals or contamination. The main confounding factor is that most bitumen found was < 0.1% of the total rock, with most samples having 0.00 to 0.01% extractable organic contents. This allows even the most minute contaminant to swamp the original biomarker signature. However, the evidence for contamination does not exclude the possibility that the bitumens comprise mixtures of hydrocarbons generated from rocks of different ages, including Neoproterozoic.

The abnormalities found include: a high ratio of $C_{28}/(C_{28} + C_{29})$ steranes (samples from Ukraine, China, Canada, Russia, and Australia), high 24-nordiacholestanes ratio (samples from Ukraine, China, Canada, Russia, and Australia), very low maturity (mainly samples from Russia), a significant difference in C_{28} vs. C_{29} $\alpha\alpha\alpha$ 20S/ (S + R) values (samples from Ukraine, China, Canada, and Australia), an odd over even predominance in the higher carbon *n*-alkanes (samples from Ukraine, Russian and, Australia), bimodal *n*-alkane distributions (samples from Ukraine, Russian, and Australia), and a large UCM (samples from Canada).

The level of severity of each of these abnormalities differs. The age parameters are primarily derived from ratios of biomarkers found in oil samples. However, in rocks the abundance of C_{28} steranes spikes at some extinction events, possibly due to an enhanced contribution from prasinophytes (Schwark & Empt, 2006). Though the 24-nordiacholestane ratio primarily follows diatom evolution, it may be that a precursor to diatoms also synthesized 24-norsteroids, or even that diatoms evolved much earlier than for which we currently have evidence.

A difference in C₂₈ and C₂₉ $\alpha\alpha\alpha$ 20S/ (S + R) values is not possible for molecules of the same age within the same rock. Similarly, it is very unlikely that indigenous molecules in a rock could still have the original biological configuration of hopanoids after over half a billion years. A high enough concentration of biomarkers such that they are visible in the full scan is unlikely for a rock over half a billion years old.

An odd over even predominance in the higher carbon *n*-alkanes is suggestive of an input from land plants which are not likely to have been present in the Neoproterozoic. Bimodal distributions of *n*-alkanes show a contribution from two sources, possibly with both at the time of the formation of the rock, possibly with only one indigenous to the rock and the other a younger overprint. A large UCM may be indicative of biodegradation, which means a loss of part of the original signature and possibly a more recent contamination.

References

- Brocks, J. J.; Grosjean, E.; Logan, G. A. **2008**. Assessing biomarker syngeneity using branched alkanes with quaternary carbon (BAQCs) and other plastic contaminants. *Geochim. Cosmochim. Acta* **72**, 871-888.
- Chen, J.-Y.; Bottjer, D. J.; Oliveri, P.; Dornbos, S. Q.; Gao, F.; Ruffins, S.; Chi, H.; Li, C.-W.; Davidson, E. H. **2004**. Small bilaterian fossils from 40 to 55 million years before the Cambrian. *Science* **305**, 218-222.
- Condon, D.; Zhu, M.; Bowring, S.; Wang, W.; Yang, A.; Jin, Y. **2005**. U-Pb ages from the Neoproterozoic Doushantuo Formation, China. *Science* **308**, 95-98.
- Goad, L. J.; Wither, N. **1982**. 27-Nor-(24R)-24-methylcholesta-5,22-dien-3/3-ol and brassicasterol as the major sterols of the marine dinoflagellate *Gymnodinium simplex* I. *Lipids* **17**, 853-858.
- Grantham, P. J.; Wakefield, L. L. **1988**. Variations in the sterane carbon number distributions of marine source rock derived crude oils through geological time. *Org. Geochem.* **12**, 61-73.
- Grazhdankin, D. V. **2003**. Structure and depositional environment of the Vendian complex in the Southeastern White Sea area. *Stratigr. Geol. Correlation* **11**, 313-331.
- Grazhdankin, D. V. **2004**. Patterns of distribution in the Ediacaran biotas: facies versus biogeography and evolution. *Paleobiology* **30**, 203-221.
- Grazhdankin, D. V.; Podkovyrov, V. N.; Maslov, A. V. **2005**. Paleoclimatic environments of the formation of upper Vendian rocks of the Belomorian-Kuloi plateau, Southeastern White Sea region. *Lithol. Miner. Resour.* **40**, 232-244.
- Grey, K. **2005**. Ediacaran palynology of Australia. Association of Australasian Paleontologists, Canberra.

- Grey, K.; Walter, M. R.; Calver, C. R. **2003**. Neoproterozoic biotic diversification: Snowball Earth or aftermath of the Acraman impact? *Geology* **31**, 459-462.
- Grosjean, E.; Logan, G. A. **2007**. Incorporation of organic contaminants into geochemical samples and an assessment of potential sources: Examples from Geoscience Australia marine survey S282. *Org. Geochem.* **38**, 853-869.
- Grosjean, E.; Love, G. D.; Stalvies, C.; Fike, D. A.; Summons, R. E. **2009**. Origin of petroleum in the Neoproterozoic-Cambrian South Oman Salt Basin. *Org. Geochem.* **40**, 87-110.
- Haines, P. W. **2000**. Problematic fossils in the late Neoproterozoic Wonoka Formation, South Australia. *Precambrian Res.* **100**, 97-108.
- Hayes, J. M.; Kaplan, I. R.; Wedeking, K. W. **1983**. Precambrian organic geochemistry; preservation of the record. In: Origin and Evolution of the Earth's Earliest Biosphere. (J. W. Schopf, ed.) Princeton University Press, Princeton NJ, pp. 93-132.
- Hoering, T. C.; Navale, V. **1987**. A search for molecular fossils in the kerogen of Precambrian sedimentary rocks. *Precambrian Res.* **34**, 247-267.
- Holba, A. G.; Tegelaar, E. W.; Huizinga, B. J.; Moldowan, J. M.; Singletary, M. S.; McCaffrey, M. A.; Dzou, L. I. P. **1998**. 24-norcholestanes as age-sensitive molecular fossils. *Geology* **26**, 783-786.
- Iosifidi, A. G.; Khramov, A. N.; Bachtadse, V. **2005**. Multicomponent magnetization of Vendian sedimentary rocks in Podolia, Ukraine. *Russ. J. Earth Sci.* **7**, 1-14.
- Kaufman, A. J.; Knoll, A. H.; Narbonne, G. M. **1997**. Isotopes, ice ages, and terminal Proterozoic earth history. *Proc. Natl. Acad. Sci. USA* **94**, 6600-6605.
- Knoll, A. H. **2009**. Pers. comm.
- Knoll, A.H.; Summons, R. E.; Waldbauer, J; Zumberge, J. **2007**. The geological succession of primary producers in the oceans. In: The Evolution of Primary Producers in the Sea. (P. Falkowski & A.H. Knoll, eds.), Elsevier, Burlington, pp. 133-163.
- Kodner, R. B.; Pearson, A.; Summons, R. E.; Knoll, A. H. **2008**. Sterols in red and green algae: quantification, phylogeny, and relevance for the interpretation of geologic steranes. *Geobiology* **6**, 411-420.
- Kokke, W. C. M. C.; Spero, H. J. **1987**. Sterol pattern determination as a probe for new species of zooxanthellae in marine invertebrates: Application to the dinoflagellate symbiont of the foraminifer *Orbulina universa*. *Biochem. Syst. Ecol.* **15**, 475-478.
- Leonov, Yu. G. **1976**. Tectonic origin of the Devonian orogenesis. Nauka, Moscow.
- Logan, G. A.; Summons, R. E.; Hayes, J. M. **1997**. An isotopic biogeochemical study of Neoproterozoic and Early Cambrian sediments from the Centralian Superbasin, Australia. *Geochim. Cosmochim. Acta* **61**, 5391-5409.
- Martin, M. W.; Grazhdankin, D. V.; Bowering, S. A.; Evans, D. A. D.; Fedonkin, M. A.; Kirschvink, J. L. **2000**. Age of Neoproterozoic bilaterian body and trace fossils, White Sea, Russia: Implications for metazoan evolution. *Science* **288**, 841-845.
- McKirdy, D. M. **1974**. Organic chemistry in Precambrian research. *Precambrian Res.* **1**, 75-137.
- McKirdy, D. M.; Webster, L. J.; Arouri, K. R.; Grey, K.; Gostin, V. A. **2006**. Contrasting sterane signatures in Neoproterozoic marine rocks of Australia before and after the Acraman asteroid impact. *Org. Geochem.* **37**, 189-207.

- Peters, K. E.; Walters, C. C.; Moldowan, J. M., eds. **2005**. The Biomarker Guide, second edition. Cambridge University Press.
- Qiu, Y.-L.; Li, L.; Wang, B.; Chen, Z.; Knoop, V.; Groth-Malonek, M.; Dombrovskaya, O.; Lee, J.; Kent, L.; Rest, J.; Estabrook, G. F.; Hendry, T. A.; Taylor, D. W.; Testa, C. M.; Ambros, M.; Crandall-Stotler, B.; Duff, R. J.; Stech, M.; Frey, W.; Quandt, D.; Davis, C. C. **2006**. The deepest divergences in land plants inferred from phylogenomic evidence. *Proc. Natl. Acad. Sci. USA* **103**, 15511-15516.
- Ragozina, A. L.; Weis, A. F.; Afonin, S. A. **2003**. Colonial cyanobacteria of the genus *Ostiana* (*Microcystis*) from the Upper Vendian of Arkhangelsk region. In: Instruments, methods, and missions for astrobiology VI. (R. B. Hoover, A. Y. Rozanov & J. H. Lipps, eds.) Proceedings of SPIE Vol. 4939, pp. 53-59.
- Rampen, S. W.; Schouten, S.; Abbas, B.; Panoto, F. E.; Muyzer, G.; Campbell, C. N.; Fehling, J.; Sinninghe Damsté, J. S. **2007**. On the origin of 24-norcholestanes and their use as age-diagnostic biomarkers. *Geology* **35**, 419-422.
- Schwark, L.; Empt, P. **2006**. Sterane biomarkers as indicators of palaeozoic algal evolution and extinction events. *Palaeogeogr. palaeoclimatol. palaeoecol.* **240**, 225-236.
- Seifert, W. K.; Moldowan, J. M. **1980**. The effect of thermal stress on source-rock quality as measured by hopane stereochemistry. *Physics and Chemistry of the Earth* **12**, 229-237.
- Seifert, W. K.; Moldowan, J. M. **1986**. Use of biological markers in petroleum exploration. In: Methods in Geochemistry and Geophysics Vol. 24 (R. B. Johns, ed.), Elsevier, Amsterdam, pp. 261-290.
- Sokolov, B. S.; Fedonkin, M. A. (eds.) **1990**. The Vendian System. Vol. 2. Regional Geology. Springer-Verlag, Berlin, Heidelberg, New York.
- Sokolov, B. S.; Iwanowski, A. B. (eds.) **1990**. The Vendian System. Vol 1. Paleontology. Springer-Verlag, Berlin, Heidelberg, New York.
- Steiner, M.; Li, G.; Qian, Y.; Zhu, M.; Erdtmann, B.-D. **2003**. Lower Cambrian small shelly faunas from Zhejiang (China) and their biostratigraphical implications. *Prog. Nat. Sci.* **13**, 852-860.
- Summons, R. E.; Walter, M. R. **1990**. Molecular fossils and microfossils of prokaryotes and protists from Proterozoic sediments. *Am. J. Sci.* **290A**, 212-244.
- Thomson, P. G.; Wright, S. W.; Bolch, C. J. S.; Nichols, P. D.; Skerratt, J. H.; McMinn, A. **2004**. Antarctic distribution, pigment and lipid composition, and molecular identification of the brine dinoflagellate *Polarella glacialis* (Dinophyceae). *J. Phycol.* **40**, 867-873.
- Vinogradov, V. I.; Golovin, D. I.; Bujakaite, M. I.; Burzin, M. B. **2003**. Stages of the epigenetic alteration of Upper Precambrian rocks from the Central East European Platform: Evidence from Rb-Sr and K-Ar isotope-geochemical investigations. *Lithol. Miner. Resour.* **38**, 177-182.
- Volkman, J. K. **1986**. A review of sterol markers for marine and terrigenous organic matter. *Org. Geochem.* **9**, 83-99.
- Waldbauer, J. R.; Sherman, L. S.; Sumner, D. Y.; Summons, R. E. **2009**. Late Archean molecular fossils from the Transvaal Supergroup record the antiquity of microbial diversity and aerobiosis. *Precambrian Res.* **169**, 28-47.
- Walter, M. R.; Veevers, J. J.; Calver, C. R.; Grey, K. **1995**. Neoproterozoic stratigraphy

- of the Centralian Superbasin, Australia. *Precambrian Res.* **73**, 173-195.
- Walter, M. R.; Veevers, J. J.; Calver, C. R.; Gorjan, P.; Hill, A. C. **2000**. Dating the 840-544 Ma Neoproterozoic interval by isotopes of strontium, carbon, and sulfur in seawater, and some interpretative models. *Precambrian Res.* **100**, 371-433.
- Xiao, S.; Zhang, Y.; Knoll, A. H. **1998**. Three-dimensional preservation of algae and animal embryos in a Neoproterozoic phosphorite. *Nature* **391**, 553-558.
- Xiao, S.; Hu, J.; Yuan, X.; Parsley, R. L.; Cao, R. **2005a**. Articulated sponges from the Lower Cambrian Hetang Formation in southern Anhui, South China: their age and implications for the early evolution of sponges. *Palaeogeogr. Palaeoclimatol. Palaeoecol.* **220**, 89-117.
- Xiao, S.; Shen, B.; Zhou, C.; Xie, G.; Yuan, X. **2005b**. A uniquely preserved Ediacaran fossil with direct evidence for a quilted bodyplan. *Proc. Natl. Acad. Sci. USA* **102**, 10227-10232.
- Yuan, X.; Xiao, S.; Parsley, R. L.; Zhou, C.; Chen, Z.; Hu, J. **2002**. Towering sponges in an Early Cambrian lagerstätte: disparity between nonbilaterian and bilaterian epifaunal tierers at the Neoproterozoic-Cambrian transition. *Geology* **30**, 363-366.
- Zang, W. L.; Walter, M. R. **1989**. Latest Proterozoic plankton from the Amadeus Basin in central Australia. *Nature* **337**, 642-645.

Appendix 1: Biomarker Trends in Neoproterozoic to Lower Cambrian Rocks from the Centralian Superbasin in Australia

Abstract

Sedimentary bitumens from the Amadeus and Officer Basins of Australia were analyzed for their hydrocarbon biomarker contents in order to further our understanding of the Neoproterozoic environment and its microbial and metazoan communities.

Introduction

The Australian rock samples studied have been collected from the Officer and Amadeus Basins which, although now are discrete geological provinces, were likely contiguous regions of marine sedimentation over much of central and western Australia as the Centralian Superbasin during the critical interval (Figure 1) (Logan et al., 1997; Walter et al., 1995). Crustal sagging and deposition of marine and fluvial sands ~800 Ma led to the formation of this superbasin that was later broken up by tectonic events, 540-600 Ma and in the mid Carboniferous, into several basins including the Officer and Amadeus (Walter et al., 1995). Stratigraphic columns for these two basins are shown in Figure 2. This region is of interest because of the wide range of depositional environments represented and the rich faunal and acritarch assemblages observed in these sediments. In the Centralian Superbasin, both major Neoproterozoic snowball events are observed and detailed carbon, sulfur and strontium data have been collected, allowing us to correlate these sections with others worldwide (Walter et al., 1995; Walter et al., 2000).

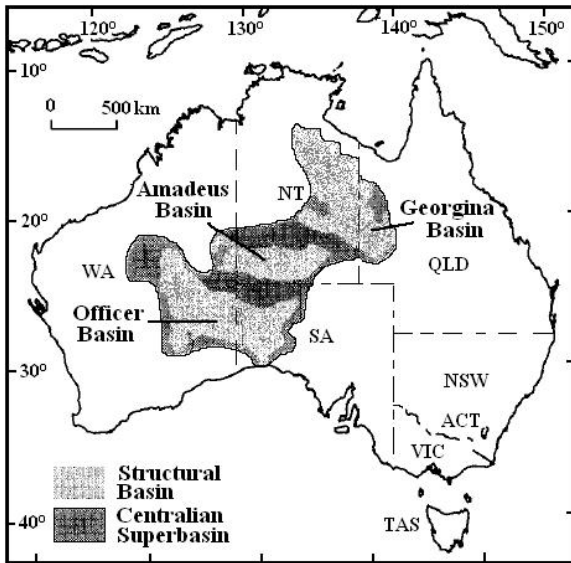


Figure 1. Location of the Centralian Superbasin adapted from Logan et al., 1997.

The Officer Basin sediments sampled include the Dey Dey Mudstone and the Tanana formations. Both of these units are Ediacaran in age and part of the Ungoolya Group, which is composed of deep water, sandy shales, minor carbonate and some turbidites. The palynoflora of the lower Dey Dey Mudstone consists of leiospheres, however in the upper Dey Dey Mudstone, acanthomorphic acritarchs quickly diversify (Grey et al., 2003). Species number increases into the members above including the Tanana Formation (Grey et al., 2003). The lower Dey Dey Mudstone is comprised of deep water sediments and the upper part is comprised of turbidites from a slope, so it is not surprising that the total organic carbon (TOC) for the Dey Dey Mudstone is low (McKirdy et al., 2006). The TOC for the Tanana Fm. is also low, though it represents a shelf to slope environment (McKirdy et al., 2006).

Amadeus Basin sediments were sampled from the Bitter Springs Formation., through the Areyonga Fm., Aralka Fm., Pioneer Sandstone, Pertatataka Fm., and Arumbera Sandstone. The Bitter Springs is Tonian (850-1000 Ma) in age and varies widely from shallow marine facies to lacustrine facies (Walter et al., 1995). The lithology is carbonate and evaporite and it also contains stromatolites and acritarchs (Walter et al., 1995). The Areyonga Formation is Cryogenian (635-850 Ma) in age and is composed of tillite and phosphatic sediments (Walter et al., 1995). The Aralka Fm. is also Cryogenian and is

composed of siltstones and shales (Walter et al., 1995). The Pioneer Sandstone is Ediacaran in age and is capped by a dolomite likely to be the Marinoan cap carbonate. The Pertatataka Fm. is Ediacaran in age and is a siltstone and shale facies with minor turbidite and sandstone (Zhang & Walter, 1989; Walter et al., 1995). It is likely from a foreland-basinal to marine outer shelf setting (Logan et al., 1997; Zhang & Walter, 1989). The fossils found include stromatolites and acritarchs that have become known as the Pertatataka acritarch assemblage (Zhang & Walter, 1989; Walter et al., 1995; Grey, 2005). The Arumbera is a sandstone unit with minor siltstone, conglomerate, shale and carbonate that contains the Neoproterozoic-Cambrian boundary, Ediacaran fauna and diverse trace fossils (Walter et al., 1995; Zhang & Walter, 1989). It is also low in TOC.

		Amadeus	Officer
Neoproterozoic	G	Arumbera	
		Julie	
			Tanana
			Karlaya
			Dey Dey
		Pertatataka	
		Cap	
		Pioneer	
		Aralka	
		Areyonga	
		BSF	

Figure 2. Stratigraphic columns of the eastern Officer Basin and the Amadeus Basin, where BSF stands for the Bitter Springs Formation, adapted from Walter et al., 2000.

Experimental

Sampling.

Samples from Australia were collected from fully cored petroleum exploration and stratigraphic wells. Samples from the Lake Maurice West-1 (LMW1) and Karlaya-1 (K1) wells of the Officer Basin were selected at the Glenside Drill Core Storage Facility which is managed and run by the Primary Industries and Resources South Australia. The samples from the Wallara-1 (W1) well of the Amadeus Basin were selected at the

Northern Territory Geological Survey's core library in Alice Springs. These core samples were sectioned at the core facility, wrapped in aluminium foil pre-heated to 550°C and then placed into twist bags for transport to MIT and storage prior to analysis.

General Procedure.

Organic free solvents from OmniSolv were used. Prior to use, all glassware and aluminum foil were fired at 550°C for 8h and glass wool; pipettes and silica gel were fired at 450°C for 8h.

Sediment samples were cleaned with de-ionised water, rinsed with methanol and dichloromethane and crushed manually with the sample wrapped in fired aluminum foil. They were then ground to a fine powder in a SPEX 8510 Shatterbox fitted with an 8505 alumina ceramic puck mill that was carefully cleaned between samples with aqueous detergent, fired sand and finally rinsed with distilled water, methanol, dichloromethane and hexane. Rock powders were extracted using an accelerated solvent extractor (Dionex ASE) using a 9:1 mixture of dichloromethane and methanol. The resultant extracts were carefully evaporated under nitrogen to a volume of approximately 2 mL whereupon activated Cu was added to remove elemental sulfur. The sample was then separated by liquid chromatography on a silica gel 60 (Merck, 230-400 mesh) column using hexane to elute the saturate fraction, 4:1 hexane/dichloromethane to elute the aromatic fraction and 7:3 dichloromethane/methanol to elute the polar fraction. One milligram aliquots of the saturate and aromatic fractions were then reduced to 0.1 mL and added to insert vials with an internal standard that served as an index of relative retention time and for quantification. The saturate fraction was run on the Autospec with the following standards: 50 ng D4 (D₄-ααα-ethylcholestane, Chiron) or 50 ng D4 (D₄-ααα-ethylcholestane, Chiron) + 1 μg aiC₂₂ (3-methylheneicosane, ULTRA Scientific). The aromatic fraction was run with 100 ng of D14 standard (d₁₄ p-terphenyl, Cambridge Isotope Laboratories).

Gas Chromatography-Mass Spectrometry (GC-MS) was performed using a Micromass Autospec-Ultima instrument equipped with an Agilent 6890N Series gas chromatograph.

Biomarkers in the saturated hydrocarbon fraction were analyzed by GC-MS with the Autospec operated in the metastable reaction monitoring (MRM) mode. A 60 m J&W Scientific DB-1 fused silica capillary column (0.25 mm i.d., 0.25µm film thickness) was used with helium at constant flow as carrier gas. Samples were injected in splitless mode. The oven was programmed 60°C, held for two minutes, ramped to 150°C at 10°C/min, then to 315°C at 3°C/min where it was held isothermal for 24 min. The source was operated in EI-mode at 70 eV ionization energy. Peak identification was based on retention time comparisons with the hydrocarbons present in a synthetic standard oil (AGSO Standard Oil) and abundances measured by comparing peak areas to the internal D₄ sterane standard without any adjustment for possible differential responses. Full scan analyses were acquired under the same GC conditions as described above and the scan rate was 0.80 s/decade over a mass range of 50 to 600 m/z with a total cycle time of 1.06s. Data were acquired and processed using MassLynx v4.0 software.

Results and Discussion

General.

Identity information for the Australian samples is given in Table 1.

Sample	Core	Basin	Formation
K1 1947	Karlaya-1	Officer	Tanana
K1 1985	Karlaya-1	Officer	Tanana
K1 2023	Karlaya-1	Officer	Tanana
LMW1 431	Lake Maurice West-1	Officer	Dey Dey Mudstone
LMW1 373	Lake Maurice West-1	Officer	Dey Dey Mudstone
W1 706	Wallara-1	Amadeus	Arumbera
W1 852	Wallara-1	Amadeus	Pertatataka
W1 1045	Wallara-1	Amadeus	Pertatataka
W1 1272	Wallara-1	Amadeus	Pioneer
W1 1286	Wallara-1	Amadeus	Aralka
W1 1296	Wallara-1	Amadeus	Aralka
W1 1306	Wallara-1	Amadeus	Aralka
W1 1345	Wallara-1	Amadeus	Areyonga
W1 1450	Wallara-1	Amadeus	Bitter Springs

Table 1. Australian samples and their identities.

Full scan data are shown in Table 2. The pristane (Pr)/ phytane (Ph) ratio provides information on the redox conditions under which sediments were deposited (Powell &

McKirdy, 1973; Didyk et al., 1978; ten Haven et al., 1987; Peters et al., 2005). However, as with all geochemical proxies, there needs to be caution in using one parameter in isolation. Pristane and phytane are both formed during the diagenesis of chlorophyll. When oxygen is present, pristane can be formed from phytol through a sequence of oxidation and decarboxylation reactions. When the depositional environment is anoxic, reductive processes prevail and phytane is formed. This empirical evidence suggests that a Pr/ Ph value <0.8 is diagnostic for an anoxic environment as commonly encountered in strongly stratified water columns. On the other hand, Pr/Ph >1 suggests more oxic environments, while Pr/Ph >3 is generally observed in terrestrial settings where organic matter is transported and sedimented in oxygenated water bodies (Peters et al., 2005). Further, Pr/Ph ratios that are <1 are most commonly observed in marine carbonates while values in the range of 2-4 for are common in deltaic shales. Intermediate values are common in clastic marine settings. The phytane/ $n\text{-C}_{18}$ ratio can be used as a maturity marker (ten Haven et al., 1987). Values $\gg 1$ suggest a sample is immature. The R_{22} index is $2 * n\text{-C}_{22} / (n\text{-C}_{21} + n\text{-C}_{23})$ and is considered by some to be a salinity marker; a value greater than 1.5 is typical for hypersaline environments (ten Haven et al., 1988). OEP is the odd over even carbon number preference and is measured by $(n\text{-C}_{25} + 6 * n\text{-C}_{27} + n\text{-C}_{29}) / (4 * n\text{-C}_{26} + 4 * n\text{-C}_{28})$. Values around 1 suggest that the bitumen is thermally mature (Scalan & Smith, 1970). There are two ratios provided below with $n\text{-C}_{\#} / x\text{-C}_{\#}$ and one $x\text{-C}_{20} / \text{Ph}$. The x-peaks are mid-chain monomethylalkanes which may suggest the presence of cyanobacteria, sponges or colorless sulfide oxidizing bacteria (Shiea et al., 1990; Thiel et al., 1999; Love et al., 2008).

	Pr/ Ph	Ph/ n-C ₁₈	R ₂₂ index	OEP	n-C ₂₂ / x-C ₂₂	n-C ₂₄ / x-C ₂₄	x-C ₂₀ / Ph
K1 1947			1.46	1.11	25.69	31.87	
K1 1985			1.73	0.91	23.07	12.76	
K1 2023	1.38	0.15	1.05	1.05	20.71	45.17	0.29
LMW1 373	0.70	0.30	0.98	1.07	30.36	94.11	0.23
LMW1 431	0.58	0.31	0.91	0.98	20.83	77.11	0.27
W1 706			0.84	1.53	10.94	22.48	
W1 852	0.84	0.33	1.19	1.06	13.16	16.69	0.37
W1 1045			1.15	1.03	11.06	30.25	
W1 1272			1.11	1.15	8.24	24.94	
W1 1286							
W1 1296			1.00	1.02	5.23	4.31	
W1 1306			1.39	1.16			
W1 1345	0.87	0.22	0.94	0.88	7.66	6.30	0.54
W1 1450	1.18	0.54	0.96	1.08	12.82	24.49	0.22

Table 2. Australian full scan data.

GC-MS (MRM) data are shown below, split into potential hypersalinity indicators (Table 3), maturity indicators (Table 4), and sponge and other source markers (Table 5). The two most used salinity indicators are gammacerane to hopane and the C₃₅ homohopane index, measured as C₃₅H (R + S) *100/ C₃₁-C₃₅H (R + S) %, are actually both indicators of stratification that can occur due to redox, temperature or salinity stratification (Peters et al., 2005). Gammacerane is formed through the degradation of tetrahymanol (ten Haven et al., 1989; Harvey & McManus, 1991), which is synthesized by bacterivorous ciliates that live in stratified zones of the water column (Harvey & McManus, 1991; Sinninghe Damsté et al., 1995). Use of 21-norsteranes and compound C as indicators of water column stratification, are discussed in Chapter 3.

The $\alpha\alpha\alpha$ -sterane 20S/ 20S + 20R and $\alpha\beta$ -homohopane 22S/ 22S + 22R ratios are commonly used to assess thermal maturity. Values at or near 0.55 indicate oil-mature samples (Seifert & Moldowan, 1986), as do high C₃₀ hopane/ moretane ratios (Seifert & Moldowan, 1980). Though most reliable when compared among samples of similar lithology, Ts/ Ts + Tm values are also used to indicate thermal maturity, with higher values indicating higher maturities (Seifert & Moldowan, 1978). For post-mature samples, Ts/ H can be used as a maturity marker (Volkman et al., 1983).

24-Isopropylcholestanes have been proposed as biomarkers for demosponges as discussed above. Another possible indicator of demosponges biomass contributions to sediments is a high abundance of 27-norcholestanes relative to cholestanes (Kelly et al., 2007). The ratio of steranes/ hopanes is primarily used as an indicator of input from eukaryotes relative to bacteria (Moldowan et al., 1985). The 2-methylhopane index (2MeHI) has been proposed as a molecular proxy for cyanobacteria (Summons et al., 1999) while the 3-methylhopane index (3MeHI) is potentially useful as a proxy for methanotrophic proteobacteria (Farrimond et al., 2004; Collister et al., 1992).

Potential Hypersalinity Indicators							
	HomoH Index %	γ / C ₃₀ H	21-norchol/ 27-norchol	21-norC ₂₈ St/ C ₂₈ $\alpha\beta\beta$ R	21-norC ₂₈ St/ C ₂₈ Sts	C/ A+B	C/ A
K1 1947	2.80	0.08	0.00	0.20	0.03	0.32	3.58
K1 1985	3.12	0.12		0.19	0.03	0.22	1.66
K1 2023	1.49	0.06		0.25	0.04	0.06	0.21
LMW1 431	0.00	0.01		0.29	0.05	0.04	0.18
LMW1 373	0.16	0.02	0.00	0.16	0.02	0.02	0.10
W1 706	2.25	0.05		0.29	0.04	0.05	0.40
W1 852	5.44	0.06	0.75	0.35	0.06	0.05	0.30
W1 1045	4.17	0.03		0.27	0.04	0.10	0.79
W1 1272	6.28	0.04	0.71	0.26	0.03	0.06	0.61
W1 1286	6.25	0.08		0.42	0.06		
W1 1296	5.56	0.05		0.63	0.10		
W1 1306	6.38	0.03	0.23	0.43	0.07	0.07	0.34
W1 1345	6.41	0.05	0.46	0.46	0.08	0.05	0.28
W1 1450	6.72	0.06	0.55	0.34	0.07	0.03	0.16

Table 3. Salinity indicators from GC-MS MRM analyses of Australian samples. H denotes hopane, γ gammacerane, and St for sterane.

Maturity					
	Ts/ (Ts+Tm)	C ₃₁ H 22S/ S+R	C ₂₉ ααα St S/ (S+R)	C ₃₀ H/ M	Ts/ H
K1 1947	0.20	0.58	0.34	1.92	0.33
K1 1985	0.18	0.59	0.38	2.07	0.27
K1 2023	0.11	0.61	0.43	5.15	0.03
LMW1 431	0.56	0.59	0.42	10.74	0.63
LMW1 373	0.03	0.58	0.25	2.16	0.04
W1 706	0.74	0.63	0.52	19.33	1.36
W1 852	0.61	0.62	0.53	25.50	1.17
W1 1045	0.62	0.58	0.40	14.07	0.49
W1 1272	0.65	0.59	0.52	16.98	0.84
W1 1286	0.66	0.58	0.56	31.25	0.66
W1 1296	0.63	0.60	0.54	17.09	0.80
W1 1306	0.65	0.57	0.48	19.36	0.83
W1 1345	0.67	0.57	0.53	23.39	0.91
W1 1450	0.58	0.58	0.49	23.75	0.85

Table 4. Maturity indicators from GC-MS MRM analyses of Australian samples. H denotes hopane, M moretane and St for sterane.

	Sponges				Other Source Markers			
	27-norSt/ ΣC ₂₇ -C ₂₉ St	27-norSts/ C ₂₇ Sts	i-C ₃₀ / n-C ₃₀	i-C ₃₀ αααR/ n-C ₃₀ αααR	Sts/ Hs	2αMe HI%	3βMe HI%	C ₂₇ Sts/ C ₂₉ Sts
K1 1947	0.01	0.03	0.47		0.09	5.25	1.94	0.91
K1 1985	0.00	0.00	0.39	0.56	0.07	3.58	2.78	0.60
K1 2023	0.00	0.00	1.16	1.21	0.05	1.08	1.04	0.33
LMW1 431	0.00	0.00	0.17		0.22	6.92	1.24	1.59
LMW1 373	0.00	0.00	1.54	1.31	0.04	0.48	1.87	0.38
W1 706	0.00	0.00	0.68	0.28	0.44	16.94	2.22	2.13
W1 852	0.00	0.00	0.74	0.35	0.68	11.68	1.81	1.37
W1 1045	0.00	0.00	0.16	0.05	0.37	8.84	2.08	1.13
W1 1272	0.00	0.00	0.40	0.20	0.63	13.75	2.62	1.98
W1 1286	0.00	0.00	0.00	0.00	0.35	14.60	2.78	1.46
W1 1296	0.00	0.00	0.00	0.00	0.29	13.55	1.50	1.25
W1 1306	0.01	0.02	0.00	0.00	0.30	14.40	2.38	1.20
W1 1345	0.01	0.02	0.03	0.13	0.44	13.20	2.26	1.01
W1 1450	0.02	0.04	0.36	0.48	0.56	11.74	2.50	1.30

Table 5. Sponge and other source markers from GC-MS MRM analyses of Australian samples. H denotes hopane and St for sterane.

Interpretations for Australian samples.

Low homohopane indices and gammacerane to hopane ratios suggest that the depositional environment was not an evaporitic basin. This interpretation is supported by the lithology. All of the samples studied were thermally mature, with the samples from the Amadeus Basin being more mature than those of the Officer basin. As expected, the

demosponge markers 24-isopropylcholestanes are not abundant in the Amadeus Basin where sediments are either too old to find sponge markers or are from deep waters, which were not oxygenated enough to support sponge life in the Neoproterozoic (McCaffrey et al., 1994; Love et al., 2009). Two samples from the Officer basin do clearly show the presence of demosponges. Neither of the samples have an appreciable amount of 27-norcholestane, though that may be due to preferential loss of light compounds due to over evaporation. The Amadeus Basin samples have a much higher steranes to hopanes ratio, suggestive of a higher eukaryotic over bacterial input (Brocks et al., 1999). The 2-methylhopane index suggests the presence of cyanobacteria in all samples, but with a higher prevalence in the Amadeus Basin. The 3-methylhopane index suggests a low abundance of methanotrophic bacteria.

Conclusions

From this new biomarker data we have a better understanding of the environment during the Neoproterozoic in Australia. Demosponge markers are found in substantial abundance in the Officer basin. The Amadeus Basin samples have higher eukaryotic to bacterial input than the Officer Basin.

References

- Brocks, J. J.; Logan, G. A.; Buick, R.; Summons, R. E. **1999**. Archean molecular fossils and the early rise of eukaryotes. *Science* **285**, 1033-1036.
- Collister, J. W.; Summons, R. E.; Lichtfouse, E.; Hayes, J. M. **1992**. An isotopic biogeochemical study of the Green River oil shale. *Org. Geochem.* **19**, 265-276.
- Didyk, B. M.; Simoneit, B. R. T.; Brassell, S. C.; Eglinton, G. **1978**. Organic geochemical indicators of palaeoenvironmental conditions of sedimentation. *Nature* **272**, 216-222.
- Farrimond, P.; Talbot, H. M.; Watson, D. F.; Schulz, L. K.; Wilhelms, A. **2004**. Methylhopanoids: Molecular indicators of ancient bacteria and a petroleum correlation tool. *Geochim. et Cosmochim. Acta* **68**, 3873-3882.
- Grey, K. **2005**. Ediacaran palynology of Australia. Association of Australasian Paleontologists, Canberra.
- Grey, K.; Walter, M. R.; Calver, C. R. **2003**. Neoproterozoic biotic diversification: Snowball Earth or aftermath of the Acraman impact? *Geology* **31**, 459-462.
- Harvey, H. R.; McManus, G. B. **1991**. Marine ciliates as a widespread source of tetrahymanol and hopan-3 β -ol in sediments. *Geochim. Cosmochim. Acta* **55**, 3387-3390.
- Kelly, A. E.; Love, G. D.; Grosjean, E.; Zumberge, J. E.; Summons, R. E. **2007**.

- Temporal and facies controls on the distributions of uncommon steranes from Neoproterozoic sediments and oils. Abstr. 23rd IMOG. Torquay, P203.
- Logan, G. A.; Summons, R. E.; Hayes, J. M. **1997**. An isotopic biogeochemical study of Neoproterozoic and Early Cambrian sediments from the Centralian Superbasin, Australia. *Geochim. Cosmochim. Acta* **61**, 5391-5409.
- Love, G. D.; Stalvies, C.; Grosjean, E.; Meredith, W.; Snape, C. E. **2008**. Analysis of molecular biomarkers covalently bound within Neoproterozoic sedimentary kerogen. In: *Paleontological Society Papers, Volume 14*. (P. H. Kelley & R. K. Bambach, eds.), The Paleontological Society, 67-83.
- Love, G. D.; Grosjean, E.; Stalvies, C.; Fike, D. A.; Grotzinger, J. P.; Bradley, A. S.; Kelly, A. E.; Bhatia, M.; Meredith, W.; Snape, C. E.; Bowring, S. A.; Condon, D. J.; Summons, R. E. **2009**. Fossil steroids record the appearance of Demospongiae during the Cryogenian Period. *Nature* **457**, 718-721.
- McCaffrey, M. A.; Moldowan, J. M.; Lipton, P. A.; Summons, R. E.; Peters, K. E.; Jeganathan, A.; Watt, D. S. **1994**. Paleoenvironmental implications of novel C₃₀ steranes in Precambrian to Cenozoic age petroleum and bitumen. *Geochim. Cosmochim. Acta* **58**, 529-532.
- McKirby, D. M.; Webster, L. J.; Arouri, K. R.; Grey, K.; Gostin, V. A. **2006**. Contrasting sterane signatures in Neoproterozoic marine rocks of Australia before and after the Acraman asteroid impact. *Org. Geochem.* **37**, 189-207.
- Moldowan, J. M.; Seifert, W. K.; Gallegos, E. J.; **1985**. Relationship between petroleum composition and depositional environment of petroleum source rocks. *Am. Assoc. Pet. Geol. Bull.* **69**, 1255-68.
- Peters, K. E.; Walters, C. C.; Moldowan, J. M., eds. **2005**. *The Biomarker Guide*, second edition. Cambridge University Press, 41-44.
- Powell, T. G.; McKirby, D. M. **1973**. Relationship between ratio of pristane and phytane, crude oil composition and geological environment in Australia. *Nature Phys. Sci.* **243**, 37-39.
- Scalan, R. S.; Smith, J. E. **1970**. An improved measure of the odd-even predominance in the normal alkanes of sediment extracts and petroleum. *Geochim. et Cosmochim. Acta* **34**, 611-620.
- Seifert, W. K.; Moldowan, J. M. **1978**. Applications of steranes, terpanes and monoaromatics to the maturation, migration and source of crude oils. *Geochim. Cosmochim. Acta* **42**, 77-95.
- Seifert, W. K.; Moldowan, J. M. **1980**. The effect of thermal stress on source-rock quality as measured by hopane stereochemistry. *Physics and Chemistry of the Earth* **12**, 229-237.
- Seifert, W. K.; Moldowan, J. M. **1986**. Use of biological markers in petroleum exploration. In: *Methods in Geochemistry and Geophysics Vol. 24* (R. B. Johns, ed.), Elsevier, Amsterdam, pp. 261-290.
- Shiea, J.; Brassell, S. C.; Ward, D. M. **1990**. Mid-chain branched mono- and dimethyl alkanes in hot spring cyanobacterial mats: a direct biogenic source for branched alkanes in ancient sediments? *Org. Geochem.* **15**, 223-231.
- Sinninghe Damsté, J. S.; Kenig, F.; Koopmans, M. P.; Köster, J.; Schouten, S.; Hayes, J. M.; de Leeuw, J. W. **1995**. Evidence for gammacerane as an indicator of water-column stratification. *Geochim. Cosmochim. Acta* **59**, 1895-1900.

- Summons, R. E.; Jahnke, L. L.; Hope, J. M.; Logan, G. A. **1999**. 2-Methylhopanoids as biomarkers for cyanobacterial oxygenic photosynthesis. *Nature* **400**, 554-557.
- ten Haven, H. L.; de Leeuw, J. W.; Rullkötter, J.; Sinninghe Damsté, J. S. **1987**. Restricted utility of the pristane/ phytane ratio as a palaeoenvironmental indicator. *Nature* **330**, 641-643.
- ten Haven, H. L.; de Leeuw, J. W.; Sinninghe Damsté, J. S.; Schenck, P. A.; Palmer, S. E.; Zumberge, J. E. **1988**. Application of biological markers in the recognition of palaeohypersaline environments. Geological Society Special Publication No. 40, 123-130.
- ten Haven, H. L.; Rohmer, M.; Rullkötter, J.; Bissert, P. **1989**. Tetrahymanol, the most likely precursor of gammacerane, occurs ubiquitously in marine sediments. *Geochim. Cosmochim. Acta* **56**, 1993-2000.
- Thiel, V.; Jenisch, A.; Wörheide, G.; Löwenberg, A.; Reitner, J.; Michaelis, W. **1999**. Mid-chain branched alkanolic acids from “living fossil” demosponges: a link to ancient sedimentary lipids? *Org. Geochem.* **30**, 1-14.
- Volkman, J. K.; Alexander, R.; Kagi, R. I.; Woodhouse, G. W. **1983**. Demethylated hopanes in crude oils and their applications in petroleum geochemistry. *Geochim. Cosmochim. Acta* **47**, 785-794.
- Walter, M. R.; Veevers, J. J.; Calver, C. R.; Grey, K. **1995**. Neoproterozoic stratigraphy of the Centralian Superbasin, Australia. *Precambrian Res.* **73**, 173-195.
- Walter, M. R.; Veevers, J. J.; Calver, C. R.; Gorjan, P.; Hill, A. C. **2000**. Dating the 840-544 Ma Neoproterozoic interval by isotopes of strontium, carbon, and sulfur in seawater, and some interpretative models. *Precambrian Res.* **100**, 371-433.
- Zang, W. L.; Walter, M. R. **1989**. Latest Proterozoic plankton from the Amadeus Basin in central Australia. *Nature* **337**, 642-645.

Appendix 2: Biomarker Trends in Ediacaran Rocks from the White Sea Region of Russia

Three outcrop samples from St. Petersburg were studied. Sponge biomarkers are not apparent in any of the samples and all of these samples contain 2,3,6-methylaryl isoprenoids. It cannot be specified whether these aryl isoprenoids are derived from isorenieratane or chlorobactane, but in either case it suggests the presence of green sulfur bacteria (*Chlorobiacea*) and thus a euxinic photic zone. These samples also contain Ni(II) porphyrins, as confirmed by their polarity and absorption at 392 nm (Saitoh et al., 2001; Grosjean et al., 2004). The presence of Ni(II) is suggestive of an oxic zone, though supporting evidence from other biomarkers is necessary (Lewan, 1984; Schaeffer et al., 1993; Sundararaman et al., 1993). The pristane/phytane ratio of these samples is near one, which supports the idea of an at least partially oxygenated water column. If true, the Ni(II) porphyrins and aryl isoprenoids together suggest a stratified water column. The mere fact that many of the samples have both aryl isoprenoids and large Ediacaran fauna is suggestive of this as well, since these organisms are assumed to need oxygen to respire. In Felitsyn et al. (1998), they too studied the Eastern European Platform and found evidence for a shallow low-energy marine environment, blooms of cyanobacteria that then lead to enrichment in Co and tetrapyrrole complexes, elevated Ni, signatures that suggest both an oxic and an anoxic environment, and organic circulation by methanogens. No 2-methylhopanoids were found, but that in no way discounts the cyanobacteria proposal (Rohmer et al., 1984). In support of the methanogen suggestion, 3-methylhopanoids have been identified. The elevation of tetrapyrrole complexes and Ni can be seen with the Ni porphyrins found. The confusion with oxic and anoxic environments and evidence for a shallow, low energy system supports the idea of a stratified water column that has enough oxygen in the surface layer to support Ediacaran

life and a euxinic zone that permeated up into the photic zone enough for *Chlorobiacea* to survive.

References

- Felitsyn, S. B.; Vidal, G.; Moczyłowska, M. **1998**. Trace elements and Sr and C isotopic signatures in late Neoproterozoic and earliest Cambrian sedimentary organic matter from siliciclastic successions in the East European Platform. *Geol. Mag.* **135**, 537-551.
- Grosjean, E.; Adam, P.; Connan, J.; Albrecht, P. **2004**. Effects of weathering on nickel and vanadyl porphyrins of a Lower Toarcian shale of the Paris basin. *Geochim. Cosmochim. Acta* **68**, 789-804.
- Lewan, M. D. **1984**. Factors controlling the proportionality of vanadium to nickel in crude oils. *Geochim. Cosmochim. Acta* **48**, 2231-2238.
- Rohmer, M.; Bouvier-Navé, P.; Ourisson, G. **1984**. Distribution of hopanoid triterpenes in prokaryotes. *J. Gen. Microbiol.* **130**, 1137-1150.
- Saitoh, K.; Tanji, H.; Zheng, Y. **2001**. Practical approach to chemical speciation of petroporphyrins. *Analytical Sciences* **17** supplement, i1511-i1513.
- Schaeffer, P.; Ocampo, R.; Callot, H. J.; Albrecht, P. **1993**. Extraction of bound porphyrins from sulfur-rich sediments and their use for reconstruction of palaeoenvironments. *Nature* **364**, 133-136.
- Sundararaman, P.; Schoell, M.; Littke, R.; Baker, D. R.; Leythaeuser, D.; Rullkötter, J. **1993**. Depositional environment of Toarcian shales from northern Germany as monitored with porphyrins. *Geochim. Cosmochim. Acta* **57**, 4213-4218.